INVERSE GAS CHROMATOGRAPHIC AND STATIC MEASUREMENTS OF WATER-POLYMER INTERACTIONS

A Thesis

by

JOSEPH S. ASPLER

B.Sc. (McGill); M.Sc. (Toronto)

Submitted to the Faculty of Graduate Studies
and Research of McGill University in partial
fulfillment of the requirements for the
degree of Doctor of Philosophy

Department of Chemistry
McGill University
Montreal, Canada

August 1980

ABSTRACT

The interaction of water with several cellulosic polymers at low water contents is measured by inverse gas chromatography. Various non-ideal kinetic contributions to the GC results are discussed, and corrections are determined.

Several gas chromatographic and static techniques were used to measure the activity of water vapor over concentrated solutions of hydroxypropyl cellulose. At 25°C, the results are compared to osmotic pressure measurements in the literature. It is suggested that in this system, the polymer-solvent interaction parameter may have the same value at each end of the concentration range, but the entropy of mixing changes from that predicted by Flory's theory for rod-like mixing at high polymer concentrations to that for Flory-Huggins mixing in dilute solution. Activities of water vapor measured from 15 to 55°C show the effect of the lower critical solution temperature above 40°C, in that activities approach unity and heats of mixing calculated from the temperature dependence of the sorption isotherms go to zero.

Infinite dilution thermodynamic parameters and heats of mixing of water with several cellulose acetates, methyl cellulose and ethyl cellulose are reported, and the effect of substitution is discussed. Finite concentration sorption isotherms are also given, and are interpreted by Zimm's cluster integral theory.

RESUME

L'interaction de l'eau avec plusieurs polymères cellulosiques aux teneurs en eau faibles est mesurée par la chromatographie inverse en phase gazeuse. Quelques contributions cinétiques non-idéales aux résultats de "GC"sont discutées, et les corrections sont determinées.

Quelques techniques chromatographiques et statiques furent utilisées pour mesurer l'activité de l'eau dans les solutions concentrées d'hydroxypropyl cellulose. A 25°, les résultats sont comparés avec des mesures de pressions osmotiques tirées de la littérature. Il est suggeré que, pour ce système, le paramètre de l'interaction polymère-solvant a la même valeur aux deux extremités de l'échelle de concentration. A des concentrations élevées de polymère, l'entropie est en accord avec les prédictions de la théorie de Flory pour un mélange de bâtonnets, alors qu'en solution diluée l'entropie est plutôt en accord avec la théorie de mélange de Flory-Huggins. Les activités de vapeur d'eau mesurées de 15° à 55° démontrent l'effet de la température critique de démixtion inférieure au dessus de 40°. Les activités s'approchent de l'unité, et les chaleurs de mélange calculées à partir de la dépendence des isothermes d'absorption sur la température tendent vers zéro.

Les chaleurs de mélange et les paramètres thermodynamiques à dilution infinie de l'eau avec quelques acétates de cellulose, méthyle cellulose, et éthyle cellulose sont rapportées, et l'effet de la substitution sur la cellulose est discuté. Les isothermes d'absorption à concentration finie sont donnés, et sont interpretés par la théorie intégral de groupement de Zimm.

ACKNOWLEDGEMENTS

The author wishes to express his deep appreciation to the many people who gave their assistance to this project. Thanks go especially to:

Dr. D.G. Gray, my research director, for instruction, advice, guidance, and (especially) patience; in addition to four years of practice in studying a handwriting worse than my own.

Dr. S. Tseng, Dr. D.A.I. Goring, Dr. R. St. John Manley, and Professor D. Patterson for advice and helpful discussions.

Mr. G. Suranyi for technical assistance.

Dr. G.J. Courval for some preliminary gas chromatographic work on hydroxypropyl cellulose.

Dr. J.F. Revol for checking the French translation of the abstract.

Ms. B. Brown for typing this manuscript.

My fellow graduate students for many useful and/or entertaining conversations; especially Dr. G.M. Dorris, Mr. B. Favis, Ms. S. Katz, Ms. R. Werbowyj, and Mr. P. Whiting.

The Pulp and Paper Research Institute of Canada for the use of their facilities and services, and for the award of the F.L. Mitchell Memorial Fellowship, 1977-1980.

The Natural Sciences and Engineering Research Council of Canada for the award of a post-graduate fellowship, 1976-1977.

The Department of Chemistry of McGill University for a teaching assistantship, 1978.

Finally, I wish to express my appreciation to my parents for their understanding in this difficult period I've been going through these last 27 years.

TABLE OF CONTENTS

page

CHAPTER 1

CHAPTER 2

CHAPTER 3

page

CHAPTER 4

CHAPTER 5

CHAPTER 6

A STUDY OF THE SORPTION OF WATER BY CELLULOSE DERIVATIVES.I. RESULTS AT FINITE CONCENTRATION AND INFINITE DILUTION

page

CHAPTER 7

A STUDY OF THE SORPTION OF WATER BY CELLULOSE DERIVATIVES.II. A SORPTION MODEL

CHAPTER 8

APPENDIX A

page

APPENDIX B

APPENDIX C

APPENDIX D

LIST OF FIGURES

CHAPTER 2

CHAPTER 3

CHAPTER 4

CHAPTER 5

CHAPTER 6

Figure page

CHAPTER 7

APPENDIX A

LIST OF TABLES

Table page

CHAPTER 3

CHAPTER 4

CHAPTER 6

CHAPTER 7

APPENDIX A

APPENDIX B

CHAPTER 1

INTRODUCTION

Aqueous polymer systems have been the object of many studies over the years (1). This interest is natural, considering the importance of water-polymer interactions in biological systems, and in many technologically important processes.

Cellulose and its derivatives remain one of the most important classes of polymers used today. The importance of water in cellulose and paper technology is well known. Because of this, the behavior of aqueous systems of cellulosic polymers has been examined in some detail with a very wide range of experimental techniques (1,2). X-ray, infrared, and nuclear magnetic resonance techniques have been used to study the changes which occur as cellulose and its derivatives absorb water. Sorption isotherms and calorimetric measurements have also been employed (2,3).

One concentration region not frequently studied by sorption methods is the region of very low water content, from zero to a few percent of water. In the past, information has been obtainable only by extrapolation from higher water concentrations. However, a new technique has been developed over the last few years which is ideally suited to the very low water concentration region. This technique is "inverse gas chromatography".

Gas chromatography (GC) is now universally accepted as a tool in analytical and in preparative organic chemistry. More recently, physical properties of polymers have been measured by inverse GC. The term "inverse" refers to the fact that the method is used to examine the stationary phase, rather than the injected sample, which is often referred to as the "probe" Inverse GC on polymeric stationary phases has been developed over the last ten years, and has been reviewed fairly recently (4,5). Since then, two comprehensive books on inverse GC have also been published (6,7).

Measurements by inverse GC have proven to be successful for non-polar systems at temperatures well away from any polymer glass transtion temperature. However, several problems were apparent from the start of the present work, due to the choice of water as probe and the polar cellulosics as substrates. Careful attention had to be paid to the materials used in constructing the GC columns, in order to avoid the introduction of extraneous polar sites into the columns. The existence of polymer-polymer or polymer-water hydrogen bonding presents the possibility of non-equilibrium kinetic effects, and furthermore may cause sorption hysteresis and curvature of the sorption isotherm. Finally, with water as probe, it was necessary to use a gas chromatograph equipped with a thermal conductivity detector rather than the more sensitive flame ionization detector. Of these problems, the most serious is the combination of isotherm curvature with peak spreading caused by non-equilibrium kinetic effects.

As stated previously, inverse GC is of particular use in the study of very low solvent concentrations in the polymer. However, this advantage of inverse GC is also one of its disadvantages: that it is confined to this region of low solvent content. Therefore, other sorption methods had to be used to extend the GC data to higher water contents.

One unusual aspect of the work in this thesis is that the mixing of water with one of the polymers produces an ordered or liquid crystalline phase at high polymer concentrations. Although non-polymeric liquid crystalline materials have been known for nearly a century (8), it has only been recently that these have been anything other than laboratory curiosities. Liquid crystals are characterized according to their structural order and their mechanism of formation. Thermotropic liquid crystals form upon heating certain crystalline solids; on further heating they melt to form an isotropic liquid. Lyotropic liquid crystals form upon the dissolution of one component in a critical amount of an appropriate solvent (9). Structures are defined as "smectic" (molecules parallel and aligned in layers) and "nematic" (molecules with parallel axes not arranged in layers). A third structure is the "cholesteric", originally seen in cholesterol derivatives. This is considered to be a twisted nematic in which the long axes of the molecule are no longer parallel, but rather are aligned at a small angle to each other, so that a structure with a fixed pitch may develop.

Recently, polymers with sufficiently stiff chains have been shown to form nematic liquid crystalline phases at high polymer concentration. Theoretical work by Flory (10-12) has pointed out that the asymmetry of the long-chained, stiff polymer molecules is by itself enough to produce a mesophase. Both natural and synthetic, optically active polymers with stiff chains have been found to form lyotropic liquid crystalline mesophases with cholesteric structure. This has been seen for various polypeptides (9), for solutions of hydroxypropyl cellulose in both water (13) and various organic solvents (14), and for other cellulosics (15) including cellulose itself (16).

Under the appropriate conditions of temperature and concentration, cholesteric liquid crystals often shown bright iridescent colors. These colors result from the reflection of radiation from the cholesteric structure of the mesophase. Some form of cholesteric structure has been suggested as the origin of the iridescent colors of certain beetles (17). Liquid crystalline polymer solutions are currently of great technological interest. Very strong fibers have been spun from such solutions. It has been suggested that this extra strength is derived from the pre-orientation of the polymer in the liquid crystalline phase (18), but few previous measurements of solvent activity over such solutions have been reported in the literature.

Scope and Aims of the Thesis

The basic aim of this project was the examination of water-polymer interactions at low water content. This region is suitable for examination by inverse gas chromatography, a technique that has been little used for aqueous polymer systems. Where necessary , sorption isotherms were measured at higher water content by means of classical, static methods. The polymers chosen were cellulose acetates of different degrees of substitution, methyl cellulose, ethyl cellulose, and hydroxypropyl cellulose (HPC). The latter forms lyotropic mesophases with cholesteric structure in water and in other organic solvents.

Chapter 2 provides a background to the theory of gas chromatography, as applied to polymer solution thermodynamics. Chapter 3 details the experimental methods used in the thesis. In Chapter 4, results of sorption measurements on HPC at 25°C as well as osmotic pressure data from the literature are compared to the Flory-Huggins and the Flory-Daoust models for the behavior of flexible coils in dilute solution, and to Flory's model for a system of rod-like molecules at very high polymer content. In Chapter 5, partial molar heats and entropies of mixing are calculated at different concentrations of water from sorption isotherms measured at several temperatures, and possible effects on the sorption process and the phase separation behavior are discussed.

In Chapter 6, the effect of non-ideal GC response in a polar system is discussed in detail. Sorption isotherms and infinite dilution thermodynamic parameters are given for the cellulosic polymers mentioned previously. Zimm's clustering integral is suggested as a model for these isotherms in Chapter 7.

Appendix A summarizes the results of sorption measurements on HPC using a large number of organic probes. Included are sorption isotherms, infinite dilution thermodynamic parameters, and a discussion of a newly-discovered HPC glass transition temperature. Appendix B shows the detailed thermodynamic data for water and hydroxypropyl cellulose referred to in Chapter 5. Appendix C gives a glossary of symbols, while Appendix D gives the detailed information used in calculating the infinite dilution heats of mixing of water in the cellulosic polymers in Chapter 6.

The thesis concludes with several claims to original research and suggestions for further work.

References

1) "Water: A Comprehensive Treatise", F. Franks, ed., Plenum Press, New York, 1975.

2) "Cellulose and Cellulose Derivatives", second edition, E. Ott and H.M. Spurlin, ed., Interscience Publishers, New York, 1955, 1970.

3) J.L. Morrison and M.A. Dzieciuch, Can. J. Chem., 37, 1379 (1959).

4) D.G. Gray, Progr. Polym. Sci., 5, 1 (1977).

5) J.-M. Braun and J.E. Guillet, Adv. Polym. Sci., 21, 107 (1976).

6) J.R. Conder and C.L. Young, "Physicochemical Measurements by Gas Chromatography", John Wiley and Sons, Chichester, 1979.

7) R.J. Laub and R.J. Pecsok, "Physicochemical Applications of Gas Chromatography", Wiley-Interscience, New York, 1978.

8) F. Reinitzer, Monatsh. Chem., 9, 421 (1888).

9) C. Robinson, Tetrahedron, 13, 219 (1961).

10) P.J. Flory, Proc. Roy. Soc. London Ser. A., 234, 60 (1956).

11) P.J. Flory, ibid, 73 (1956).

12) P.J. Flory, Ber. Bunsenges. Phys. Chem., 81, 891 (1977).

13) R.S. Werbowyj and D.G. Gray, Mol. Cryst. Liq. Cryst., 34, 97 (1976).

14) R.S. Werbowyj and D.G. Gray, Macromolecules 13, 69 (1980).

15) M. Panar and O.B. Willcox, Demande de Brevet d'Invention No. 7703473, Paris, 1977.

16) H. Chanzy, A. Peguy, S. Chaunis, and P. Monzie, J. Polym. Sci., Polym. Phys. Ed., 18, 1137 (1980).

17) A.C. Neville and S. Caveney, Biol. Rev., 44, 531 (1969).

18) W.G. Miller, Ann. Rev. Phys. Chem., 29, 519 (1978).

CHAPTER 2

BACKGROUND

A. Gas Chromatographic Measurements at Infinite Dilution

GC measurements on polymers are divided somewhat arbitrarily into two concentration regions. The region of finite concentration GC extends across the sorption isotherm up to high relative partial pressures of probe vapor. The region of infinite dilution, in GC terminology, is that portion of the isotherm where the concentration of the probe approaches zero, so that the system is essentially 100% polymer. In this limit, the partition isotherm should be linear, and peak retention times should be independent of injection size. If not, then the value of the infinite dilution retention time must be obtained by careful extrapolation of retention time to zero probe size.

A sample injected into the GC column that is not at all retained by the stationary phase will elute with a retention time t_M. The retention volume of this non-interacting probe is:

$$V_M = \dot{V}t_M = a\ell \tag{2-1}$$

where $\dot{V}$ is the carrier gas flow rate, ℓ is the length of the column, and a is the volume of the gas phase per unit length of the column. An interacting sample will have some retention time t_R, such that $t_R > t_M$. The retention volume of this sample corrected for the dead volume of the column is thus:

$$V_{R'} = (t_R - t_M)\,\dot{V} \tag{2-2}$$

It should be noted that the common method of flow rate measurement by soap bubble flowmeter requires a correction for the saturation of the carrier gas with water vapor from the soap solution:

$$\dot{V}_{corr} = \dot{V}_{observed} \left(\frac{P_o - p_{o,flo}}{P_o} \right) \qquad (2\text{-}3)$$

where P_o is the outlet pressure (normally atmospheric) and $p_{o,flo}$ is the saturated vapor pressure of water at the temperature of the flowmeter.

The finite pressure drop of carrier gas across the column, caused by the viscosity of the gas passing between the column packing particles, necessitates a correction for the gas compressibility. Because of compressibility, the flow at the outlet of the column will be greater than at the inlet. James and Martin (1) derived the correction factor j for the pressure drop:

$$j = \frac{3}{2} \left(\frac{(P_i/P_o)^2 - 1}{(P_i/P_o)^3 - 1} \right) \qquad (2\text{-}4)$$

where P_i is the inlet pressure.

The net retention volume V_N is defined as:

$$V_N = j\, V_{R'} = j(t_R - t_M)\, \dot{V} \qquad (2\text{-}5)$$

A more useful quantity is the specific retention volume V_g defined by Littlewood <u>et al</u> (2):

$$V_g = \frac{273.2}{T_c w} V_N \qquad (2\text{-}6)$$

where T_c is the column temperature and w the weight of the column loading. Thus V_g in mL g^{-1} is the elution volume of carrier gas corrected to 0° C, per gram of stationary phase in the column.

At low probe concentration (the "infinite dilution region") the concentration of vapor may obey a linear partition equation of the form:

$$q = \beta c \qquad (2\text{-}7)$$

where q is the probe concentration in the stationary phase (mol g^{-1}), c is the gas phase probe vapor concentration (mol mL^{-1}), and β (mL g^{-1}) is a partition coefficient per unit mass of stationary phase. In this limit, equation 2-6 becomes:

$$V_g = \frac{273.2}{T} \beta \qquad (2\text{-}8)$$

since the GC retention volume is related to the partition coefficient by the relation:

$$V_{R'} = \beta w \qquad (2\text{-}9)$$

B. Polymer Solution Thermodynamics

1. Theory

Present-day polymer solution theories have their origin in vapor pressure measurements on mixtures of small molecules (3). The simplest case is that of Raoult's law, where the activity of a component is equal to its mole fraction in solution:

$$\frac{p_1}{p_1^o} = x_1 = a_1 \qquad (2\text{-}10)$$

where p_1^o is the vapor pressure of the pure component and p_1 is its vapor pressure over the solution. This law is generally valid only for mixtures of non-polar molecules of the same approximate size, shape, and structure, such as benzene and toluene. However, at low concentrations of other molecules, the activity may still be linearly related to the mole fraction of the components:

$$\frac{p_1}{p_1^o} = \gamma_1 x_1 \qquad (2\text{-}11)$$

This expresses Henry's law where γ_1 is the activity coefficient.

The "strictly regular solution theory" is based upon the assumption that the solution is a rigid lattice such that each molecule has its own place, and all lattice sites are the same. Under these conditions, there is no volume change on mixing ($\Delta V_m = 0$). The entropy of mixing ΔS_m is equal to the ideal combinatorial (geometric, or statistical) term:

$$\Delta S_m = -k(N_1 + N_2)\ (x_1 \ln x_1 + x_2 \ln x_2) \qquad (2\text{-}12)$$

where x_1 and x_2 are mole fractions and N_1 and N_2 are numbers of molecules of the two species, and k is the Boltzmann constant. The heat of mixing ΔH_m is:

$$\Delta H_m = (N_1 + N_2)\, z\, w\, x_1\, x_2 \tag{2-13}$$

where z is the lattice coordination number, and w is derived from the energy of a (1-2) contact between unlike molecules on the lattice. Introducing the well-known Flory-Huggins interaction parameter:

$$\chi = zw/kT \tag{2-14}$$

the heat of mixing is:

$$\Delta H_m = (N_1 + N_2)\chi_{12} x_1 x_2 kT \tag{2-15}$$

which leads to the expression for the free energy of mixing:

$$\frac{\Delta G_m}{RT} = x_1 \ln x_1 + x_2 \ln x_2 + \chi_{12} x_1 x_2 \tag{2-16}$$

Subsequently, the χ parameter was given the character of a free energy term:

$$\chi = \chi_H + \chi_S \tag{2-17}$$

where χ_H and χ_S are the enthalpic and entropic contributions to χ, respectively. The free energy of mixing as defined by equation 2-16 is often written:

$$\Delta G_m = \Delta G_{m,comb} + \Delta G_{m,noncomb} \tag{2-18}$$

$\Delta G_{m,comb}$ is the combinatorial part of the free energy of mixing, given by the first two terms on the right hand side of equation 2-16. $\Delta G_{m,noncomb}$ is the non-combinatorial part of the free energy calculable from the χ parameter, and consists of all other contributions to ΔG_m, both enthalpic and entropic.

Attempts to fit the preceding expressions to polymer solutions give unrealistic and unacceptable values for the entropy of mixing. These values result from the use of mole fractions for polymer and solvent molecules of vastly diffent sizes. Under these conditions, volume fractions should replace mole fractions, such that:

$$\phi_1 = \frac{N_1}{N_1 + xN_2} \tag{2-19}$$

$$\phi_2 = \frac{xN_2}{N_1 + xN_2} \tag{2-20}$$

where $x = V_2/V_1$ is the ratio of the molar volumes of the two components. As is customary in inverse GC, components 1 and 2 are the probe and the polymeric stationary phase, respectively. The free energy of mixing of polymer and solvent maintains the same form as equation 2-16:

$$\frac{\Delta G_m}{kT} = N_1 \ln \phi_1 + N_2 \ln \phi_2 + (N_1 + xN_2)\chi_{12}\phi_1\phi_2 \tag{2-21}$$

Differentiation of equation 2-21 gives the familiar Flory-Huggins expression for the activity of a solvent over a polymer solution:

$$\ln a_1 = \ln(1 - \phi_2) + \left(1 - \frac{1}{x}\right)\phi_2 + \chi_{12}\phi_2^2 \tag{2-22}$$

By taking the following limits, we obtain the expression for the Henry's law coefficient at infinite dilution:

$$\lim_{\substack{\phi_2 \to 1 \\ x \to \infty}} (a_1/\phi_1) = \exp(1 + \chi) \tag{2-23}$$

The expression for the critical point of the solution is obtained by differentiation of equation 2-22:

$$\chi_{crit} = \tfrac{1}{2}(1 + x^{-\frac{1}{2}})^2 \tag{2-24}$$

so that for a polymer of high molecular weight:

$$\lim_{x \to \infty} \chi_{crit} = 0.5 \tag{2-25}$$

Equations 2-24 and 2-25 define the "Upper Critical Solution Temperature" (UCST), below which the polymer is insoluble. The frequently observed "Lower Critical Solution Temperature" (LCST) is not predicted by the Flory-Huggins theory, and requires further treatment. (The LCST is the point above which the polymer becomes insoluble, and below which the solutions are stable. Perversely, the LCST of a polymer solution is at a higher temperature than its UCST).

The sometimes very large change in volume upon mixing solvent and polymer not recognized by the Flory-Huggins theory is recognized in the "free volume theories", in which the rigid Flory-Huggins lattice is replaced by a lattice of cells that may be affected by changes in pressure, temperature, and composition of the solution (4-6). The molecules in these systems are allowed to possess a free volume associated with their internal degrees of freedom, so that the free volume of the solvent molecules is greater than that of the polymer. The solution of a polymer may therefore be likened to a "condensation" of a gas onto a larger substrate (4). This highly negative volume change upon mixing corresponds to a highly unfavorable, negative entropy of mixing, and thus explains the existence of the LCST. It can be shown that at an LCST, ΔH is less than zero (favorable) and ΔS is less than zero (unfavorable), so that the phase separation is caused by the increasingly unfavorable entropy of mixing from the free volume term as the temperature increases. At the UCST, the opposite holds true: ΔH is greater than 0 (unfavorable) and ΔS is greater than 0 (favorable), and the phase separation is caused by the increasingly unfavorable enthalpy term as the temperature is lowered. However, Patterson (4) has pointed out that caution must be used when dealing with polar systems, since some other effect such as diminishing hydrogen bond strength with increased temperature may also play an important role in the LCST.

2. Relationship Between Solution Theories and Gas Chromatographic Measurements

The original expressions relating activity coefficients to GC at infinite dilution were determined by Littlewood (7), who showed that in the Henry's law region where equation 2-11 is followed, equations 2-7 and 2-8, defining the partition coefficient β and the specific retention volume V_g respectively, may be written as:

$$\gamma_1 = \frac{RT}{\beta M_2 p_1^o} = \frac{273.2R}{V_g M_2 p_1^o} \qquad (2\text{-}26)$$

where M_2 is the molecular weight of the stationary phase.

Obviously, the use of equation 2-26 is not appropriate to high polymer solutions, due to the unrealistic values of γ_1^∞ that result from high numerical values of M_2. This problem was circumvented by Patterson et al (8), who derived an expression for the weight fraction based activity coefficient that in effect extended the Flory-Huggins theory to infinite dilution:

$$\begin{aligned} \ln(\Omega_1^\infty) &= \ln\left(\frac{a_1}{w_1}\right)^\infty \\ &= \ln\left(\frac{273.2R}{V_g M_1 p_1^o}\right) - (B_{11} - V_1)\frac{p_1^o}{RT} \qquad (2\text{-}27) \end{aligned}$$

From equation 2-27, the volume fraction based activity coefficient may be obtained in the limit as $\phi_2 \rightarrow 1$ from:

$$\begin{aligned} \ln\left(\frac{a_1}{\phi_1}\right)^\infty &= 1 - \frac{1}{x} + \chi \\ &= 1 + \chi \text{ as } x \rightarrow \infty \qquad (2\text{-}28) \end{aligned}$$

Equation 2-27 can also be used to give the value of χ in terms of the weight fraction based activity coefficient:

$$\begin{aligned} \ln(\Omega_1^\infty) &= \ln\left(\frac{a_1}{w_1}\right)^\infty \\ &= \ln\left(\frac{v_1}{v_2}\right) + 1 - \left(\frac{V_1}{M_2 v_2}\right) + \chi \qquad (2\text{-}29) \end{aligned}$$

Thus by combining the previous three equations we obtain an expression for χ_{12}^{∞}, the Flory-Huggins interaction parameter for an infinitely dilute solution of volatile component 1 in polymer 2:

$$\chi_{12}^{\infty} = \ln\left(\frac{273.2Rv_2}{p_1^o V_g V_1}\right) - \left(1 - \frac{V_1}{M_2 v_2}\right) - \frac{p_1^o}{RT}(B_{11} - V_1) \qquad (2\text{-}30)$$

$$\simeq \ln\left(\frac{273.2Rv_2}{p_1^o V_g V_1}\right) - 1 \qquad (2\text{-}31)$$

This parameter will also be referred to as χ_{FH}, in order to show its origin in the Flory-Huggins theory.

The "excess partial molar free energy" is the difference between the measured and ideal free energies of mixing of the two components and can be calculated from the GC-derived activity coefficient:

$$\Delta\overline{G}_m^{\infty} = RT \ln \gamma_1^{\infty} \qquad (2\text{-}32)$$

This means that χ_{12}^{∞} is directly related to $\Delta\overline{G}_m^{\infty}$ from equation 2-28. The excess enthalpy of mixing is:

$$\Delta\overline{H}_m^{\infty} = R\frac{\partial(\Delta\overline{G}_m^{\infty}/T)}{\partial(1/T)} \qquad (2\text{-}33)$$

$$= R\frac{\partial \ln \gamma_1^{\infty}}{\partial(1/T)} \qquad (2\text{-}34)$$

(where γ_1^{∞} can be replaced by an activity coefficient based upon another concentration term), and the excess entropy of mixing is readily obtained:

$$\Delta\overline{S}_m^{\infty} = \frac{(\Delta\overline{H}_m^{\infty} - \Delta\overline{G}_m^{\infty})}{T} \qquad (2\text{-}35)$$

The excess enthalpy of mixing is related to the temperature dependence of χ_{12}^{∞} by:

$$\Delta\overline{H}_m^{\infty} = RT\,\chi_H = [(\partial\chi/\partial(1/T)]/T \qquad (2\text{-}36)$$

The temperature dependence of the retention volume may be related to enthalpies of mixing by:

$$\Delta\overline{H}_m^{\infty} = -R(\Delta H_v + \Delta H_s) \qquad (2\text{-}37)$$

$$= -R\left(\frac{\partial \ln p_1^o}{\partial(1/T)} + \frac{\partial \ln V_g}{\partial(1/T)}\right) \qquad (2\text{-}38)$$

where the first term in the preceding equations, ΔH_v, is the latent heat of vaporization of the pure liquid probe, and the second term, ΔH_s, is the heat of sorption of the probe in the polymer. However, if the experimental retention data is not very precise (i.e., within < ± 1%), then it is preferable to use equations 2-33 or 2-34.

3. Polymer-Solvent Interactions at Infinite Dilution

Many polymers have been examined in the infinite dilution region by inverse GC. Values of the χ_{12}^{∞} parameter or some form of the activity coefficient, and heats of solution, have been reported. Those can be found in the various books and review articles cited in the references to Chapter 1. In general, good agreement has been found between these GC results, and results extrapolated from measurements by other techniques at higher solvent concentration.

Work performed has also included the measurement of probe diffusion coefficients and polymer solubility parameters. Three component systems - either solvent/polymer/polymer or solvent/solvent/polymer - have been examined. The last major area for inverse GC measurements is the examination of polymer glass transitions and melting points. This type of measurement is based on the change in accessibility of a polymer to a probe with temperature that may occur near T_g or T_m. The glass transition region in particular has been the source of many erroneous GC measurements in the literature due to the neglect of the slow diffusion that occurs through the glassy polymer.

Figure 2-1 shows a generalized infinite dilution retention curve of ln V_g vs. reciprocal absolute temperature for a hypothetical semi-crystalline polymer. In the segment AB, the polymer is below its glass transition temperature. The bulk of the polymer is not available to the probe, and hence the retention mechanism is confined to surface adsorption. The slope of the line AB is given by $-\Delta H_A/R$, where ΔH_A is the heat of adsorption of the probe onto the surface.

The glass transition temperature is generally taken as the first deviation from linearity as the temperature is raised to the point B. In the region BC, bulk sorption is possible. However, this is a non-equilibrium region due to the slow diffusion of the probe within the bulk. In the region CD, retention occurs by a combination of equilibrium bulk sorption and surface adsorption:

$$V_N = K_b V_L + K_a A_L \tag{2-39}$$

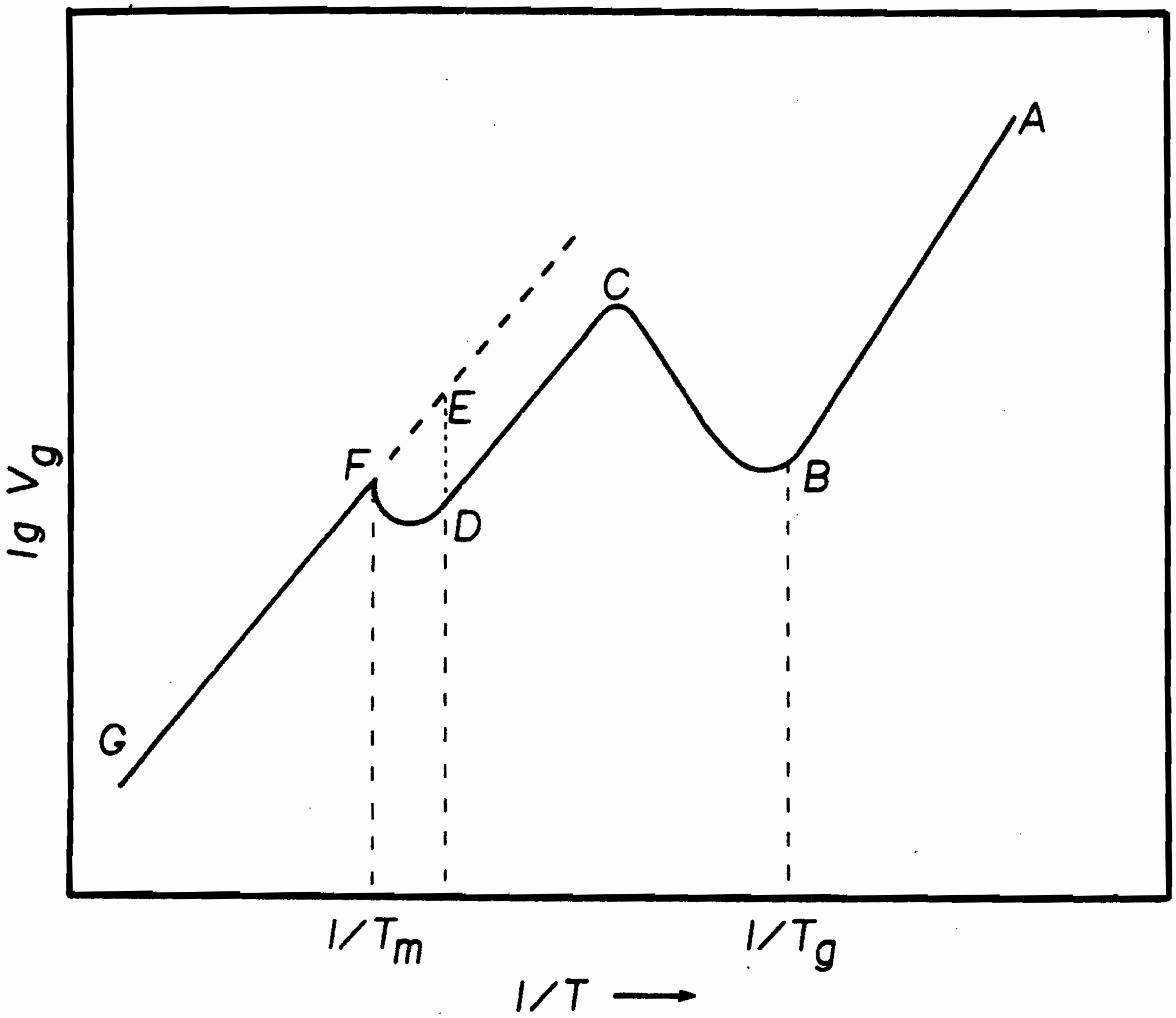

FIGURE 2-1 Generalized retention diagram for a semicrystalline polymer (9).

where K_a and K_b are partition coefficients for surface and bulk sorption, and V_L and A_L are the volume and surface area of the stationary phase. The weight of the stationary phase, w, may be substituted for V_L. The slope in this equilibrium region is $- \Delta H_s/R$ (equations 2-37 and 2-38).

If the probe is excluded from the crystalline regions of the polymer, a second discontinuity (region D - F) will be seen near the melting point (F) as the amount of stationary phase accessible to the probe increases.

C. Mixing with Rod-like Molecules

The original Flory-Huggins theory did not consider the effect of relative orientation of polymer molecules. However, for the stiff molecules introduced in Chapter 1, an additional factor becomes evident at high polymer concentrations, where parallel arrangements must be favored over random orientations of the rigid rods. Flory (10) has developed a lattice theory for semi-flexible and rod-like molecules which predicts the appearance of an anisotropic or ordered phase above a certain polymer concentration. The solvent activity over such a phase is given by (11,12):

$$\ln a_1 = \ln \phi_1 + \frac{2}{y} + \left(\frac{y - 1}{x}\right)\phi_2 + \chi_R\phi_2^2 \qquad (2\text{-}40)$$

where the degree of orientation of the rods is given by y ($1 \leq y < x$) with y = 1 for perfect orientation. The subscript on the polymer-solvent interaction parameter, χ_R, is used to indicate its origin in the rigid-rod theory. For high polymer concentration and large x, y approaches 1 and so equation 2-40 becomes:

$$\ln (a_1/\phi_1) = 2 + \chi_R\,\phi_2^2 \qquad (2\text{-}41)$$

The theory has recently been extended to include systems with different rod lengths (13,14).

Using the principles already set out, it is also possible to relate the rigid rod theory to GC data. Combining equations 2-28, 2-31, and 2-41 yields for perfectly oriented rods (y = 1):

$$\chi^{\infty}_{R} \simeq \ln\left(\frac{273.2Rv_2}{p_1^{o}V_gV_1}\right) - 2 \qquad (2\text{-}42)$$

The value of the polymer-solvent interaction parameter at infinite dilution over an ordered solution of rods should thus be easily obtainable. Treating the same data according to the Flory-Huggins theory would give a different value of χ:

$$\chi^{\infty}_{12} = \chi^{\infty}_{R} + 1 \qquad (2\text{-}43)$$

D. Measurements at Finite Concentration

The dependence of the GC retention volume on probe concentration in the gas phase can be used to determine sorption isotherms (15). The gradient $\partial q/\partial c$ of the partition isotherm is:

$$\left(\frac{\partial q}{\partial c}\right)_T = \frac{V_{R'}(c)}{w} \qquad (2\text{-}44)$$

where $V_{R'}$ is the concentration dependent, corrected retention volume. At infinite dilution, $(\partial q/\partial c)_T^{\infty} = \beta$, and this reduces to equation 2-9, $V_R' = \beta w$. Therefore, at a given gas phase concentration c, the amount of sorbed vapour is obtained by the integration of equation 2-44:

$$qw = \int_0^c V_R'(c)dc \qquad (2\text{-}45)$$

and this equation -- with appropriate corrections -- is the basis of all sorption isotherm measurements by GC. In GLC, the polymer weight w may be replaced by its volume V_L. Figure 2-2 shows the effect of the GC experimental chromatogram shape on the corresponding partition isotherm, for the case of a linear and a signoidal-shaped isotherm. Surface adsorption isotherms can be measured by this method if q is replaced by the Gibb's surface excess Γ and w is replaced by the surface area A_L. The surface coverage a_s (mol g^{-1}) is given by the product ΓA_L.

Conder and Purnell (16-19) investigated in great detail various non-ideal effects in the measurement of sorption isotherms by different

(a) INFINITE DILUTION

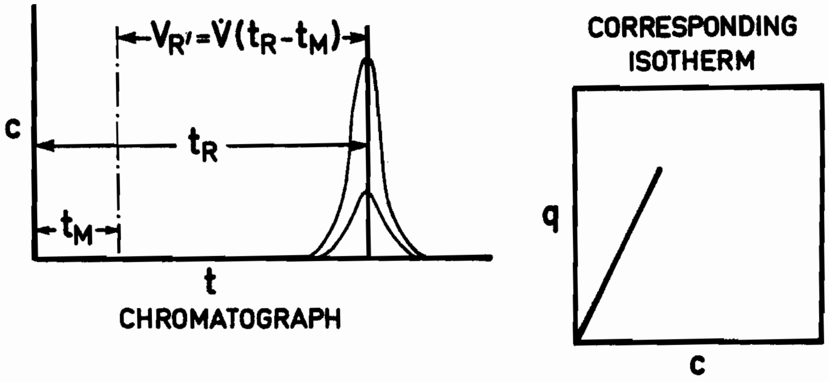

(b) FINITE CONCENTRATION

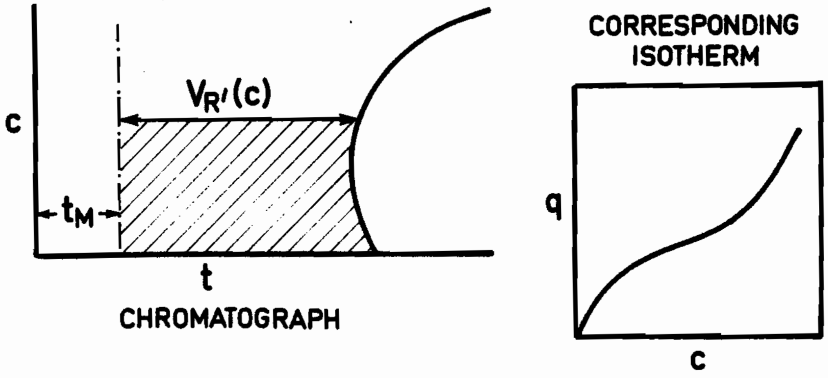

FIGURE 2-2 Simplified relationship between chromatographic results and isotherm shape (21):

(a) linear isotherm in infinite dilution region

(b) finite concentration where the curve on the right of the chromatogram represents t_R as a function of c and the shaded area is the integral in equation 2-46.

GC methods. Their work was summarized in an excellent review by Conder (20), which will be referred to in detail.

Conder and Purnell discussed a number of effects which can complicate the ideal situation implied in equations 2-44 and 2-45, and which must be considered in any finite-concentration work. These include the sorption effect, which results from the change in gas flow rate across a sorption-desorption boundary. They showed that the flow rate of the carrier gas transporting the peak is increased, according to the approximate expression:

$$\frac{F(y)}{F(0)} = \frac{1 + K}{1 + K(1 - y)} \qquad (2\text{-}46)$$

where F(0) is the zero concentration flow rate, F(y) is the flow rate of a peak whose gas phase mole fraction concentration of probe is y, and K is the partition coefficient.

According to the terminology of Conder and Purnell, sorption isotherm measurements can be divided into four types. The first three types differ only slightly in the methods for measuring the GC experimental curve, and the isotherms can be determined by variations of the basic equation 2-45. These three are "frontal analysis by a characteristic point" (FACP); "frontal analysis" (FA); and "elution by a characteristic point" (ECP). The two frontal analysis methods require a "plateau" concentration of probe vapor, achieved by means of some type of gas saturator or solvent pump. The experimental frontal chromatograms are obtained by following the sorption and desorption processes at the probe front as the flow system is changed from pure carrier gas at t = 0 to carrier gas + probe vapor and then back to pure carrier gas. Illustrations of these methods are given in the work of Conder and Purnell (16-19).

The ECP method is the most versatile and most commonly used of the three. The experimental chromatogram is obtained by "instantaneous" syringe injection of probe onto the column. If $j = 1$ (pressure gradient $\simeq 0$) and $\overline{y} << 1$ (sorption effect $\simeq 0$), equation 2-45 becomes:

$$
\begin{aligned}
\overline{qw} &= \int_0^{\overline{c}} (V_R - V_M)\, dc \\
&= \frac{PF}{RT} \int_0^{\overline{y}} (t_R - t_M)\, dy \qquad (2\text{-}47) \\
&= \frac{PF}{RT}\, \alpha'
\end{aligned}
$$

where α' is the shaded area so marked in figure 2-3. The "characteristic point" $\overline{y}_o$ is the point on the experimental curve at the vapor pressure corresponding to the height of the cross-hatched area. Thus the partition isotherm can be built up by measuring α' for various values of $\overline{y}_o$ on the chromatogram.

A more rigorous equation takes into account gas compressibility and the sorption effect, but not gas phase imperfection (20):

$$
\begin{aligned}
qw = \frac{P_o}{RT} \Bigg\{ & \frac{(\alpha + \beta)(1 + K)\ F(0)}{y_o} \ln \left[1 + \frac{jy_o}{(1 + K)(1 - jyo)} \right] \\
& + V_M \ln(1 - jy_o) - \beta F(0.8y_o) \Bigg\} \qquad (2\text{-}48)
\end{aligned}
$$

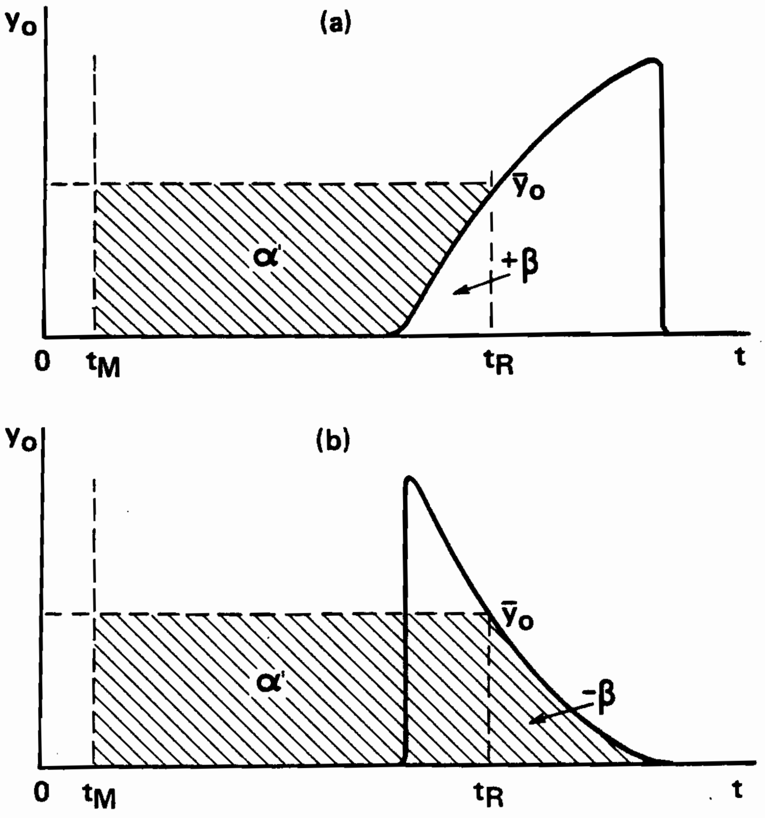

FIGURE 2-3 ECP chromatogram when (20):

(a) diffuse side of peak is a front boundary

(b) diffuse side of peak is a rear boundary.

where α is equal to the area α' in figure 2-3 plus the area between $t = 0$ and $t = t_M$; $F(0)$ is the measured flow rate (corrected by equation 2-3 for water vapor in the flowmeter, but not for the sorption effect); and V_M and p_o are as defined earlier. K is the bulk partition coefficient:

$$K = \frac{t_R - t_M}{t_M} \qquad (2\text{-}49)$$

Equation 2-48 can be simplified by successive approximations until it reduces to equation 2-47.

Conder and Purnell found that their results were in good agreement with static measurements in the literature, and pointed out that errors may exist in the earlier GC literature, where the factors mentioned here were not considered. In a similar vein, Conder and Young (22) have pointed out a very important criterion for successful measurements by the ECP method that is often ignored. This criterion requires that the diffuse sides of peaks of different injection size used to construct figure 2-3 be superimposable. Failure to observe this indicates the existence of a non-equilibrium chromatogram, possibly due to the slow diffusion of probe through the polymer.

The fourth GC technique is that of "elution on a plateau" or EP. In this method, a constant concentration or plateau of probe vapor is continually added to the carrier gas. The retention time of a small additional injection is measured, and once this has been repeated at several plateaus, the resultant curve has the same form as the ECP chromatogram in figure 2-3. The isotherm can then be calculated in a similar way.

Finite concentration GC measurements have proven useful in several areas. Sorption isotherms have been measured for a few polymers, and in general agreement has been very good with static measurements. Inverse GC methods have been used to measure adsorption of amounts too small to measure with any precision by other methods. GC measurements have also been used in measuring the surface area of polymers by the BET theory as well as isosteric heats of adsorption. Investigation of cellulose surfaces have yielded the surface area of fibers and of paper, and have been able to show the change in the area of paper with water content (23).

E. References

1) A.T. James and A.J.P. Martin, Biochem. J., 50, 679 (1952).

2) A.B. Littlewood, C.S.G. Phillips and D.T. Price, J. Chem. Soc., 1480 (1958).

3) For a complete review of the early solution theory work, see P.J. Flory, "Principles of Polymer Science", Cornell University Press, Ithaca, 1953.

4) I. Prigogine (with the collaboration of A. Bellemans and V. Mathot), "The Molecular Theory of Solutions", The North Holland Publishing Co., Amsterdam, 1957.

5) B.E. Eichinger and P.J. Flory, Trans. Farad, Soc., 64, 2035; 2053; 2061; 2066 (1968).

6) D. Patterson, Rubber Chem. Technol., 40, 1 (1967).

7) A.B. Littlewood, "Gas Chromatography", J.H. Purnell, ed., p.209, Wiley-Interscience, N.Y., 1968.

8) D. Patterson, Y.B. Tewari, H.P. Schreiber and J.E. Guillet, Macromolceules 4, 356 (1971).

9) J.-M. Braun and J.E. Guillet, Adv. Polym. Sci., 21, 107 (1976).

10) P.J. Flory, Proc. Roy. Soc. London, Ser. A, 234, 60 (1956).

11) P.J. Flory, ibid, 73 (1956).

12) P.J. Flory and W.J. Leonard, Jr., J. Am. Chem. Soc., 87, 2101 (1965).

13) P.J. Flory and A. Abe, Macromolecules, 11, 1119 (1978), et. seq.

14) P.J. Flory and G. Ronca, Mol. Cryst. Liq. Cryst., 54, 289 (1979).

15) J.R. Conder in "Progress in Gas Chromatography", J.H. Purnell, ed., Interscience Publishers, N.Y., 1968.

16) J.R. Conder and J.H. Purnell, Trans. Farad, Soc., <u>64</u>, 1505 (1968).

17) J.R. Conder and J.H. Purnell, <u>ibid</u>, <u>64</u>, 3100 (1968).

18) J.R. Conder and J.H. Purnell, <u>ibid</u>, <u>65</u>, 824 (1969).

19) J.R. Conder and J.H. Purnell, <u>ibid</u>, <u>65</u>, 839 (1969).

20) J.R. Conder, Chromatographia, <u>7</u>, 387 (1974).

21) D.G. Gray, Progr. Polym. Sci., <u>5</u>, 1 (1977).

22) J.R. Conder and C.L. Young, "Physicochemical Measurements by Gas Chromatography", John Wiley and Sons, Chichester, 1979.

23) G.M. Dorris, Ph.D. Thesis, McGill University, 1979.

CHAPTER 3

EXPERIMENTAL

A. Polymers and Columns

The HPC sample used for the GC measurements was a Klucel "L" from Hercules with a nominal $\overline{M}_w$ of 100 000 and an average molar substitution (M.S.) of four. Static sorption measurements were done on a sample of HPC of the same nominal $\overline{M}_w$ from Aldrich. Bergmann and Sundelöf (1) have reported a value of $\overline{M}_n$ of 35000 measured by osmometry for their Klucel "L" sample.

The cellulose triacetate sample (CTA) and the cellulose acetate sample (CA, degree of substitution or D.S. = 2.45) were both obtained from Eastman. The cellulose ethers were Dow "ethocel" ethyl cellulose (D.S. = 1.4) and "methocel" methyl cellulose (D.S. = 1.9). Alkoxyl analyses of these cellulose ethers were performed by Schwartzkopf Microanalytical Laboratories, Woodside, N.Y..

The third cellulose acetate (CMA; D.S. = 0.89) was prepared by the method of Malm _et al_ (2), where CTA dissolved in glacial acetic acid was subjected to partial saponification at 40° with sulfuric acid as catalyst. The analysis for acetyl content was the standard method of saponification of a known amount of polymer in excess NaOH followed by back titration with sulfuric acid (3).

The polymers were coated onto a poly (tetrafluoroethylene) support (Fluropak 80) by slow evaporation from solution. The coated supports were packed into 1.8 m, 0.25 in. o.d. polypropylene columns, and the ends of the columns were filled with silanized glass wool. This choice of packing and column material minimized extraneous water-support interactions.

Loadings on the supports were determined by Soxhlet extraction, with the exception of the CMA columns, where a modification of the acetyl group analysis was used. An unknown weight of polymer of known acetyl content coated onto a known weight of support was saponified, and the weight of polymer was determined from the amount of base required. The methyl cellulose column was used only for the determination of the heat of mixing at infinite dilution, since the loading could not be determined reliably. (Methyl cellulose is soluble in water, but insoluble in all common organic solvents, and a Soxhlet extraction with water from PTFE powder was not possible due to the non-wettability and low density of this material).

The data on the polymers and the columns are summarized in Table 3-1.

Table 3-1

Analytical Data for Polymers and GC Columns

Sample	Degree of Substitution (D.S.) of Polymer	Column Number	Column Loading g(%)
Cellulose triacetate	3.0	CTA-1	0.565 (2.44%)
		CTA-2	1.13 (4.70%)
Cellulose acetate	2.45	CA	0.550 (2.41%)
Cellulose monoacetate	0.89	CMA-1	0.378 (1.67%)
		CMA-2	0.171 (0.817%)
		CMA-3	0.0873 (0.415%)
Ethyl cellulose	1.4	-	0.464 (2.35%)
Methyl cellulose	1.9	-	(nominal loading=2%)
Hydroxypropyl cellulose	M.S. = 4	HPC	0.646 (2.39%)

B. Gas Chromatographic Measurements

A Hewlett-Packard model 5722A gas chromatograph equipped with a thermal conductivity detector was used for these measurements. The instrument was modified to give a controlled amount of water vapor in the helium carrier gas stream, as shown in figure 3-1. By the appropriate use of the "wet" and "dry" flow controls and by changing the temperature of the gas saturator, it is possible to vary the relative partial pressure of water over the column from 0 to 100%.

The thermal conductivity detector block was kept at 250°C and the filament current at 200 mA. These values are in the range recommended by the manufacturer for the maximum detector sensitivity consistent with the maximum detector filament lifetime. The injection port was maintained at 150°C, far enough above the boiling point of water to ensure the instantaneous vaporization of injected samples. The injection port was set to higher temperature when required for other solvents (4).

Column temperatures below 35°C were controlled to within ± 0.05° by an external circulating bath, while higher temperatures were controlled to ±0.1° by the built-in air oven. Where necessary, the temperatures were corrected for the emergent stem of the thermometer. Injections were made with a Hamilton microlitre syringe, with retention times at infinite dilution obtained by extrapolation of the peaks of small injections to zero peak height. Typical injection sizes at infinite dilution were from 0.05 to 0.001 μL. The smallest injections were obtained by inserting into the injection port a syringe from which water had

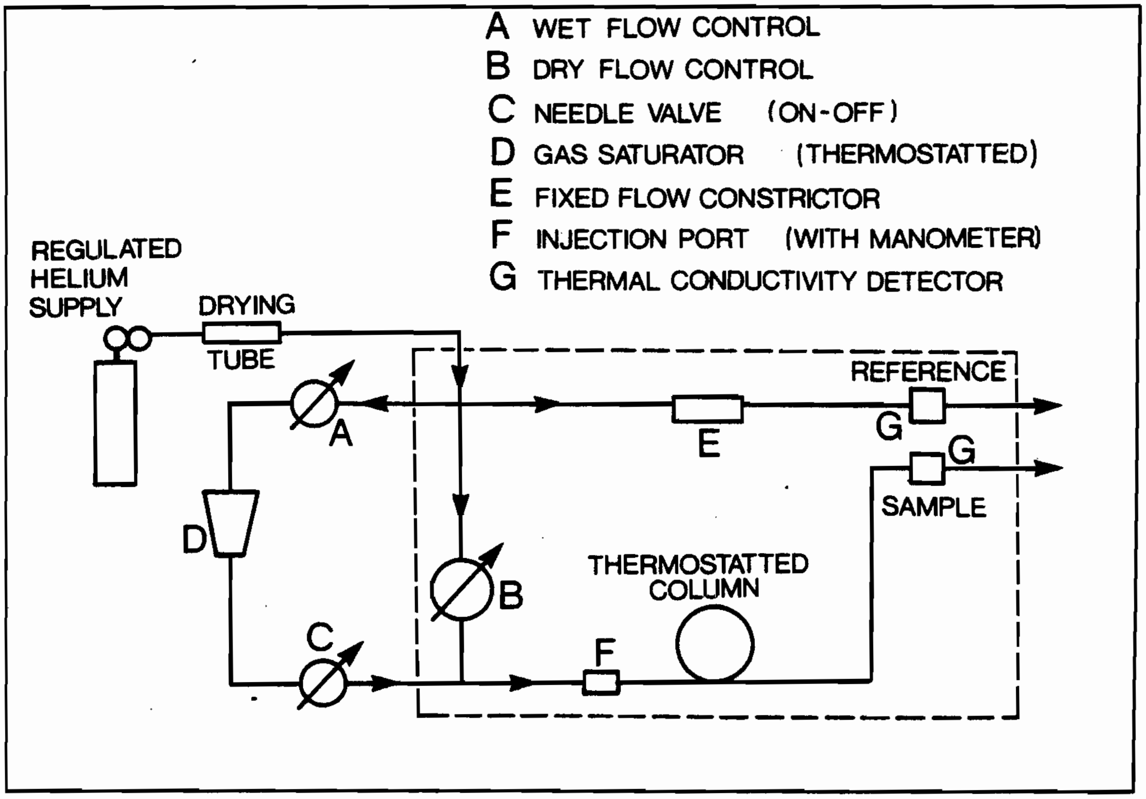

FIGURE 3-1 Gas chromatographic apparatus modified to give constant water vapor pressure in carrier gas.

previously been expelled, and injecting the resulting air-water vapor mixture. Finite concentration measurements were carried out by injecting up to 10 μL of water into the GC. Flow rates of the helium carrier gas were measured with a soap bubble flowmeter and were corrected for column pressure drop and for the water vapor content of the flowmeter (equations 2-3 and 2-4).

A chromatogram suitable for ECP calculations measured on HPC at 25°C is shown in figure 3-2. These peaks are acceptable from the criterion of the superimposability of the diffuse edges described in the previous chapter. Because of the effect of a non-linear sorption isotherm on a peak shape, in finite concentration GC a non-linear response does not necessarily indicate non-ideal behavior.

A calibration line for detector response as peak height vs. gas phase vapor pressure of water was constructed by injecting a large amount of water onto an empty column at various temperatures, and plotting the vapor pressure of probe at these temperatures vs. the height of the eluted plateaus. The height of any point on the experimental chromatogram could thus be converted to a vapor pressure of water, and the values of y calculated directly. ECP isotherms were calculated using equation 2-48 and various "characteristic points" along the chromatographic curve. Air was the non-interacting marker used to determine t_M.

Since the areas α and β (equation 2-48 and figure 2-3) were originally obtained in units of cm^2 of recorder chart paper, they had to be multiplied by a calibration factor C_A:

$$C_A = \frac{y_o}{HM} \qquad (3-1)$$

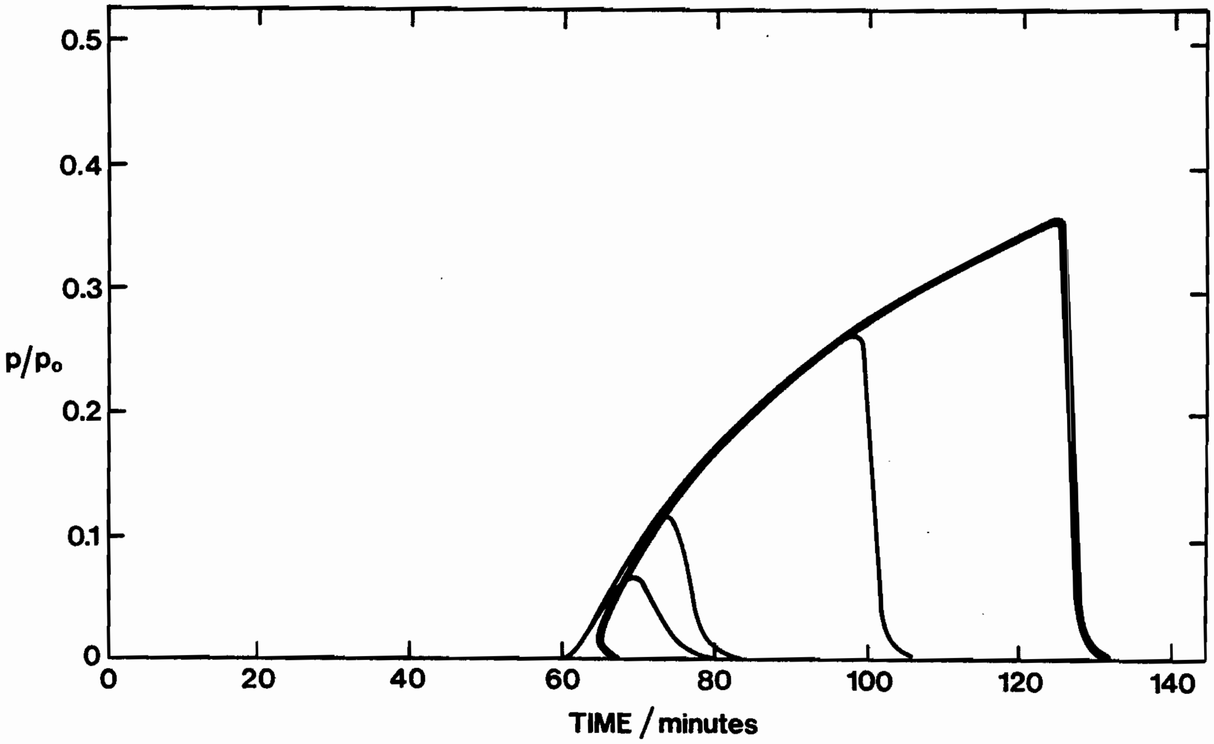

FIGURE 3-2 GC chromatogram suitable for calculations by the ECP technique (HPC at 25°C). The largest injection was 10 μL. The curve at low water content is the locus of peak maxima of small injections of water (not shown).

where H is the recorder pen deflection (cm) at a gas phase mole fraction of probe of y_o and M is the recorder chart speed (cm min^{-1}).

Results from the EP method are illustrated in figure 3-3. Retention times for small additional injections at each plateau were measured and extrapolated to zero peak height on the plateau. The variation in retention time at infinite dilution on top of a plateau with plateau height has the same form as the characteristic chromatogram of figure 3-2, and the sorption isotherm may be calculated in the same way. However, Dorris (5) has pointed out that if water vapor is used for the plateau, the correction to the flow rate due to the vapor pressure of water in the flowmeter changes with plateau height, and becomes:

$$\dot{V}_{corr} = \left(\frac{P_{\upsilon} - p_{o,flo}}{P_o \; (1 - p_{o,sat}/P_i)} \right) \dot{V} \qquad (3\text{-}2)$$

where $p_{o,sat}$ is the vapor pressure of water at the saturator temperature. For this reason, a graphical integration derived by Conder and Purnell (6) was used to calculate the EP isotherms. In this method, the retention volumes at each plateau were corrected for the sorption effect, gas compressibility, and the effect of the changing water content of the carrier gas, to $(V_R - V_M)/(1 - jy_o)$. These were then plotted against the gas phase probe concentration at the plateau, c, where:

$$c = \frac{\bar{p}}{RT} \qquad (3\text{-}3)$$

and $\bar{p}$ is the average probe vapor pressure in the column, given by the

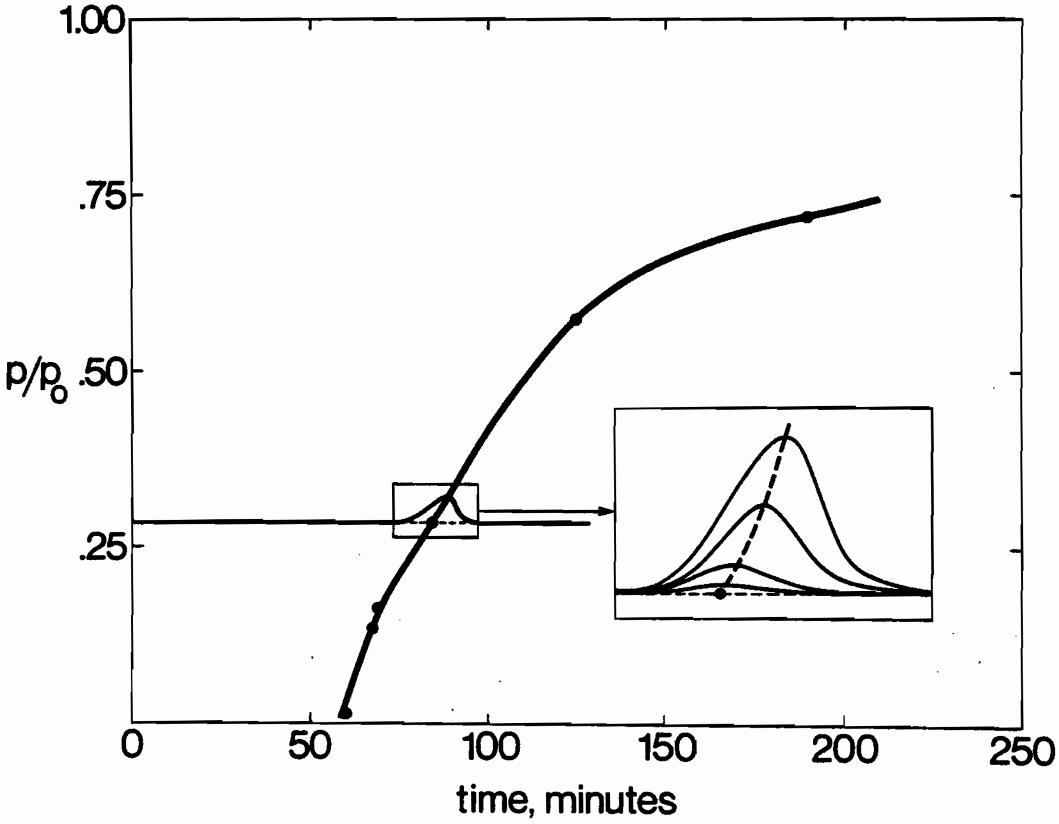

FIGURE 3-3 Typical results for the EP method. The dotted line in the inset extrapolates to the retention time at the plateau water vapor concentration (solid point). The adsorption isotherm can be calcuated from the line through the solid points at different plateau concentrations.

partial pressure of water at the outlet divided by j. The plateau heights were calibrated by passing the wet carrier gas stream from the column through a drying tube for a known period, and measuring the uptake of water.

The EP method has two advantages over the ECP technique. The gas saturator allows a higher partial pressure of water to be achieved than is possible by syringe injection of a large amount of water. Secondly, the retention times represent the perturbation of the equilibrium plateau by a small amount of additional water vapor, reducing problems that may arise from the injection of a large volume of water onto a dry column. The major disadvantage of the EP technique is that at high relative partial pressures of water it is difficult to see small amounts of water injected on top of the plateau. This problem would become even more serious if at the same time a highly curved isotherm were being followed.

C. Other Sorption Methods

Two static methods were also used to determine sorption isotherms. Since both are well established in the literature, only a brief description is necessary.

Microbalance measurements were performed on a Cahn AG electrobalance enclosed within a vacuum system. The sample well was enclosed in a jacket connected to an external constant temperature water circulator, and the temperature was maintained to within ±0.05°. The laboratory in which these experiments were done was kept at a constant temperature, at least 1° higher than the temperature within the sample well, in order to prevent condensation of water vapor on the balance components. Sample weights were from 50 to 75 mg. For each point on the isotherm, a small amount of water vapor was admitted to the system, or withdrawn from the system for desorption isotherms. Changes in sample weight were monitored on a calibrated strip-chart recorder until no further change was seen. The vapor pressure was then measured from a U-tube mercury manometer by means of a precision cathetometer. When necessary, the pressures were corrected for different miniscus heights in the U-tube.

In the second method, nickel-chromium wires were fixed to the lids of 120 mL wide mouthed sample bottles with epoxy cement. Glass weighing bottles containing dried HPC (0.3 to 0.6 g) were suspended from these wires over aqueous solutions of sulfuric acid, and the sealed bottles were submerged in constant temperature baths. Glass "marbles" were used as weights inside the sample bottles. The uptake of water by these samples was followed gravimetrically until equilibrium was reached. The concentration of sulfuric acid was determined by titration, and the corresponding partial pressures of water vapor were obtained from the literature (7).

Because of the requirements of the constant temperature laboratory, the vacuum microbalance could only be used for measurements at temperatures of 30° or less. Reproducible results were obtained only at relative partial pressures of water less than 90%. The acid method, while slower, gave sorption isotherms at high water content in the 15 - 30° range, and complete isotherms in the range 35 - 55°.

The four sorption methods are summarized in Table 3-2. The differences between them are in the amount of water that can be sorbed, and the length of time required to measure each isotherm. As the results will show, the four methods are equivalent within the appropriate concentration regions.

Table 3-2

Comparison of methods used to measure sorption of water onto HPC

method	volume fraction range of water	relative partial pressure range of water	approximate time required
Elution by a characteristic point (ECP)	0-0.03	0-0.4	1 day per isotherm
Elution on a plateau (EP)	0-0.06	0-0.6	1 day per point on an isotherm
Static sorption (on microbalance)	0-0.30	0-0.90	1 to 2 days per point on an isotherm
Static sorption (over aqueous H_2SO_4 solution)	0-0.50	0-0.99	1 to 2 months per isotherm

D. Errors and Calculations

In this section, the sources of error in each experimental technique are explained, and contributions to the total experimental error are considered. This will be followed by a brief discussion of the calculations.

There were two possible sources of error in the sorption measurements on the vacuum microbalance. The cathetometer readings were reproducible to within ± 0.05 mm, which corresponds to an error in the activity of water of up to ± 0.003. The sample weights were precise to within ± 0.02 mg, corresponding to an error in the volume fraction of water sorbed of less than 0.001, a negligible amount.

In the measurements of sorption by samples suspended over aqueous sulfuric acid, equilibrium was considered to have been reached when weights remained constant to within ± 0.5 mg over several days, again resulting in a negligible error in ϕ_1. The calculated activities of water vapor were precise to about ± 0.003, given the scatter in the titrimetric determination of the H_2SO_4 concentration, and assuming that the vapor pressures of water vapor over aqueous sulfuric acid presented in the literature are precise to ± 1 in the last significant figure.

The GC measurements are open to a greater variety of errors. Each of these will be considered separately.

In infinite dilution GC, the greatest source of error is in the extrapolation of the retention times to zero peak height. The estimated precision is about ± 2 - 3%, although the error can be as high as ± 5%

at slow flow rates or very long retention times due to the instability of the detector baseline. Errors in measuring both atmospheric pressure and column back pressure were negligible. The reproducibility in the gas flow rates measured with the soap bubble flow meter was about ± 0.2 - 0.4%. No error was detected in the speeds of the strip-chart recorder. The reproducibility in polymer loading determinations was within ± 1%. Errors in loading would affect absolute properties such as sorption isotherms, χ parameters, or comparisons between columns of different loadings, but would not have any effect on the reported heats of mixing.

The greatest source of error in the finite concentration GC measurements was in the calibration of the GC detector response of peak height vs. vapor pressure of water. The calibration is limited by the lowest temperature at which a constant vapor pressure plateau could be measured, since the vapor pressures of water below this temperature had to be obtained by extrapolation. At high temperatures and pressures, the uncertainty in a_1 is about ± 0.002. The uncertainty in a_1 rises to ± 0.02 at low temperatures and pressures, affecting volume fractions of water up to $\phi_1 \simeq 0.015$. This larger uncertainty is the cause of the very large error bars in this concentration region for the heats of mixing of water with HPC in Chapter 5.

Linear regression analyses were calculated using the Fortran subroutine LINFIT (8). Given a set of experimental data, x, y, and standard deviation of each value y, this subroutine determines the slope and the intercept of the best straight line by a least squares approach, along with the standard deviations. When a multiterm fitting was required, it was generally calculated by means of a polynomial least squares fitting program available as part of the statistical package of the McGill University System for Interactive Computing ("MUSIC STATPAK"). Several polynomial fittings in chapter 5 were calculated using the Fortran subroutine POLFIT (8).

E. References

1) R. Bergmann and L.O. Sundelöf, Eur. Polym. J., 13, 881 (1977).

2) C.J. Malm, K.T. Barkey, M. Salo and D.C. May, Ind. Eng. Chem., 49, 79 (1957).

3) American Standard Test Method, ASTM D871-72, American National Standards Institute, 1973.

4) This Thesis, Appendix A.

5) G.M. Dorris, Ph.D. Thesis, McGill University, 1979.

6) J.R. Conder and J.H. Purnell, Trans. Farad. Soc., 65, 824 (1969).

7) "International Critical Tables", Vol. III, 1st ed., McGraw-Hill, New York, 1928, p.303.

8) P.R. Bevington, "Data Reduction and Error Analysis for the Physical Sciences", McGraw-Hill Book Co., New York, 1969.

CHAPTER 4*

MIXING OF WATER WITH HYDROXYPROPYL CELLULOSE. I. SORPTION ISOTHERM AT 25°C AND INFINITE DILUTION RESULTS

---

*This chapter was published in a somewhat different form as a paper by J.S. Aspler and D.G. Gray in Macromolecules 12, 562 (1979)

A. Introduction

Hydroxypropyl cellulose (HPC) is a cellulose ether, soluble in water and in most polar organic solvents. It is prepared by the reaction of cellulose (cotton linters) with propylene oxide (1). Figure 4-1 shows a schematic of an HPC molecule with an average molar substitution (M.S.) of 4. The diagram shows the possible existence of unsubstituted hydroxyl groups on the cellulose, as well as the possibility of one hydroxypropyl group substituted on top of another. The interesting properties that HPC has shown are derived from the combination of these flexible side chains with the stiff cellulosic backbone.

HPC has been shown to form a liquid crystalline mesophase with cholesteric structure in water, as well as in several organic solvents (2,3). Dilute aqueous solutions also show a sharp lower critical solution temperature (LCST) at about 42^o. Above this temperature, the solutions precipitate, coalescing into a white gel at yet higher temperatures. The LCST gives a useful reference point in the measurement of the thermodynamic properties of the system. This system is more tractable that most mesogenic polymer-solvent systems, not the least because of the benign nature of the components and the general desireability of water as solvent.

In this chapter the sorption of water by HPC using infinite dilution and finite concentration GC is studied. Few finite concentration GC measurements have been made previously, so static sorption measurements at 25^o are also presented.

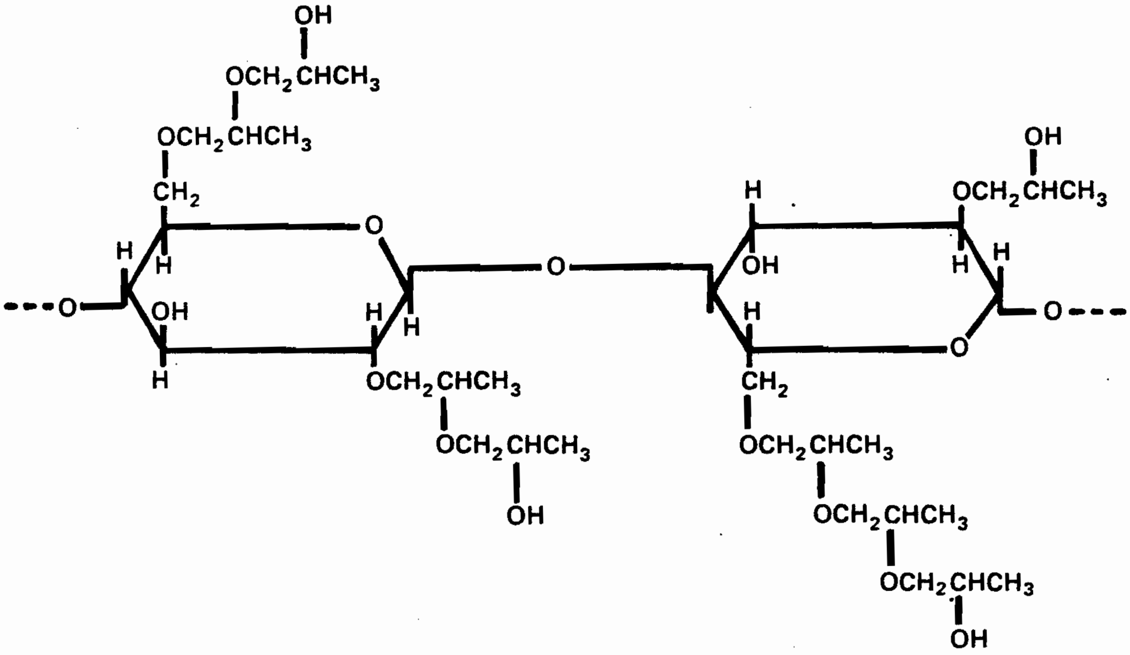

FIGURE 4-1 Idealized structure of hydroxypropyl cellulose with an average of four hydroxypropyl groups per anhydroglucose unit.

B. Results and Discussion

1. Infinite Dilution Region

The results for the interaction of water with HPC at infinite dilution are given in Table 4-1. The activity coefficients were calculated from the infinite dilution specific retention volumes measured at a flow rate of 40 mL min^{-1}, as introduced in chapter 3, section B-3. These are shown as raw values and as smoothed values calculated from specific retention volumes fitted to a second order polynomial equation. The effect of the second virial coefficient B_{11} was negligible. Preliminary measurements on columns of loadings from 1% to 10% showed that the effect of loading is small.

The value of the heat of mixing* at infinite dilution was determined to be -5.7 ± 0.6 kJ mol^{-1} from a least squares fit of the data in Table 4-1 to equation 2-34. The more precise equation 2-38 could not be used due to the scatter in the experimental points which in turn results from the curvature of the sorption isotherm at infinite dilution. Use of that equation could lead to false assumptions as to the temperature dependence of $\Delta\overline{H}_m^{\infty}$.

Values for χ at infinite dilution of water in HPC are in principle readily derived from the GC data in Table 4-1. Thus, if the entropy of mixing is given by the Flory-Huggins theory, χ_{FH} at any temperature is obtained according to equation 2-28 by simply subtracting 1 from the tabulated values of ln (a_1/ϕ_1). The χ_{FH}^{∞} values would then range from 1.38 at 15°C to 1.84 at 84.5°C, with a value of 1.51 at 40°C. However,

---

*In this discussion, heats of mixing should properly be referred to as partial molar heats of mixing of water at infinite dilution in the polymer.

Table 4-1

Activity Coefficients and Specific Retention Volumes of Water at Infinite Dilution in HPC

$\frac{T}{^\circ C}$	$\ln V_g$ ± 0.03	$\ln (a_1/\phi_1)^\infty$ ± 0.03[a]	$\ln (a_1/\phi_1)^\infty$ ± 0.03[b]
15.0	8.67	2.34	2.38
19.7	8.30	2.41	2.40
25.0	7.91	2.47	2.43
29.3	7.66	2.47	2.45
34.2	7.34	2.51	2.47
40.3	7.05	2.47	2.51
45.1	6.74	2.52	2.54
49.9	6.41	2.61	2.57
54.8	6.25	2.53	2.60
59.6	5.92	2.63	2.64
64.9	5.62	2.68	2.68
69.0	5.37	2.75	2.72
74.7	5.11	2.76	2.76
79.5	4.84	2.83	2.80
84.5	4.65	2.82	2.84

a) Calculated from V_g and equation 2-34.

b) Calculated from smoothed values of V_g and equation 2-34.

the assumption of random mixing seems unreasonable for this polymer. Hydroxypropyl cellulose film exhibits some crystallinity (4). If, as previously indicated for water at infinite dilution in poly(ethylene oxide) (5), the water only mixes with the amorphous fraction, then the retention volume in equation 2-31 should be replaced by V_g (1-C) where C is the fractional crystallinity of the stationary phase. The crystallinity may be evaluated if GC data are available above and below the melting point (5,6), but HPC has too high a melting point for this method to be useful. However, a value of 14.9% for the crystallinity of water-cast HPC film has been deduced from calorimetry, X-ray and density measurements (4). This value corresponds to a change in χ^{∞}_{FH} of ln (1 - 0.149) = - 0.16. Thus, assuming that the crystallinity remains constant from 15°C to 85°C, the values of χ^{∞}_{FH} corrected for crystallinity are given by:

$$\chi^{\infty}_{FH} = \ln (a_1/\phi_1) - 1.16 \qquad (4\text{-}1)$$

On the other hand, more precise retention measurements (7) showed a small, but definite trend to a lower retention volume at lower flow rates. This might introduce an error of up to 0.1 which should be added to $\ln (a_1/\phi_1)^{\infty}$.

The values for χ^{∞}_{FH} are very high, considering that hydroxypropyl cellulose is readily dissolved in water below 42°C. If, however, the random mixing implied in the Flory-Huggins theory becomes impossible at high polymer concentrations because of chain stiffness (8,9), an alternative model for the mixing entropy term is required. Flory's model for rod-like mixing gives equations 2-42 and 2-43 at infinite dilution; the corresponding values for χ are obtained by subtracting 2 from the ln $(a_1/\phi_1)^\infty$ data in Table 4-1. Thus at 40°C, $\chi_R^\infty \approx 0.51$, a not unreasonable value when it is remembered that dilute aqueous HPC solutions show a lower critical solution temperature at 42°C. This suggests that the polymer solvent interaction parameter might remain relatively constant with concentration but that the combinatorial entropy of mixing might change from "Flory-Huggins" to "Flory rod-like" across the concentration range.

The excellent agreement of the value of ln $(a_1/\phi_1)^\infty$ at 40° with theory may be somewhat fortuitous, considering the scatter in the points, and the corrections due to gas flow rate and polymer crystallinity that are of equal size but occur in opposite directions. Also to be considered is the fact that the phase separation at high polymer concentration is not the sharp occurence at 42° in dilute solution. Rather, it occurs over a broad temperature range starting somewhat below 40° (3). Still, bearing in mind the relative insensitivity of ln $(a_1/\phi_1)^\infty$ to temperature, it is possible that the value of ln $(a_1/\phi_1)^\infty \approx 2.5$ at 40° represents the start of the broad phase separation in the ordered polymer.

2. Finite concentration region

The obvious way to test this suggestion is to examine the solvent activity as a function of concentration. Recently, Bergman and Sundelöf published comprehensive osmotic pressure data for aqueous solutions of Klucel L (10). These authors discussed their data in terms of a virial expansion, but the Flory-Huggins theory should also be applicable for the relatively high concentrations examined. The interaction parameter χ may be calculated from the osmotic pressure data according to (11):

$$\chi = - \frac{[\pi\overline{V}_1/RT + \ln \phi_1 + \phi_2 (1 - 1/\overline{x}_n)]}{\phi_2^2} \qquad (4\text{-}2)$$

where χ (without subscripts) is the Flory-Huggins interaction parameter derived from osmotic pressure measurements, π is the osmotic pressure, $\overline{V}_1$ is the molar volume of water and $\overline{x}_n$ is the number average molar volume ratio for water and polymer. Taking $\overline{M}_n$ = 35 000, and 1.23 g cc^{-1} as the density of HPC, $\overline{x}_n \simeq 1600$. Volume fractions were calculated from component densities, assuming no volume change on mixing. A marked concentration dependence in the calculated values of χ was evident, with χ varying linearly with ϕ_2 over the experimental concentration range. The data were therefore fitted to the empirical equation (12):

$$\chi = \chi_1 + \chi_2\phi_2 \qquad (4\text{-}3)$$

where χ_2 is the slope and χ_1 is the intercept at $\phi_2 = 0$ of a plot of χ versus ϕ_2. Values for χ_1 and χ_2 are presented in Table 4-2. The values for χ_1 reach the expected value of 0.50 as the temperature approaches the observed cloud point of 42°C. Furthermore χ_2 is 0.33 at this point. Flory and Daoust (12) indicate that a value of $\chi_2 \leq 1/3$ is a necessary condition for a critical point at $\phi_2 = 0$, whereas a finite critical concentration requires $\chi_2 > 1/3$. Measurements (3) on a similar sample of HPC give a virtually constant cloud point temperature for aqueous solutions from 40% polymer down to a few ppm, in accord with values of χ_2 close to 1/3.

Table 4-2

Values for χ_1 and χ_2, calculated* from the osmotic pressure data of Bergmann and Sundelöf (10)

Temperature	χ_1	χ_2
25°C	0.482	0.371
30°C	0.486	0.372
35°C	0.492	0.357
40°C	0.500	0.333

---

*Calculated from equations 4-2 and 4-3. Values are linear least squares fit.

The value of χ at $\phi_2 = 1$ may be estimated from an extrapolation of these data. From equation 4-2, $\chi = 0.83$ at $40^{o}C$. The value from infinite dilution GC, assuming Flory-Huggins mixing and correcting for both crystallinity and flow rate is about 1.45. On the other hand the value of χ_R^{∞} at $40^{o}C$, assuming rod-like mixing at $\phi_2 = 1$, is nearly the same as that for χ from osmometry at $\phi_2 = 0$. This agreement may be fortuitous, because the values for χ, calculated from osmotic pressure data according to equation 4-2, are rather sensitive to the value for $\bar{x}_n$. However, it seems noteworthy that with appropriate models for mixing, the same polymer-solvent interaction parameter is obtained at the extremes of the concentration range.

The results of static and GC measurements of water vapor activity at $25^{o}C$ across the intermediate concentration range are shown in figure 4-2 along with values for water activity calculated from the osmotic pressure measurements. Sorption isotherms of water at low concentrations measured by the two GC techniques at 25^{o} are shown in figure 4-3. There was no sign of hysteresis in sorption/desorption cycles on the vacuum microbalance for this polymer. The agreement between the four sorption methods is good, with deviation only at the highest water contents, where the measurement of small changes in vapor pressure with large changes in water content becomes more difficult. The solid curves in figures 4-2 and 4-3 were calculated from equation 4-3 with the values for χ at $25^{o}C$ shown in Table 4-2. The broken curve was calculated from equation 2-41, with a value of 0.43 for χ_R from Table 4-1. At the high

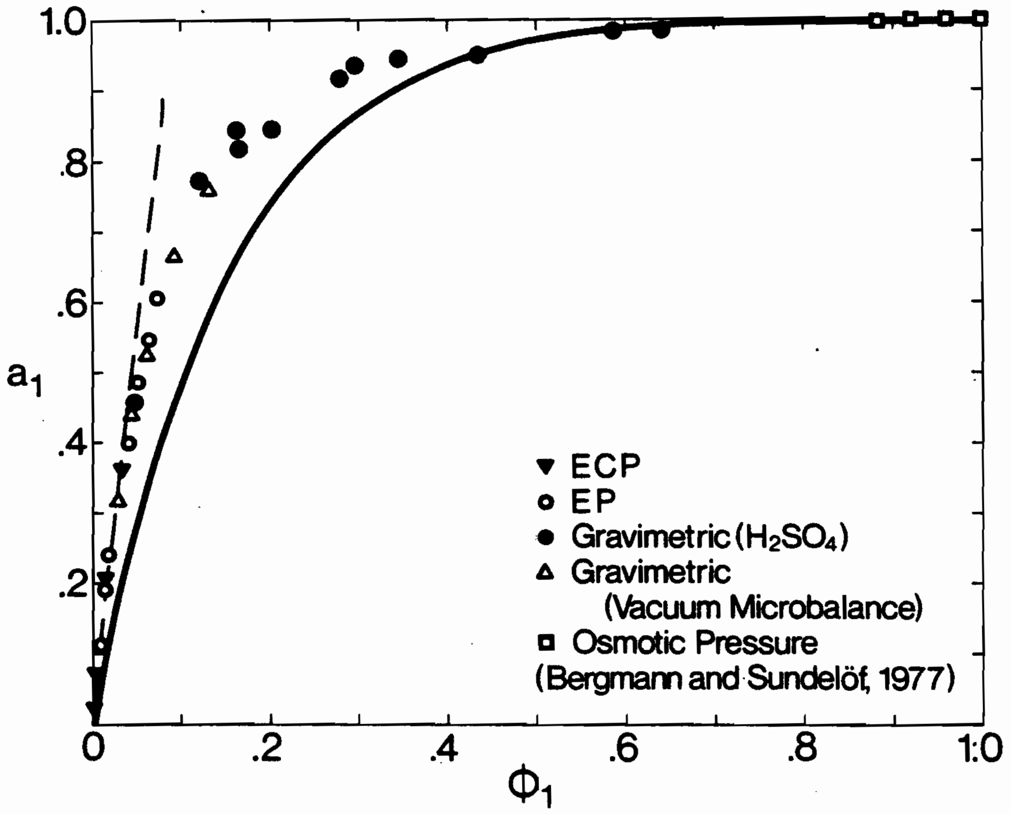

FIGURE 4-2 Sorption isotherm for water on HPC at 25°C. Experimental points were measured by the techniques indicated on the figure. Solid and broken lines are calculated for normal and rod-like mixing respectively (see text).

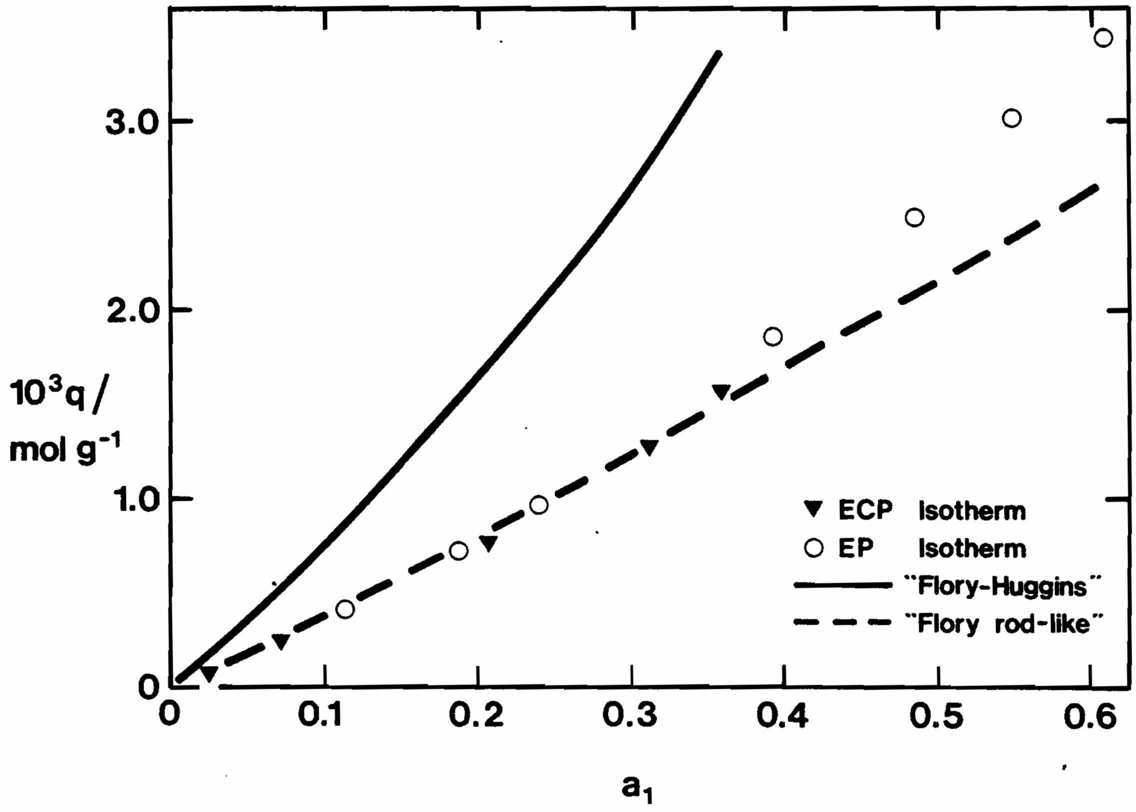

FIGURE 4-3 Low concentration GC sorption isotherm for water on HPC at 25°C. Experimental points and calculated lines as indicated on the figure and in the text.

water side, the results thus are in accord with Flory-Huggins mixing, while at high polymer concentrations the system follows the rigid-rod theory. Optical observations (3) indicate that the anisotropic mesophase is found at water concentrations less than $\phi_1 = 0.62$. This is a lower concentration of water than that predicted by Flory's theory (13) for rod-like molecules, and is most readily rationalized by noting that HPC, like most cellulosics, is moderately flexible in dilute solution (14,15). The experimental points for water vapor pressure over the mesophase deviate from the line for rod-like molecules when ϕ_1 is greater than ~ 0.05. This again may be due to molecular flexibility. Values for the activity as a function of concentration are given in Table 4-3, along with values of y calculated from equation 2-40 with $\chi_R = 0.48$ and $x \gg y$. The value of y indicates the disorder in the mesophase, although its significance is questionable if the molecules are not rigid. There is no evidence of a discontinuity or plateau in the variation of water activity with volume fraction. For monodisperse rods, the activity should remain constant over the concentration range where the isotropic phase and mesophase coexist. This must occur around $\phi_1 \simeq 0.6$, but the water activity is too close to that of pure water for the detection of a plateau by direct sorption measurements.

The value of the volume fraction activity coefficient, a_1/ϕ_1, increases with decreasing water content, except at the lowest water contents, where a slight decrease occurs. Although this effect is too slight to be apparent on the adsorption isotherm (figure 4-3), the raw ECP data (figure 3-2) show clearly that the retention volumes increase

Table 4-3

Experimental activities and order parameters for an aqueous hydroxypropyl cellulose mesophase at 25°C

a_1	a_1/ϕ_1	y[a]
0.0	11.3[b]	1.0
0.03	15.	0.9
0.07	13.	1.0
0.11	12.	1.0
0.206	12.	1.0
0.239	11.	1.0
0.313	11.	1.0
0.317	12.	1.0
0.356	11.	1.0
0.392	9.9	1.1
0.455	11.	1.0
0.486	9.2	1.1
0.527	8.7	1.1
0.548	8.8	1.1
0.606	8.3	1.2
0.668	7.2	1.3
0.772	6.3	1.4
0.835	5.1	1.6
0.926	3.26	2.1
0.948	2.75	2.5
0.960	2.23	3.1
0.987	1.61	5.0

[a] Order parameter given by equation 2-40. See text.
[b] Limiting value at infinite dilution.

with decreasing water content at very low relative humidities, and the effect is also evident when the data is plotted as χ_{FH} vs. ϕ_1 (figure 4-4). Possible explanations include an initial hydration of the polymer, or disruption of crystalline regions. Figure 4-4 also shows the change-over from "rod-like" behavior at high polymer concentration to "Flory-Huggins" behavior at low polymer concentrations. This change-over occurs in the same concentration region in which optical measurements have shown the development of mesophase structure (3).

Viscometric studies of HPC solutions have shown that the value of the Mark-Houwink parameter, a, ($[\eta] = kM^a$) is close to one (3). This is far from the theoretical value of 1.8 expected for a rod-like molecule in dilute solution, but is similar to values reported for other cellulosics and is suggested to represent an expanded, but freely draining coil. This lead to the conclusion (3) that mesophase formation at about 40% polymer - a much higher concentration than predicted - is due to the existence of a series of short, connected rod-like structures rather than a single rigid rod.

In their examination of the activity of organic solvents over liquid crystalline solutions of poly-γ-benzyl glutamate, Flory and Leonard (16) found that the Henry's law slope a_1/ϕ_1, at $\phi_1 = 0$, was much less than expected. They obtained a better fit to their experimental data by introducing a new volume fraction term for the mixing of solvent with only the side chains of the helical polymer molecules. In our case, no such assumption was needed to fit the rigid rod-theory with a plausible value of χ.

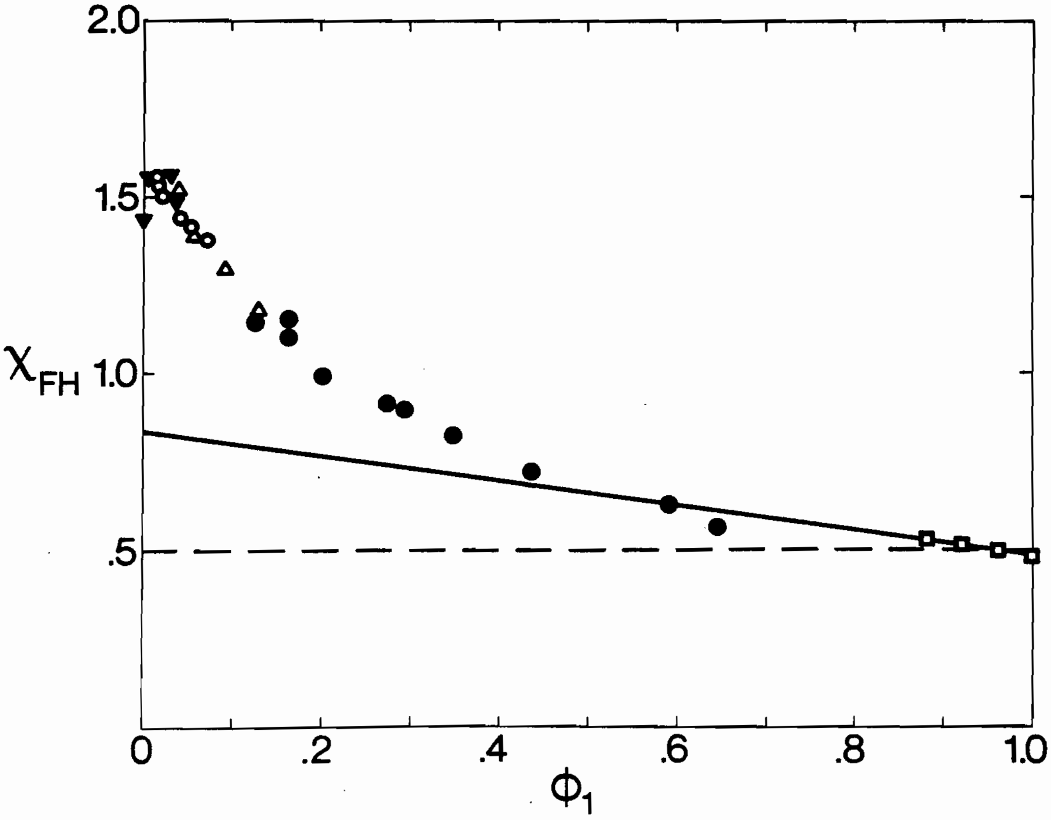

FIGURE 4-4 Values for χ_{FH} calculated according to equation 2-22. Symbols as in figure 4-2. The solid line for χ was calculated from equation 4-3 with $\chi_1 = 0.482$ and $\chi_2 = 0.371$.

C. References

1) E.D. Klug, J. Polym. Sci., Part C, 36, 491 (1971).

2) R.S. Werbowyj and D.G. Gray, Mol. Cryst. Liq. Cryst., 34, 97 (1976).

3) R.S. Werbowyj and D.G. Gray, Macromolecules, 13, 69 (1980).

4) R.J. Samuels, J. Polym. Sci., A2, 7, 1197 (1969).

5) G.J. Courval and D.G. Gray, Macromolecules, 8, 326 (1975).

6) J.E. Guillet and A.N. Stein, Macromolecules, 3, 103 (1970).

7) This Thesis, Chapter 6.

8) P.J. Flory, Proc. Roy. Soc. London, 234A, 60 (1956).

9) P.J. Flory, Ber. Bunsenges. Phys. Chem., 81, 891 (1977).

10) R. Bergmann and L.O. Sundelöf, Eur. Polym. J., 13, 881 (1977).

11) P.J. Flory, "Principles of Polymer Science", Cornell University Press, Ithaca, 1953.

12) P.J. Flory and H. Daoust, J. Polym. Sci., 25, 429 (1957).

13) P.J. Flory, Proc. Roy. Soc. London, 234A, 73 (1956).

14) M.G. Wirick and M.H. Waldman, J. Appl. Polym. Sci., 14, 579 (1970).

15) L.O. Sundelöf and B. Nystrom, J. Polym. Sci., Polym. Lett. Ed., 15, 377 (1977).

16) P.J. Flory and W.J. Leonard, Jr., J. Am. Chem. Soc., 87, 2101 (1965).

CHAPTER 5

MIXING OF WATER WITH HYDROXYPROPYL CELLULOSE. II. EFFECT OF TEMPERATURE ON SORPTION BY A POLYMERIC MESOPHASE

A. Introduction

In the previous chapter, the activity of water vapor over concentrated aqueous solutions of hydroxypropyl cellulose (HPC) was measured by inverse gas chromatographic and static methods at 25°C. Inverse GC was also used to measure the activity coefficients of water at infinite dilution on the polymer from 15 to 85°C. It was found that sorption data at high water content and the osmotic pressure data from the literature in dilute aqueous solution was best fitted to the familiar Flory-Huggins equation, while results at very high polymer concentration were best fitted to Flory's equation defining a system of very stiff or rod-like molecules.

Although an increasing number of papers is being published on lyotropic, polymeric liquid crystals, there have been very few studies on the thermodynamics of mixing. The HPC-water system is attractive because of the benign nature of the components, the reasonable vapor pressure of the solvent, and the readily accessible lower critical solution temperature. The sorption measurements of the previous chapter were therefore repeated in the same concentration range of 0 to 50% water by volume, over a temperature range of 15° to 55°, which spans the LCST of the system. Various thermodynamic parameters have been calculated in an attempt to elucidate the mesophase structure and the mechanism of sorption in this concentration range.

B. Results

The appearance of the HPC samples, observed during static measurements, was similar to that reported previously (1), progressing from the original white powder to a clear film to a gel, with the cholesteric colors developing as water content increased. Results from various sorption methods agree within experimental error up to the useful limits of each method. The experimental error was greatest at the lowest GC concentrations ($\phi_1 = 0.005$ to 0.015) due to the error inherent in the calibration of the GC detector at low partial pressures of water, and in the range $0.03 \lesssim \phi_1 \lesssim 0.07$, above the limits of the GC measurements, but at the lowest limits of the static methods.

Typical GC sorption isotherms measured by the ECP technique are shown in figure 5-1, while figure 5-2 shows isotherms measured over the entire concentration range. No hysteresis was seen in the sorption/desorption curves measured on the vacuum microbalance.

In order to determine the heats of mixing, the activities of water, $a_1 = p_1/p_1^o$, were first obtained at regular intervals by interpolation of the isotherms from a volume fraction of 0.005 to 0.030 in steps of 0.005, and above 0.030 in steps of 0.01. The average values of the activities were computed using polynomial regression over small portions of the isotherms encompassing five experimental points. While this did not provide any great advantage over the hand-fitted curve, it did help to determine the precision of the interpolation. A complete tabulation of both the experimental data and the interpolated points is given in Appendix B of this thesis.

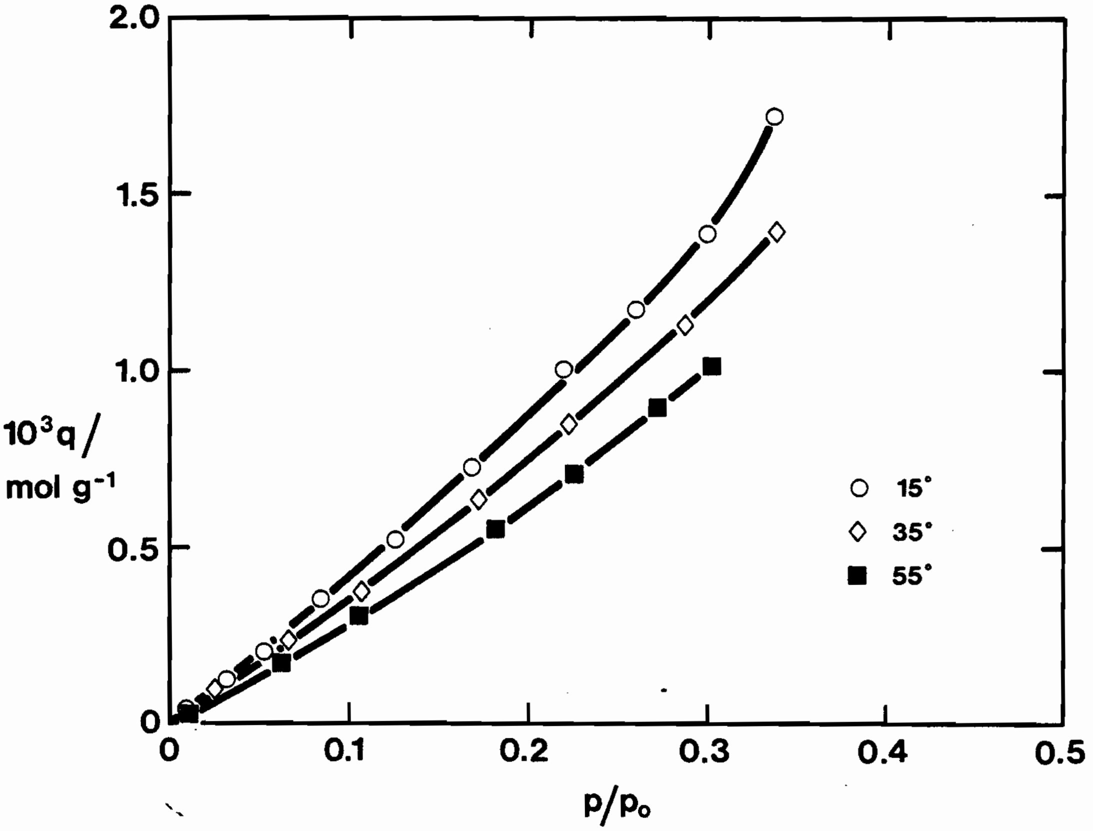

FIGURE 5-1 Sorption isotherm at 15°, 35°, and 55° for low concentrations of water on HPC. The amount of water adsorbed, in mol g^{-1}, is plotted as a function of the relative partial pressure using data from GC (ECP) measurements.

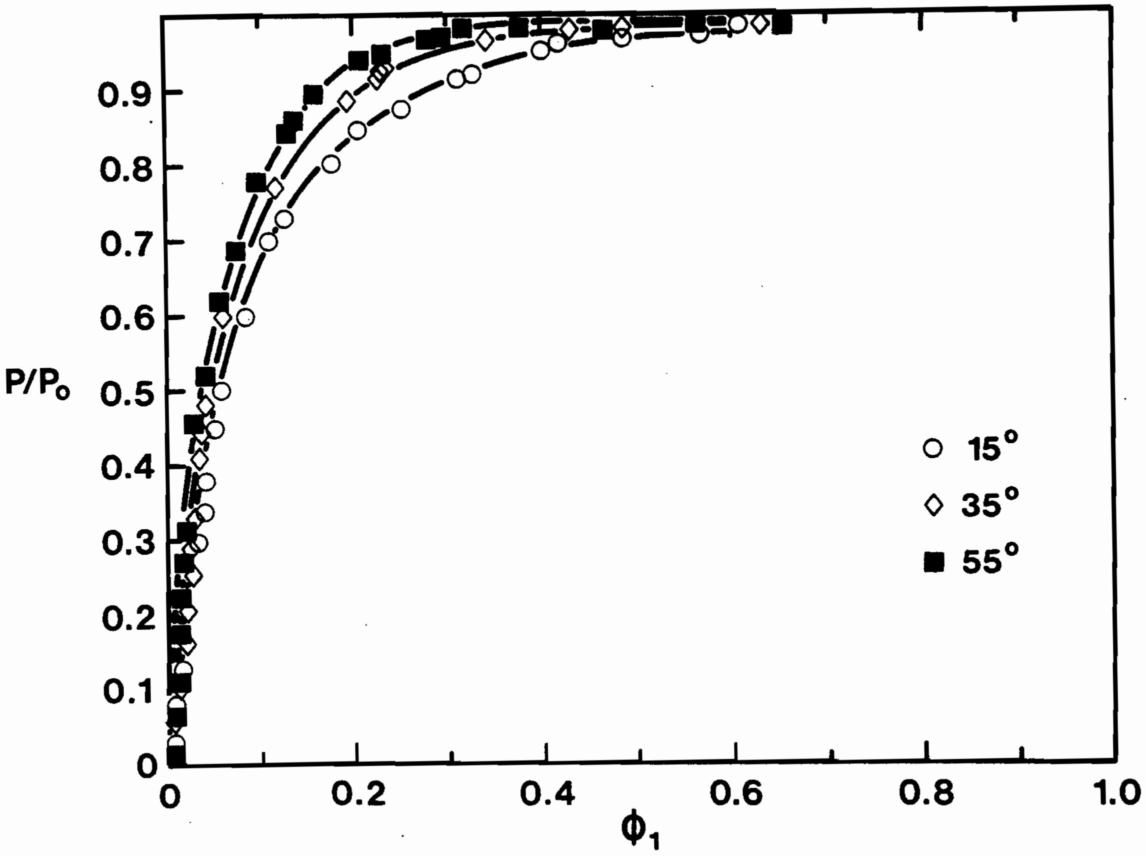

FIGURE 5-2 Sorption isotherms at 15°, 35°, and 55° for water on HPC. The activity is plotted as a function of the volume fraction of water using data from both GC and static measurements.

The partial molar heat of solution, $\Delta\overline{H}_m$,* was calculated from the activities according to:

$$\Delta\overline{H}_m = R\left(\frac{\partial \ln a_1}{\partial (1/T)}\right)_{\phi_1} \qquad (5\text{-}1)$$

The corresponding free energy of mixing with respect to a standard state of liquid water is:

$$\Delta\overline{G}_m = RT \ln a_1 \qquad (5\text{-}2)$$

and the corresponding entropy of mixing:

$$\Delta\overline{S}_m = \frac{\Delta\overline{H}_m - \Delta\overline{G}_m}{T} \qquad (5\text{-}3)$$

Figures 5-3 and 5-4 show the natural logarithm of the activities as a function of inverse absolute temperature at low water content (ϕ_1 = 0.01 to 0.10) and high water content (ϕ_1 = 0.10 to 0.40), respectively. At volume fractions of water of less than 0.2, the relationship between ln a_1 and (1/T) is linear within experimental error, indicating constant heats of mixing over the temperature range. However, at temperatures above 40°C and water contents $\phi_1 \gtrsim 0.20$, there is an inflection clearly visible in the curves of figure 5-4, with the slope and hence $\Delta\overline{H}$ above the LCST approaching zero as the water content increases. The point of the inflection is drawn with prior knowledge of the dilute solution LCST of 42°C. With this in mind, if the portions of these curves above and below the inflection point are taken as linear, then two heats of mixing may be inferred; one ($\Delta\overline{H}_1$) below the LCST and one ($\Delta\overline{H}_2$) above the LCST.

---

* It is to be understood in the following discussion that all heats of mixing are partial molar quantities, per mole of water.

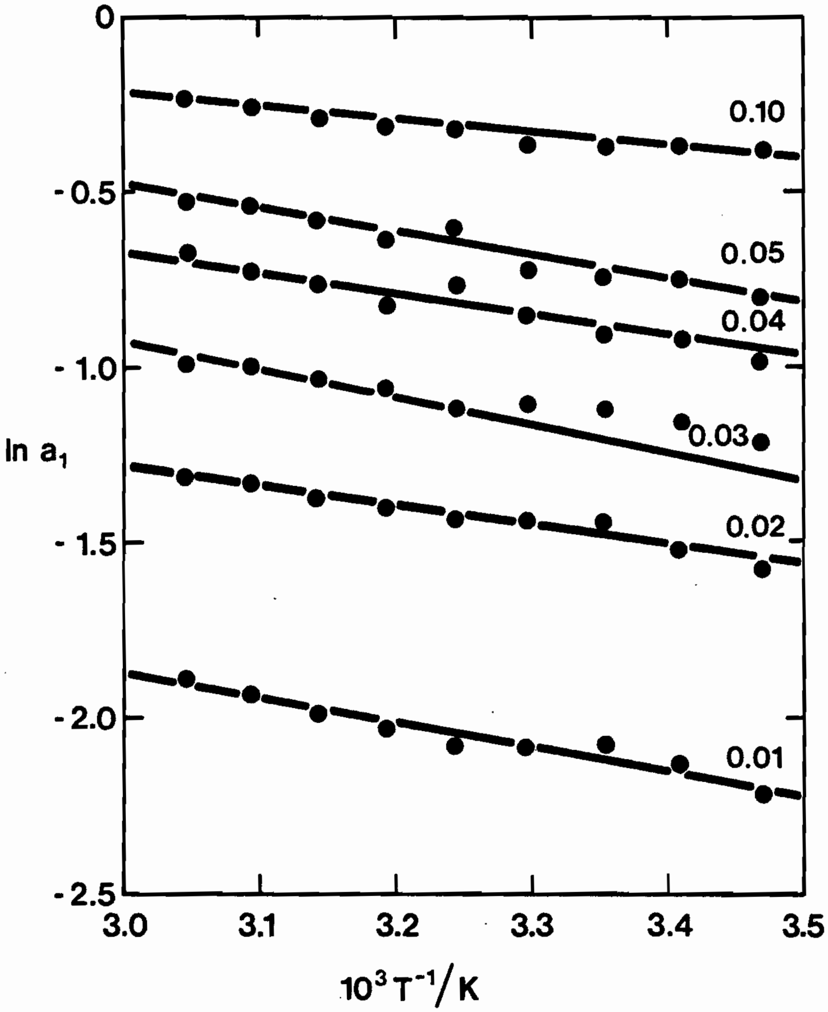

FIGURE 5-3 The natural logarithm of the activity of water vapor plotted as a function of inverse absolute temperature for volume fractions of water from 0.01 to 0.10, as indicated.

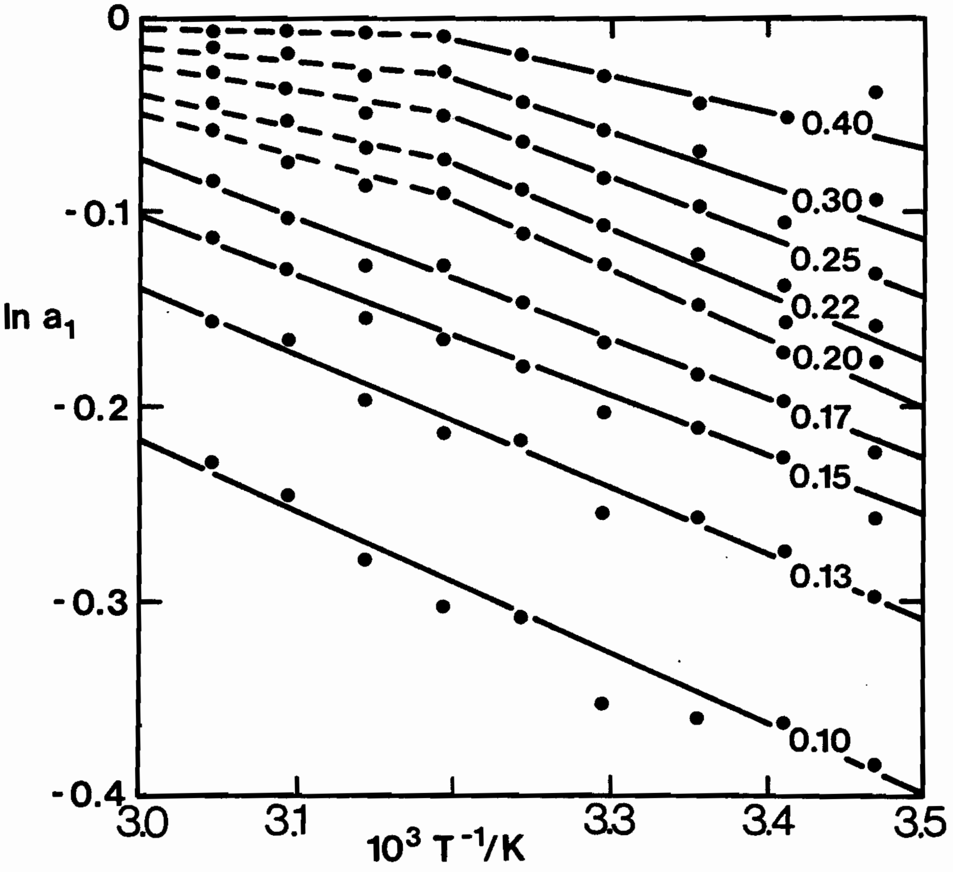

FIGURE 5-4 The natural logarithm of the activity of water vapor plotted as a function of inverse absolute temperature for volume fractions of water from 0.10 to 0.40, as indicated.

Figure 5-5 shows the heats of mixing from 0 to 50% water by volume. Typical precisions estimated from the least squares analysis of the data are given. Tabulated values of $\Delta\overline{H}$ (15 - 55°C), $\Delta\overline{H}_1$ (25 - 40°C) and $\Delta\overline{H}_2$ (45 - 55°C) are also given in Appendix B of this thesis.

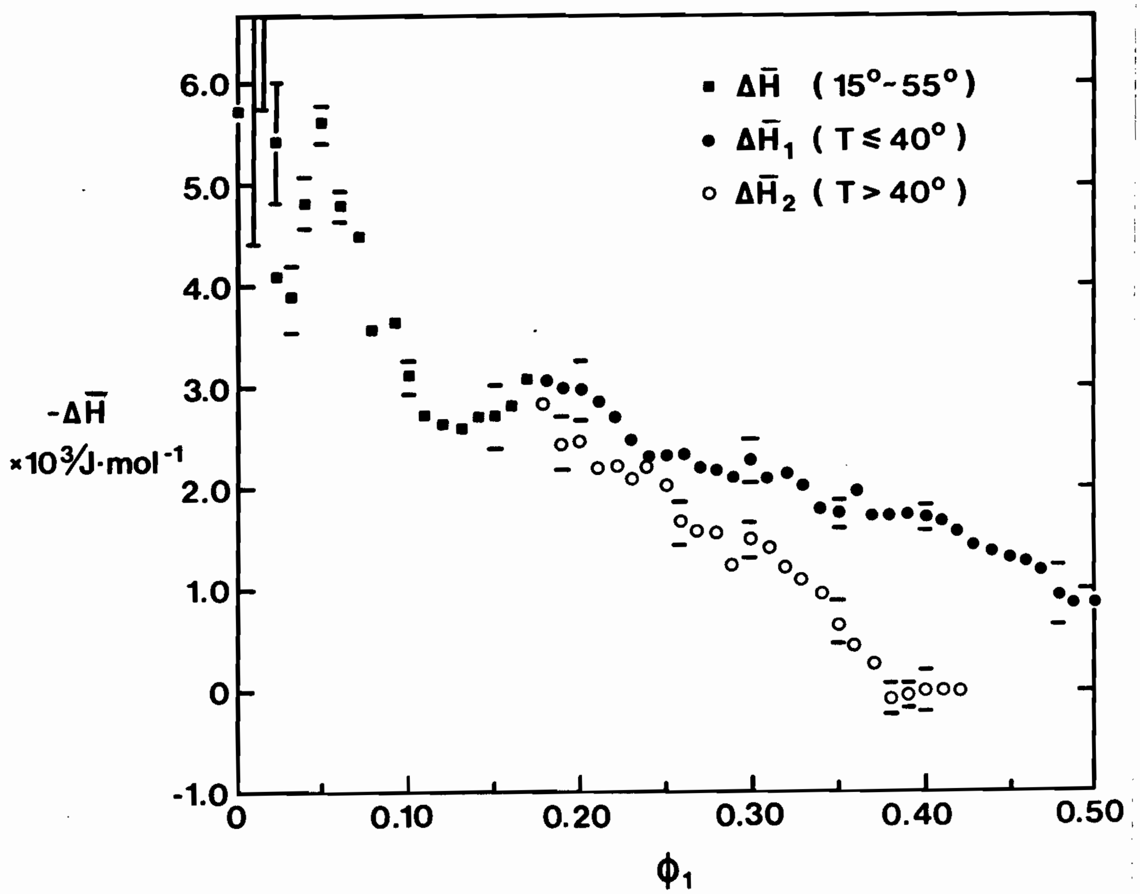

FIGURE 5-5 Partial molar heats of mixing, measured from adsorption isotherms in temperature ranges $\Delta\bar{H}$ (15 - 55°C), $\Delta\bar{H}_1$ (25 - 40°C), $\Delta\bar{H}_2$ (45 - 55°C).

C. Discussion

In common with other lyotropic polymeric mesophases, a two phase isotropic-anisotropic region exists at intermediate concentrations of HPC in water below the LCST (1). This requires that a plateau should exist in the sorption isotherms, since for the two phases to co-exist, the water activity should remain constant with increasing HPC concentration, and the amount of anisotropic phase should increase at the expense of the isotropic material (2). However, the two phase region is narrow and the experimental activities are close to unity, and so the measurements are insufficiently precise to detect the region of constant water vapor pressure.

Above the LCST, the dilute solutions separate into a polymer rich precipitate and a very dilute aqueous phase. When the water content drops below about 60% (by volume), the liquid crystalline mesophase forms. Even in the mesophase region, the samples turn white on heating, indicating that separation of a dispersed phase still occurs, but over a much more extended temperature range than for the dilute solutions (1). This effect provides an explanation for the variation in the heats of mixing with temperature shown in figures 5-4 and 5-5.

At a sharp LCST, one would expect that the activity of water over the very dilute aqueous phase would go to unity. The heat of mixing would be expected to go to zero at the same time since the excess heat of mixing of water with water is zero. The polymeric mesophase is a far more complicated case, since the phase separation does not yield precipitate plus water but instead a still-ordered phase apparently containing a dilute dispersed phase. The non-linearity in the activity plots of figure 5-4 at high water content can be attributed to the separation of a dispersed phase above the LCST. Thus, a qualitative agreement is obtained even though the quantitative agreement is more difficult to determine.

For ϕ_1 greater than about 0.38, the activities above the LCST are close to unity, as expected for very dilute solution mixing, and $\Delta\overline{H}_2$ is zero within experimental error (figure 5-5). As the amount of water decreases, the magnitude of $\Delta\overline{H}_2$ increases until it coincides with $\Delta\overline{H}_1$ at $\phi_1 \simeq 0.20$. At lower concentrations of water, there is a single heat of mixing, $\Delta\overline{H}$.

The enthalpic interactions between water and the liquid crystalline phase are given by $\Delta\overline{H}_1$ and $\Delta\overline{H}$. The mixing process is exothermic, with the magnitude of $\Delta\overline{H}$ decreasing as the volume fraction of water increases. However, the decrease is not smooth, apparent maxima occuring at $\phi_1 \simeq 0.05$ and $\phi_1 \simeq 0.17$. Such discontinuities have been observed in the past for water adsorption on other polymers such as collagen (3), poly(N-vinyl pyrrolidone) (4), amylose (5), and cellulose (6), and have been interpreted in terms of specific states of water in the swollen adsorbate. The volume fractions at which the discontinuities occur correspond approximately to one ($\phi_1 = 0.053$) and three ($\phi_1 = 0.145$) water molecules per substituted anhydroglucose unit. As each unit contains three hydroxyl groups, the maxima may be associated with interactions between these groups and water. The second maximum near three water molecules per unit is also close to the point where the effect of the LCST is first seen in the activities of water vapour.

A second contribution to the enthalpy of mixing may result from the disruption of the partially crystalline regions of the dry polymer to give the aqueous liquid crystalline phase. The magnitude of the effect is uncertain, ΔH_c for the transition from the semi-crystalline polymer to the isotropic state being four joules per gram of polymer (7). This effect may contribute to the high value of $\Delta\overline{H}$ at very low water content.

The entropies of mixing at $40^{\circ}C$ are shown in figure 5-6. The minimum in $\Delta\overline{S}_m$ at $\phi_1 \simeq 0.05$ comes at the same place as the maximum in the $\Delta\overline{H}$ curve, and may represent the minimum of configurational entropy, at roughly one water molecule per HPC unit.

One surprising aspect of the heats of mixing of HPC and water is the fact that the heats are very low, -5.7 kJ mol^{-1} for HPC at infinite dilution (8), as compared to a value of -31.8 kJ mol^{-1} for cellulose (6). which has the same number of hydroxyl groups per unit as does HPC. The significance of this will be introduced in the next chapter during the discussion of the sorption of water by various cellulosic polymers.

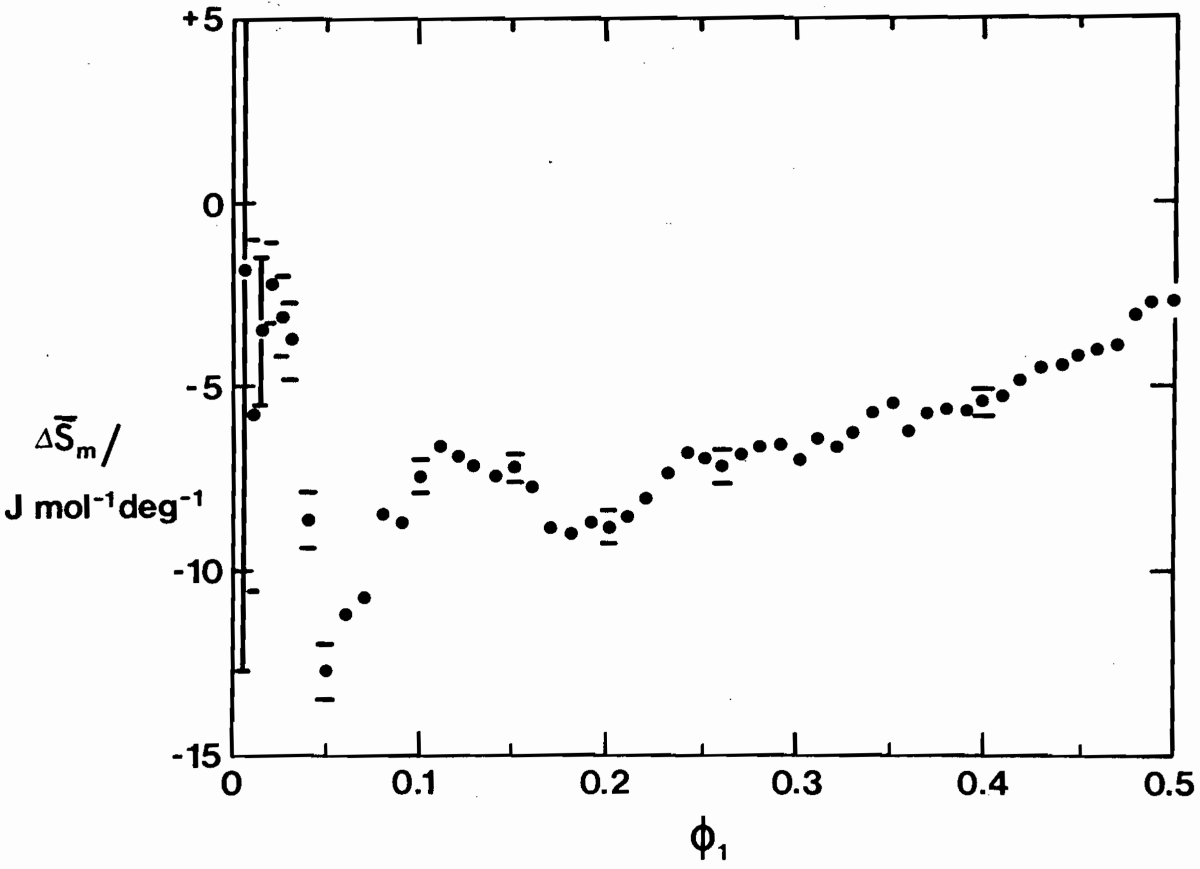

FIGURE 5-6 Partial molar entropies of mixing of water with HPC at 40°C

D. References

1. R.S. Werbowyj and D.G. Gray, Macromolecules 13, 69 (1980).
2. P.J. Flory, Proc. Roy. Soc. Ser. A, 234, 73 (1956).
3. M.H. Pineri, M. Escoubes and G. Roche, Biopolymers 18, 2799 (1978).
4. A.P. Mackenzie and D.H. Rasmussen, in "Water Structure at the Water-Polymer Interface", H.H.G. Jellinek, ed., p.146, Plenum Press, N.Y., 1972.
5. D.J. Macchia and F.A. Bettelheim, Polym. Lett. 2, 1101 (1964).
6. J.L. Morrison and M.A. Dzieciuch, Can. J. Chem. 37, 1379 (1959).
7. R.J. Samuels, J. Polym. Sci., Part A2, 7, 1197 (1969).
8. This Thesis, Chapter 4.

CHAPTER 6

A STUDY OF THE SORPTION OF WATER BY CELLULOSE DERIVATIVES. I. RESULTS AT FINITE CONCENTRATION AND INFINITE DILUTION

A. INTRODUCTION

As stated in the first Chapter of this thesis, water sorption by cellulosic polymers has been little studied, particularly at low water content. In the present Chapter, the techniques of inverse gas chromatography are applied to this problem. The polymers and columns are those described in Chapter 3 of this thesis.

In Chapter 1, the possible errors resulting from kinetic effects were introduced. It was suggested that the most serious of these problems is the combination of isotherm curvature with peak spreading caused by slow attainment of equilibrium.

In figure 6-1, curve 1 is a peak shape unperturbed by kinetic effects. The skewing is the result of different retention times for different portions of the injected peak, and thus the peak corresponds to an equilibrium non-linear sorption isotherm (BET "Type I"). Curve 2 is the peak shape after further skewing and spreading by kinetic effects.

One result of these kinetic effects was to increase the potential for error in the experimental results. While this difficulty was not insurmountable, it also meant that the final results are of lower precision than are results from measurements on non-polar systems that do not present these kinetic effects.

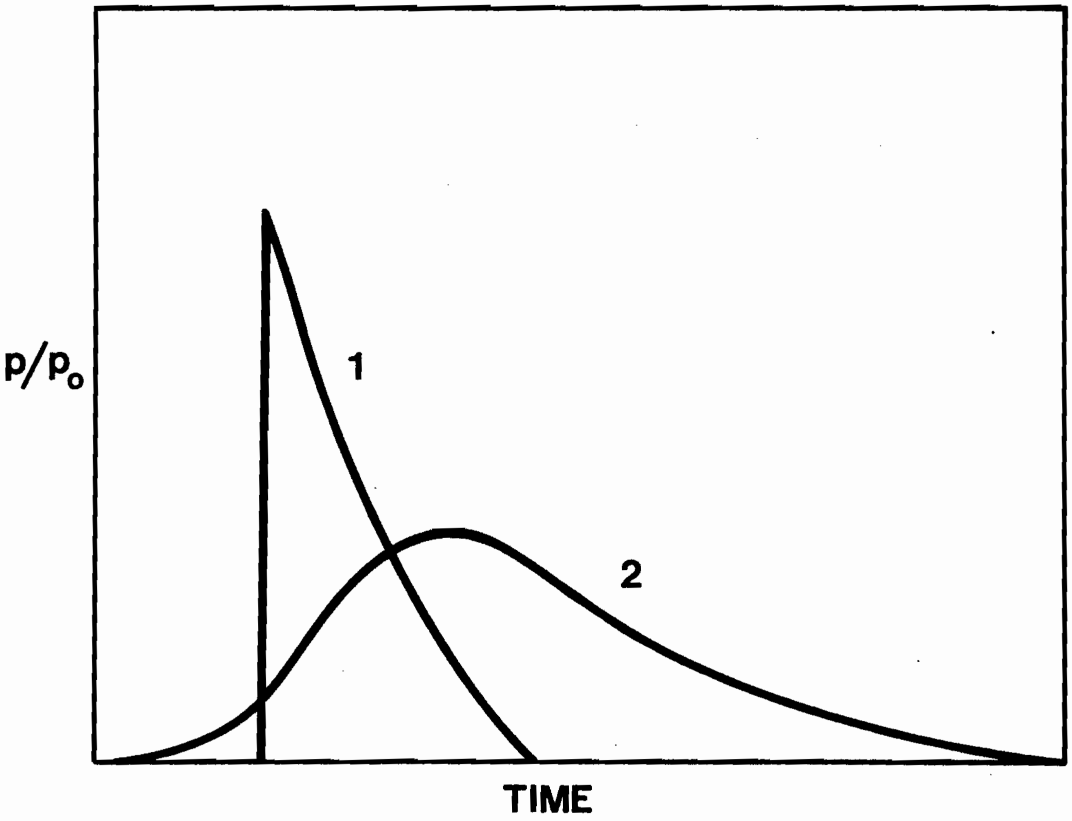

FIGURE 6-1 Peak shapes for (1) an equilibrium but non-linear isotherm and (2) a non-linear isotherm skewed and broadened by kinetic effects.

B. Results

1. Kinetic Effects

Figure 6-2 shows the shapes of experimental GC peaks resulting from injections of different amounts of water at low water content. It is evident that the retention volumes vary with sample size, indicating a non-linear isotherm; and that the peaks are very broad for these small injections, indicating a slow and non-ideal approach to equilibrium. These low concentration peaks do not meet the criterion for isotherm measurement by the ECP technique given by Conder and Young (1), namely that the diffuse side of the peaks should be superimposable. The fact that these peaks are not superimposable can be attributed to the slow attainment of equilibrium,which results in flow rate and loading effects on the peak shapes and retention volumes. The CMA-3 column at 74.6° (figure 6-2a) is the worst case. The data for the CA column at 25° shown in figure 6-2b are closer to ideality.

The loci of the peak maxima were arbitrarily chosen as the characteristic chromatographic curve. The effects of flow rate and loading on this curve, which is required to give the sorption isotherms as well as retention volumes at infinite dilution, were then examined.

Figure 6-3 illustrates how peak maxima move to longer retention volumes at faster flow rates. Two representative peak shapes are shown. This trend is the opposite to that shown in the literature for slow diffusion in non-polar systems with linear isotherms (2), but agrees with the sketch presented in figure 6-1. The true curve may then be closer to the low flow rate result, where water vapor has a longer time

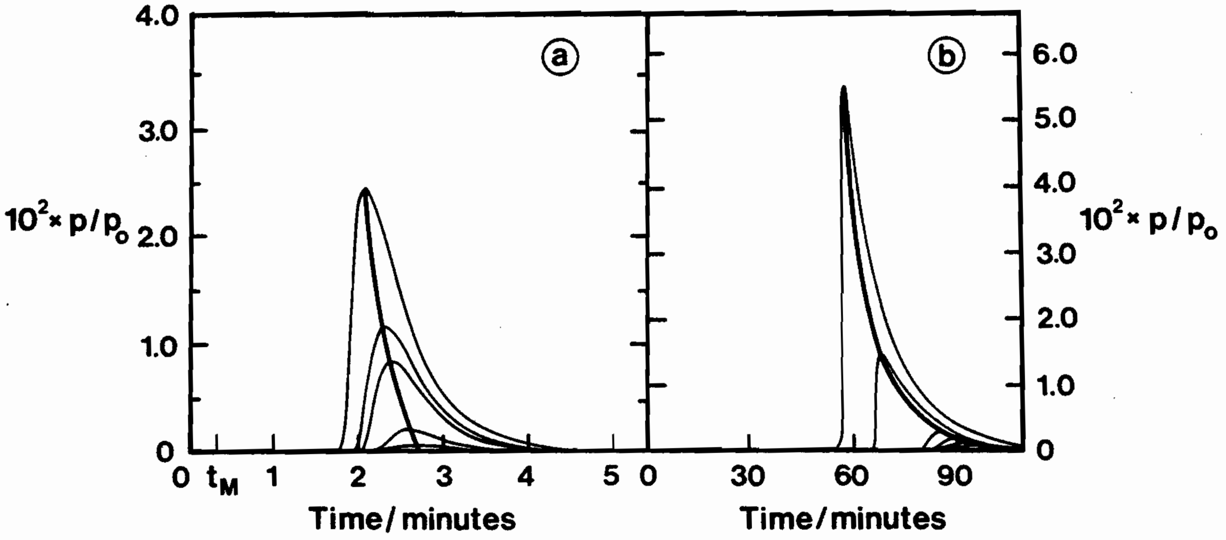

FIGURE 6-2 Experimental peaks and resultant chromatograms at low water content.

(a) CMA-3 column at 74.6° and 62.0 mL min^{-1}

(b) CA column at 25.0° and 34.2 mL min^{-1}

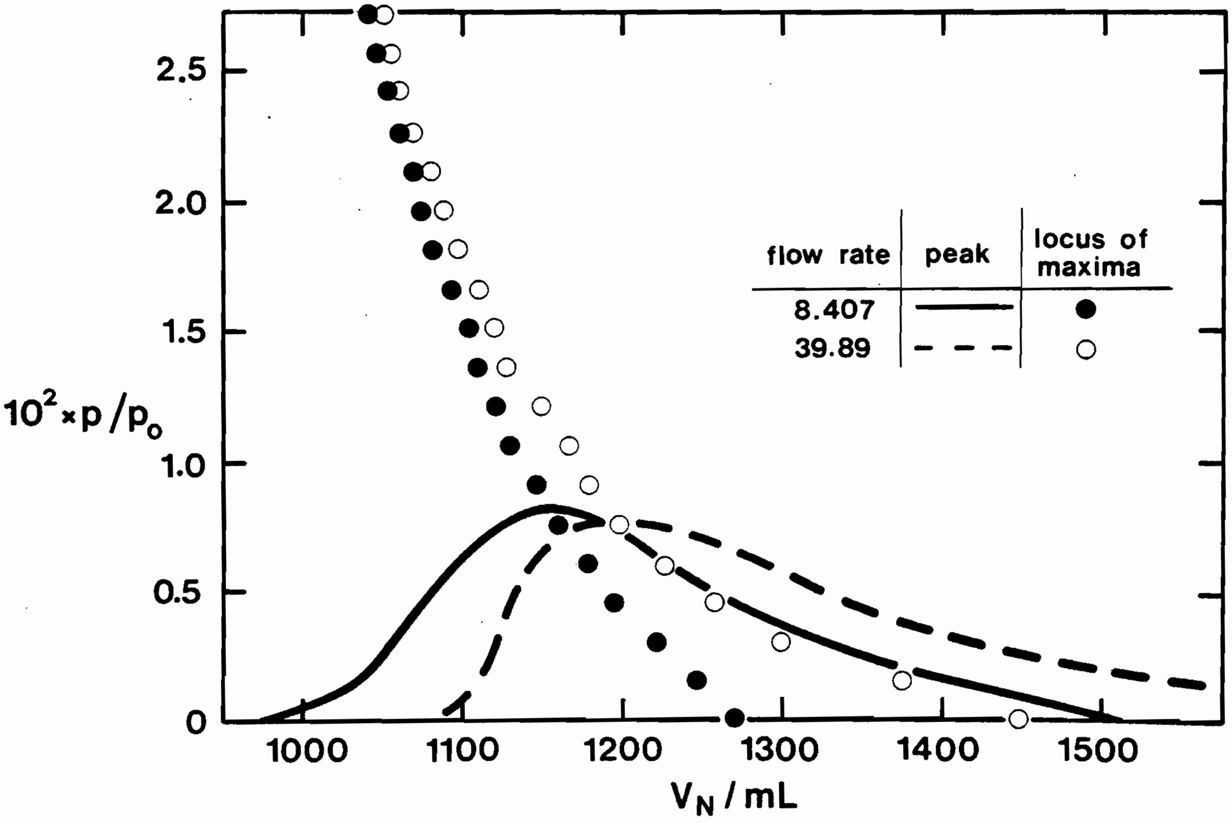

FIGURE 6-3 Experimental peak shapes and chromatograms at slow and fast flow rates for CTA-1 column at 25.0°C.

in the column to reach equilibrium. This is also suggested by the fact that peak widths increase with flow rate, but remain constant with peak height at constant flow rate.

The foregoing suggests that a true infinite dilution retention volume can be obtained by extrapolation to both zero peak height and zero flow rate. One method of doing this is illustrated in figure 6-4, where the loci of the peak maxima for the CMA-3 column at 74.6° are plotted. Curves similar to those shown in figure 6-4 were obtained for the other cellulosic polymers that were studied, but the differences between flow rates were much smaller. The zero flow rate curve in figure 6-4 was obtained by extrapolation to zero flow of each gas phase concentration of water vapor. Due to the scatter in the points, the zero flow rate curve is not too precise. However, by extrapolating this curve to zero peak height a good estimate of the infinite dilution specific retention volume under these conditions, 1000 ± 5% mL g^{-1}, can be obtained.

Aside from the decreasing retention volumes with decreasing flow rate, two other features of figure 6-4 are noteworthy. The curvature of the experimental characteristic chromatograms (loci of the peak maxima) become progressively less as flow rate decreases, and the chromatograms converge at moderate peak height. Sorption isotherms measured on the CTA-1 column at several flow rates showed -- as suggested by figure 6-4 -- that there is no effect of flow rate on the sorption isotherms at finite concentration, and so the observed effects are of importance only in the infinite dilution and low concentration regions.

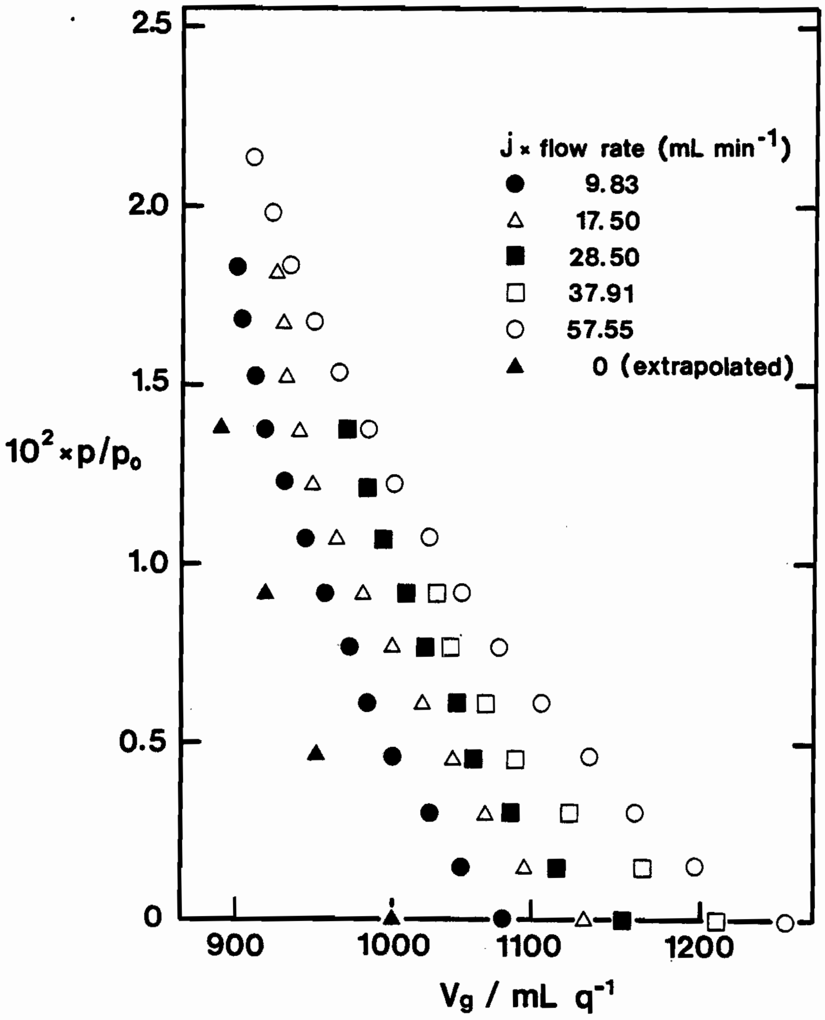

FIGURE 6-4 Experimental chromatograms for the CMA-3 column at 74.6°C as a function of flow rate. The loci of the peak maxima were determined as in figure 6-2.

Alternately, the zero flow rate value of V_g can be obtained by the extrapolation of the peaks to zero peak height as shown in figure 6-2, and then by the extrapolation of a plot of the resultant specific retention volumes to zero flow rate. The retention data on four polymers is shown in figure 6-5. A logarithmic scale was necessary to include all the data in the same figure, but disguises the marked decrease in the retention volumes at low flow rate. The severity of the kinetic effect for cellulose monoacetate at three column loadings is shown in figure 6-6, where the retention volumes drop by about 30% as the flow rate is decreased.

The hypothesis that kinetic effects increase the retention volume by causing the type of peak spreading shown in figure 6-1 is supported by the observation that increasing the layer thickness, which should also increase the time to equilibrium, causes an increase in the retention volume. The CMA samples again present the most extreme case, although the same effect -- of a lower magnitude -- was seen for the CTA columns. The direction of this loading effect is the opposite of that often observed (3) for systems where surface adsorption contributes. There is scatter in the points in figure 6-6 due to uncertainties in extrapolating to zero peak height, but for the lowest loading at zero flow rate, the value for V_g is about 970 ± 5% mL g^{-1}, in good agreement with the value obtained by the alternative extrapolation method (figure 6-4).

2. Infinite Dilution Results

The values of V_g extrapolated to zero peak height and then to zero flow rate in figure 6-5 were used to calculate the χ_{12}^{∞} parameters

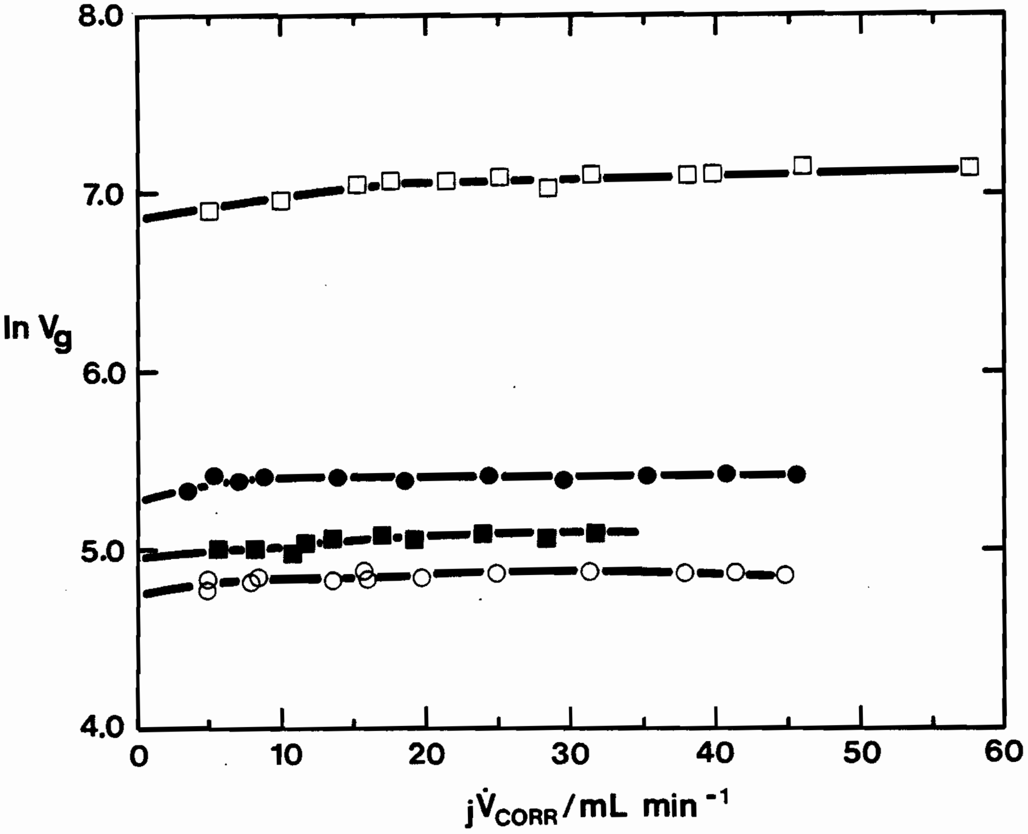

FIGURE 6-5 Log of specific retention volumes at 74.6°C as a function of flow rate for CMA-3 (□); CA (●); HPC (■); and CTA (○).

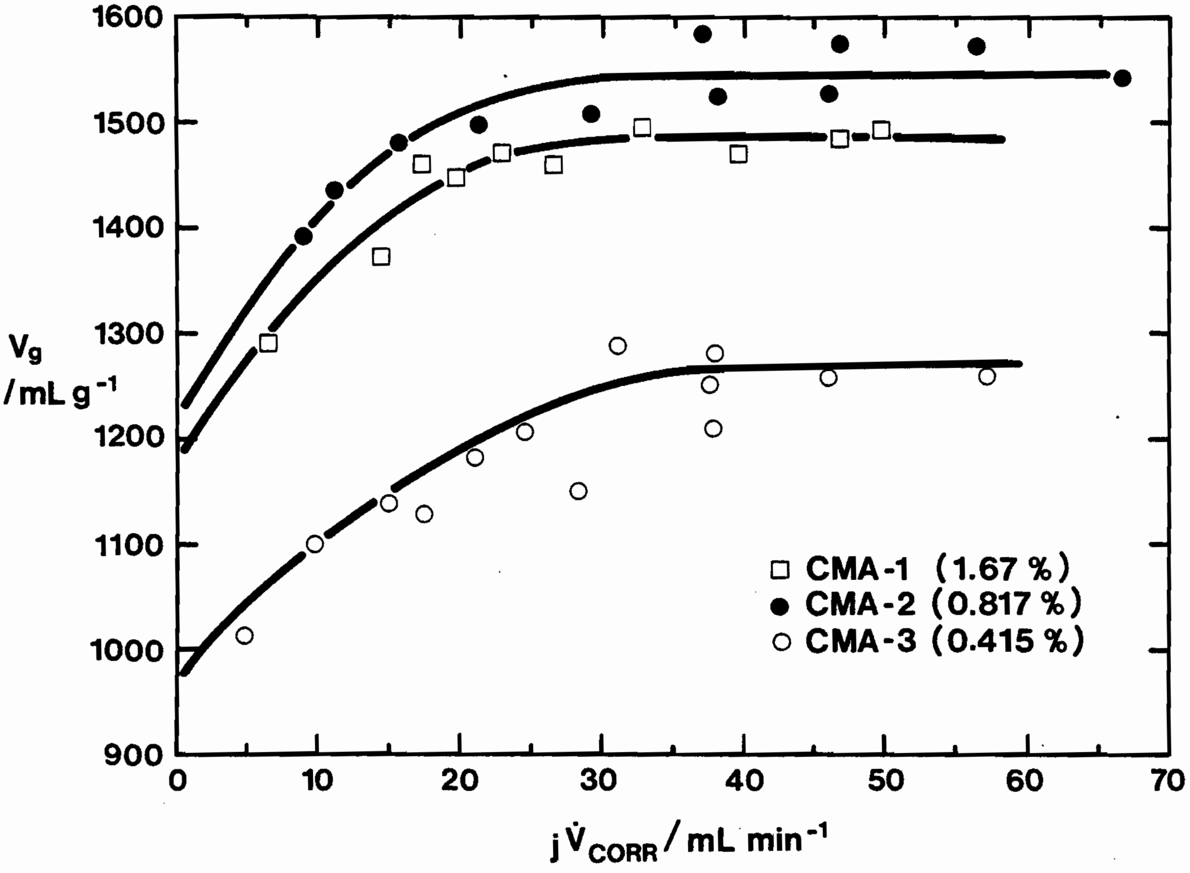

FIGURE 6-6 Specific retention volumes at 74.6°C as a function of flow rate for CMA-1 (□); CMA-2 (●); and CMA-3 (○).

by means of equation 2-31. The data for χ_{12}^{∞} for these polymers at 74.6° are shown in Table 6-1, along with a value of χ_{12}^{∞} for cotton cellulose obtained by extrapolation of the static data of Morrison and Dzieciuch (4). The order of the values of χ_{12}^{∞} reflect the increasing interaction between the polymers and water in the same way as does the order of the values of V_g in figure 6-5. These detailed measurements were done at 74.6° due to the strong interactions between water and these polymers which resulted in long retention times. Due to detector instability over very long retention times, low flow rate measurements could not be done at room temperature. Where columns of different loading were available, results are given for the lowest loading.

Also shown in Table 6-1 are the heats of mixing at infinite dilution, $\Delta\overline{H}_m^{\infty}$, calculated using equation 2-34 from data between 60° and 85°. The given error is the standard deviation of the least squares analysis of the data. These results were obtained from measurements at a single flow rate ($\approx$40 mL min^{-1}), as the change in the flow rate dependence of V_g with temperature is within experimental error over this narrow range. The heats given are those for the columns with lowest loading, where applicable. The apparent heats increased by about 25% with loading for CMA.

3. Results at Finite Concentration

Figure 6-7 shows the variation in specific retention volume with water vapor pressure at 25°C for several polymers. Curves 1 and 2 were obtained from the CA and CTA-1 columns for ECP isotherm calculations by superimposing a series of peaks resulting from injections of different

Table 6-1

Thermodynamic Data for Cellulosic Polymers and Water

Polymer	χ_{12}^{∞} (± 0.05)	$-\Delta\overline{H}_m^{\infty}$ (kJ mol^{-1})
cotton cellulose[a]	-1.0 (25°C)	31.8
cellulose monoacetate (D.S. = 0.89)	0.0	16 ± 1
cellulose acetate (D.S. = 2.45)	1.6	9.5 ± 1.5
cellulose triacetate	2.1	5 ± 1
ethyl cellulose[b] (D.S. = 1.4)	1.1	12 ± 1
methyl cellulose (D.S. = 1.9)	-----	18.5 ± 1
hydroxypropyl cellulose	1.9	5.7 ± 0.6

(a) data from reference 4 (static sorption)

(b) χ_{12}^{∞} measured at a gas flow rate of 40 mL min^{-1}

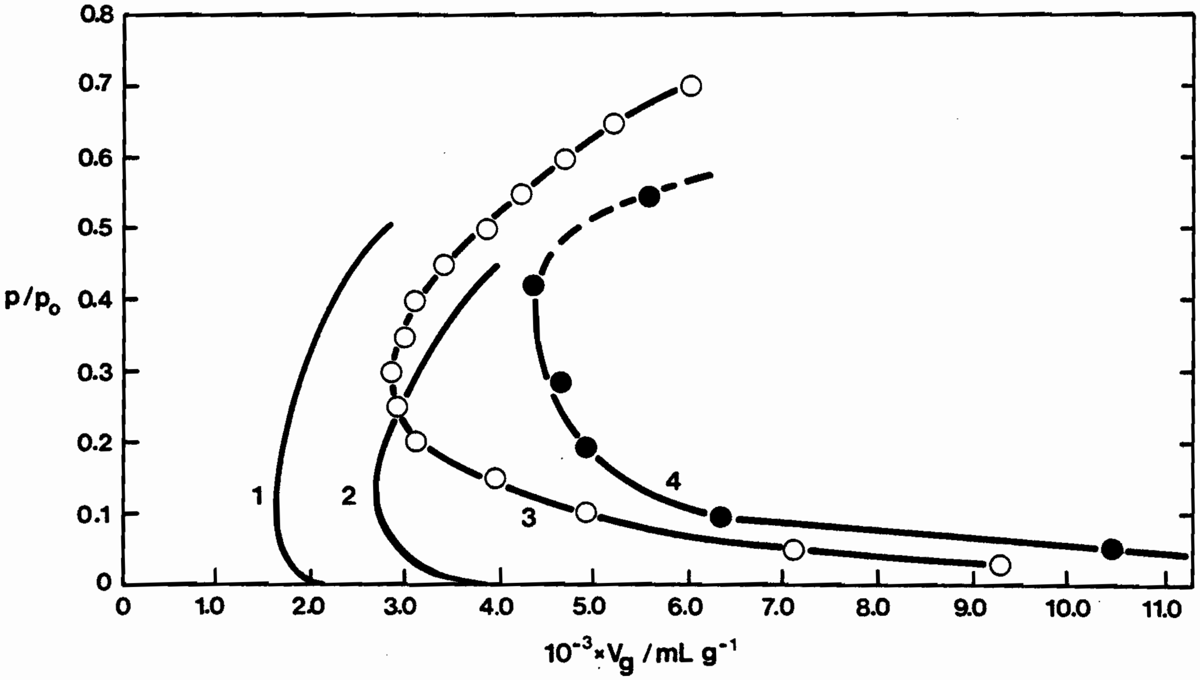

FIGURE 6-7 Experimental GC chromatograms at finite concentration. Curves 1 and 2 are the ECP curves for CTA and CA, respectively. Curve 3 (○) is a hypothetical GC chromatogram for cellulose calculated from the static data; see text. Curve 4 (●) is drawn from the points measured by the EP technique for the CMA sample.

sizes, and drawing the curve along the common diffuse peak fronts (1). In this concentration region, there was little effect of flow rate. At low water content, the diffuse side of the peaks do not superimpose as well (figure 6-2b), so the loci of the peak maxima were used. This use of peak maxima to define an ECP chromatogram has been criticized by Conder and Young (1), who also pointed out the problems of the ECP method as applied to isotherms which display a point of inflection. They stated that under these conditions, the ECP data is useable only at concentrations above the inflection point, since the elution behavior of a "characteristic point" passing through such a discontinuity is no longer described by the simple relation assumed until now.

For these reasons, cellulose monoacetate is unsuitable for ECP measurements. Therefore the isotherm was measured by the EP technique. In curve 4 of figure 6-7, the points correspond to the infinite dilution retention volumes on plateaus of the given partial pressures of water. The measurements were made in order of increasing water content. In order to check this GC method, static measurements were performed at 25° using the vacuum microbalance apparatus. Results are shown in figure 6-8. The sorption curves agreed up to $p/p_o \simeq 0.3$, while the GC method was more sensitive at low water content. The deviation at high relative partial pressure of water is due to the difficulty in detecting very small amounts of water injected on top of the high concentration plateaus.

For the sake of comparison, curve 3 in figure 6-7 shows the GC chromatogram for a hypothetical cellulose column. The points were calculated from the static isotherm in the literature (4) and equation 2-44.

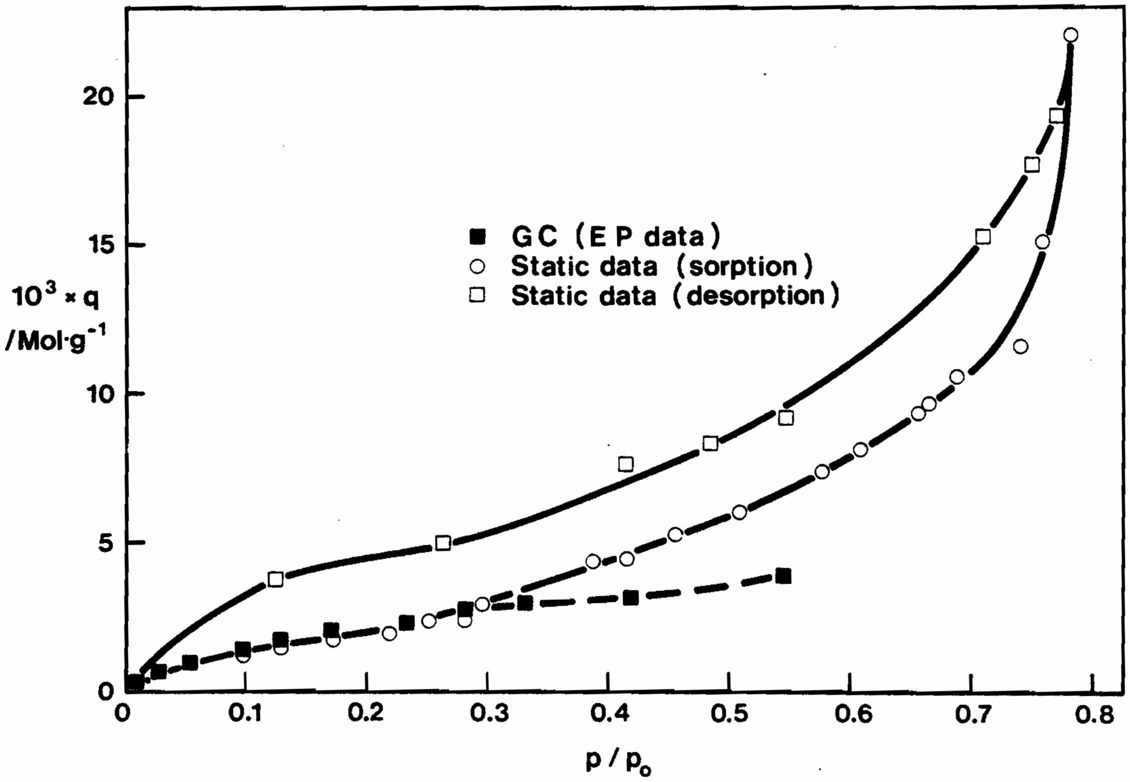

FIGURE 6-8 Sorption and desorption isotherms for water on CMA measured by GC (EP technique) and vacuum microbalance.

Figure 6-9 shows the adsorption isotherms of water on the cellulose acetate and ethyl cellulose columns, as calculated from the GC data. The literature isotherm for cellulose mentioned in the previous paragraph is also shown. The error caused by non-ideal peak shapes in the ECP isotherms (CA, CTA, and ethyl cellulose) is confined to the region of low water content ($p/p_o \lesssim 0.1$), and even at low water content the error is probably not serious.

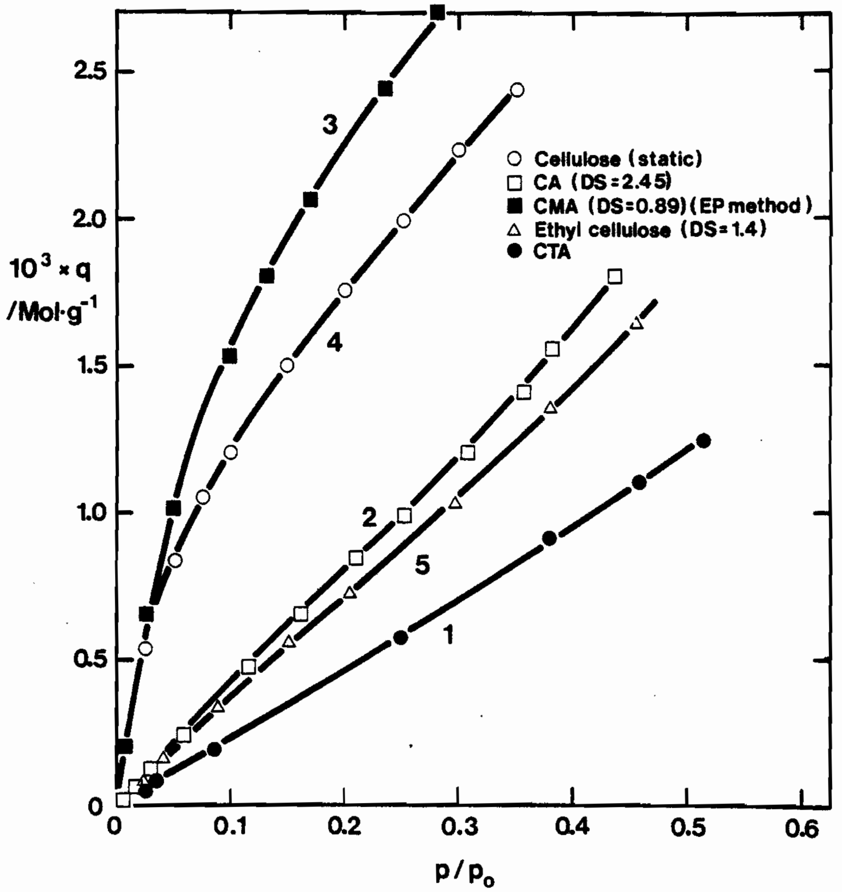

FIGURE 6-9 Sorption isotherms for water on various cellulosics at 25°C measured by both GC and static means. Curves 1 - 4 are as described in the previous figure, while curve 5 is the isotherm for ethyl cellulose.

C. Discussion

In figure 6-9, those polymers with a high degree of substitution appear to have a "type III" concave upwards isotherm shape, as reported by many others (5-11). In fact, at very low water content all of the isotherms possess a weak "type II" isotherm knee, although the type II behavior is exaggerated by the effect of the gas flow rate on the GC chromatogram curvature. The minima in V_g shown in figure 6-7 are characteristic of an isotherm knee.

The isotherms shown here should be comparable with those in the literature measured by static methods. For cellulose acetate and cellulose triacetate, the amounts of water sorbed according to the literature ranges from 10% to 50% greater than those reported here (6-9). The ethyl cellulose sample -- with a lower D.S. than that commonly seen -- sorbed more than twice the amount of water reported for other samples of this polymer (10, 11).

The interaction of water with these cellulose derivatives is obviously very sensitive to the degree of substitution of the polymers, and to their physical form, so that variations in measurements between different samples is not unexpected. However, for the samples of both HPC and CMA examined during the course of this work, the GC and static isotherms coincided, within the useful limits of each technique.
The few comparative studies on sorption by identical polymer samples (12,13) have shown the interchangeability of the two types of measurements. The exceptions (14,15) probably result from kinetic effects on the GC retention close to a glass transition temperature.

Interpretation of the results in terms of χ_{12}^{∞} is not unequivocal. The values for χ_{12}^{∞} in Table 6-1 assume that the water mixes with the total weight of polymer in the column. This may not be true for polymers that are partially crystalline. The necessary correction was was given in Chapter 4 of this thesis:

$$\chi_{12}^{\infty} = \chi_{12}^{\infty} + \ln(1 - C) \qquad (6\text{-}1)$$

where C is the fractional crystallinity of the polymer. For example, cotton cellulose is approximately 60% crystalline or 40% accessible to water (16), so the true value of χ_{12}^{∞} shown in Table 6-1 may be closer to -1.9. This also shows that an apparently favorable, negative value of χ is not sufficient for solution to occur. A very negative χ in this case indicates a strong interaction between the dry cellulose and the first incoming water molecules.

The values of χ_{12}^{∞} were calculated assuming that mixing of water with these polar polymers follows the Flory-Huggins lattice model for mixing. There is no immediate reason why this should be valid, especially since it has already been shown in Chapter 4 of this thesis that HPC follows a different mixing model. Nevertheless, the present data does allow a comparison between different polymers. The addition of unity to each value of χ_{12}^{∞} yields $\ln(a_1/\phi_1)^{\infty}$, which is model independent although still not corrected for crystallinity. The heats of mixing $\Delta\overline{H}_m^{\infty}$ are model independent, and as long as the crystallinity does not change over the narrow temperature range studied, the heats are also independent of crystallinity. Infinite dilution heats of mixing for the cellulose acetates are not obtainable from the literature, except as extrapolations of imprecise data from finite concentration.

The values of $-\Delta\overline{H}_m^{\infty}$ shown in Table 6-1 descend smoothly in the order of decreasing hydroxyl content or increasing acetyl substitution, from cellulose (D.S. = 0) to cellulose triacetate. A plot of $-\Delta\overline{H}_m^{\infty}$ vs. degree of substitution shows that the heat for ethyl cellulose falls on the cellulose acetate curve (figure 6-10). However, the value of $-\Delta\overline{H}_m^{\infty}$ for methyl cellulose is greater than predicted by figure 6-10. This suggests that the predominant interaction is the one between water and the unsubstituted hydroxyl groups. It is also likely that the interaction between water and the methoxyl groups is stronger than that between water and ethoxyl or acetyl groups. In the only case in the literature analogous to the present one, the heat of mixing of water at infinite dilution in diethylene glycol dimethyl ether (17) was more exothermic than in diethylene glycol diethyl ether (18), in qualitative agreement with the results for the cellulosics.

A qualitative result similar to the order of heats shown here was seen by de Vries and Smit (19). In an early paper using inverse GC, these authors showed that for the adsorption of various alcohols onto cellulose acetates of D.S. = 3 and D.S. = 2.5, the heat of mixing was always more exothermic in the sample of lower substitution. However, the quantitative significance of these results in suspect, since the authors did not account for non-ideal GC effects.

The value of $\Delta\overline{H}_m^{\infty}$ for HPC is about the same as that for CTA. At first this is surprising, since the hydroxyl content of HPC is the same as that for cellulose. However, HPC is known to be relatively hydrophobic at low water content (20), despite evidence (21) that the average molar substitution (M.S.) of four is distributed in such a manner as to

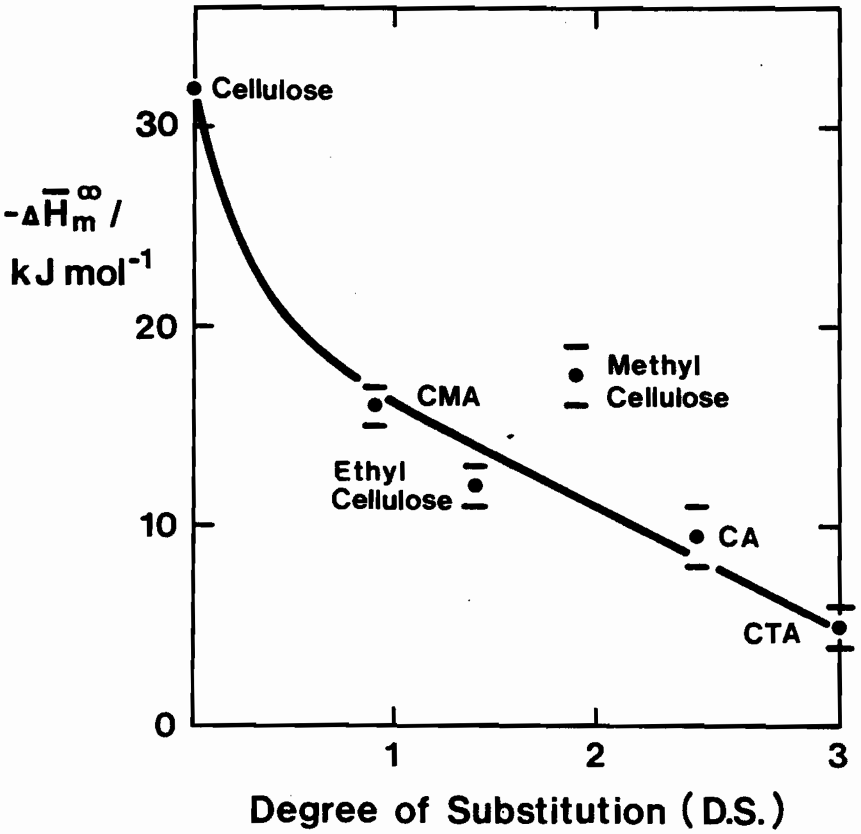

FIGURE 6-10 The negative of the heat of mixing at infinite dilution $-\Delta\overline{H}_m^\infty$ plotted as a function of the degree of substitution, D.S. Data from Table 6-1.

leave one free hydroxyl group on every anhydroglucose unit. It is also known that HPC maintains its highly ordered structure at water contents below the cholesteric mesophase, since the dry polymer is partially crystalline, and has a three-fold helical structure (21,22). The low value of $\Delta\overline{H}_m^{\infty}$ for HPC lends credence to a structure for dry HPC proposed by Samuels (21), in which all hydroxyl groups -- whether on the backbone or the side chains -- take part in some form of intramolecular hydrogen bonding. Water sorption to the HPC would then occur by lower energy hydrogen bonding to the ethereal oxygen, as suggested by Klug (20). If water sorption does occur by hydrogen bonding to the hydroxyl groups of the HPC, it could only do so at the expense of breaking the intramolecular hydrogen bonds.

Cellulose and cellulose monoacetate can be seen to be the most active of these polymers, by virtue of the fact that they show the most negative heats of mixing with water, the greatest amount of water sorbed, and the greatest change in their isotherms with water sorbed. CMA, a water soluble polymer, is the more hydrophilic due to its more accessible structure.

Attempts were made to measure the interactions of water with cellulose itself using inverse GC. However, the problems resulting from the strong water-cellulose interactions and from slow water diffusion through cellulose fibers below the cellulose glass transition have so far proved insurmountable. Several attempts were made to obtain cellulose as a thin film by coating cellulose acetate onto a chromatographic support and removing the acetyl groups by saponification. Unfortunately, it was found that saponification conditions severe enough to give a complete reaction had the additional effect of swelling the resultant cellulose and removing it from the support. Conversely, under conditions mild enough to leave the polymer coating on the support, only a small fraction of the acetyl groups were found to have been saponified. One paper was recently published claiming to give the infinite dilution specific retention volumes for water on cellulose at 100°C (23). These ranged from 106 mL g^{-1} for cotton cellulose to 240 mL g^{-1} for kraft pulp. These results have little numerical significance for several reasons. Only a single, large injection of 0.6 μL was made, with no extrapolation to zero peak height, so that these results can in no way be considered as being at infinite dilution. Only one high gas flow rate (60 mL min^{-1}) was used, but there would almost surely be a strong flow rate dependence. Finally, while the authors reported different values of V_g for the various types of cellulose, they made no allowance for varying degrees of accessibility to water (16).

D. References

1) J.R. Conder and C.L. Young, "Physicochemical Measurements by Gas Chromatography", John Wiley and Sons, Chichester, 1979.

2) G.J. Courval and D.G. Gray, Macromolecules 8, 916 (1975).

3) G.J. Courval and D.G. Gray, Can. J. Chem., 54, 3496 (1976).

4) J.L. Morrison and M.A. Dzieciuch, Can. J. Chem., 37, 1379 (1959).

5) J.A. Barrie, "Water in Polymers", Chapter 8 in "Diffusion in Polymers", J. Crank and G.S. Park, ed., Academic Press, London, 1968.

6) C. Toprak, J.N. Agar, and M. Falks, J. Chem. Soc.,Farad. Trans. 1, 75, 803 (1979)

7) D.K. Beever and L. Valentine, J. Text. Inst., 49, T95 (1958).

8) D.K. Beever and L. Valentine, J. Appl. Chem., 8, 103 (1958).

9) H. Barnes, C. Skaar, and P. Luner J. Appl. Polym. Sci., 21, 1085 (1977).

10) V. Stannett and J.L. Williams, in "Fibre-Water Interactions in Papermaking, Transactions of the Symposium held at Oxford: September, 1977", W. Clowes and Sons, Ltd., Oxford, 1978, p.497.

11) J.L. Williams, H.B. Hopfenberg, and V. Stannett, J. Macromol. Sci. -- Phys., B3, 711 (1969).

12) Y.H. Chang and D.C. Bonner, J. Appl. Polym. Sci., 19, 2457 (1975).

13) P.J.T. Tait and A.M. Abushihada, Polymer, 18, 810 (1977).

14) A.A. Tager, T.I. Kirillova, and T.V. Ikanina, Polym. Sci. USSR, 20, 2854 (1979)

15) G. Edel and B. Chabert, C.R. Acad. Sci. Paris, Ser. C, 268, 226 (1969).

16) O. Sepall and S.G. Mason, Can. J. Chem., 39, 1934 (1961)

17) W.J. Wallace and T.J. Vallenga, J. Chem. and Eng. Data, 16, 331 (1971).

18) W. Schneider, R. Vogel, and E. Mokhtari-Nejad, Ber. Bunsenges. Phys. Chem., 81, 1076 (1977).

19) M.J. de Vries and J.H. Smit, J. South African Chem. Inst., 20, 11 (1967).

20) E.D. Klug, J. Polym. Sci., 36C, 491 (1971).

21) R.J. Samuels, J. Polym. Sci. Part A2, 7, 1197 (1969).

22) R.W. Werbowyj and D.G. Gray, Macromolecules 13, 69 (1980).

23) S. Yu. Khovryakov, Z.A. Belova, and K.G. Komkova, Metody Anal. Kontrolya Kach. Prod. Khim. Promsti, 1978 (5), 5-7; also cited in Chem. Abstr., 89, 148378n (1978).

CHAPTER 7

A STUDY OF THE SORPTION OF WATER BY CELLULOSE DERIVATIVES. II. A SORPTION MODEL

A. Introduction

In the previous chapter, results were reported for the sorption of water onto various cellulosic polymers at finite concentration and at infinite dilution. Non-ideal GC effects that appeared to be confined to the region of low concentration and infinite dilution were also described. In the present chapter, the Zimm cluster integral is used as a model for sorption. The polymers studied were: hydroxypropyl cellulose (HPC); cellulose; cellulose monoacetate (CMA; D.S. = 0.89); cellulose acetate (CA; D.S. = 2.45); cellulose triacetate (CTA); and ethyl cellulose (D.S. = 1.4).

Until now, the results have been explained only in terms of thermodynamic models for mixing with randomly oriented or rod-like molecules (Flory-Huggins and "Flory-rodlike" mixing). However, there exists a variety of derivations that attempt to fit experimental isotherm data to physical or statistical models. A review published ten years ago (1) contained eighteen different isotherm equations, a list even then neither complete nor up-to-date. Most of these models depend on the existence of different states of water within a sample, and attempt to give the experimental isotherms as the sum of the relative contributions from each state of the adsorbate. These "states" of water have been investigated by NMR spectroscopy in cellulose (2) and by differential scanning calorimetry in cellulose acetate (3), among other techniques. In each case, the existence of four states of water was reported. For cellulose, these were defined to be in increasing concentration of water: water strongly hydrogen bonded to hydroxyl groups in the non-crystalline regions, water sorbed in multilayers, water sorbed in capillaries, and finally bulk water. The range of GC measurements reported here is confined to the first one or two of these regions.

A brief description of four isotherm models quoted in the recent literature follows. Of these four models, only the Zimm cluster integral will be used for a detailed analysis of the experimental results. It is the most general of the four models, and is the only one that does not require any prior assumptions regarding the structure of the substrate or the mechanism of sorption.

The best known model is that of Brunauer, Emmett, and Teller (the "BET" theory) (4). This states that monolayer surface adsorption takes place on the substrate with a heat of adsorption ΔH, followed by multilayer sorption with a heat equal to the latent heat of condensation of the adsorbate. Although the model is only applicable in a narrow range ($.05 \lesssim p/p_o \lesssim .40$) and although it has been severely criticized on the basis of its prime assumption, it has still given a reasonable fit for a wide variety of systems. Furthermore, if the area occupied by each adsorbate molecule is known, then the surface area of the substrate can be determined. Tremaine and Gray (5) have derived a method whereby the BET parameters can be calculated directly from finite concentration GC retention data, without the intermediate step of calculating the sorption isotherm.

Hailwood and Horrobin (6) proposed a model that assumed the existence of three phases in the solid: strongly bound or dissolved water; water forming hydrates with the polymer; and unhydrated polymer. They used the equation:

$$\frac{Mq}{1800} = \frac{\alpha a}{1 - \alpha a} + \frac{\alpha\beta a}{1 + \alpha\beta a} \qquad (7\text{-}1)$$

where q is the amount of water sorbed at a relative partial pressure, a;

α and β are empirical constants related to the equilibrium constants for overall and monohydrate sorption, respectively; and M is the effective "molecular weight" of the sorbing unit, or the amount of substrate per water molecule.

The previous equation was rearranged to yield:

$$A + Ba - Ca^2 = a/q \tag{7-2}$$

This was solved for the best fit values of A, B, and C, and gives a sigmoidal (BET type II) isotherm as the sum of a Langmuir isotherm (BET type I) and a multilayer isotherm (BET type III). The model has been criticized due to the existence of an extra adjustable parameter, which allows any set of data in a sigmoidal shape to be fit to equations 7-1 and 7-2 by the correct choice of parameters. On the other hand, various workers have been able to fit water sorption data to the model (7-9). One partial success of the model was the ability to relate the M factor (effective weight of polymer per water molecule) to the fraction of polymer, A, that is accessible to the water.

D'Arcy and Watt (10) proposed a model that considered three processes in the substrate: monolayer adsorption by strongly binding sites, monolayer adsorption by weakly binding sites, and multilayer adsorption. This gives a sigmoidal isotherm as the sum of a type I isotherm, a type III isotherm, and a linear isotherm. This approach therefore suffers from the same weakness as the previous one; namely that a good fit depends as much on the choice of parameters as on a physical model.

Zimm Cluster Theory

The concept of the cluster integral was first developed by Zimm (11) and by Zimm and Lundberg (12) to explain the sorption characteristics of hydrophilic polymers. It had previously been found that a rigid site model such as the Flory-Huggins theory gave poor results when applied to water-collagen mixtures. The cluster theory is based on the relationship between geometric probabilities and thermodynamic properties, eliminating the need for an arbitrary structure or model (13). As pointed out by Zimm and Lundberg (12), the theory "does not predict isotherms, but it does serve to intepret them in molecular terms". The theory has been extended by others, especially Starkweather (14,15).

The cluster integral G_{11} is defined as:

$$G_{11} \equiv \frac{1}{V}\iint [F_2(i,j) - 1]\; d(i)d(j) \qquad (7\text{-}3)$$

where the probability that two molecules i and j will be found together at the point (i,j) within the range bounded by d(i) and d(j) is:

$$\frac{1}{V^2} F_2(i,j)d(i)d(j) \qquad (7\text{-}4)$$

This defines the molecular pair distribution function F_2. The following expressions were then derived (11,13):

$$\frac{G_{11}}{v_1} = -\phi_2\left(\frac{\partial(a_1/\phi_1)}{\partial(a_1)}\right)_{P,T} - 1 \qquad (7\text{-}5)$$

or

$$\frac{\phi_1 G_{11}}{v_1} = c_1 G_{11} = -\phi_2\left(\frac{\partial \ln \phi_1}{\partial \ln a_1}\right)_{P,T} - 1 \qquad (7\text{-}6)$$

In the previous equations, a_1, ϕ_1, v_1, and c_1 are the activity, volume fraction, molar volume, and molar concentration respectively of component 1. The term $\phi_1 G_{11}/v_1$ has been shown to give (10) the concentration of type 1 molecules present in the excess of the mean in the vicinity of a given type 1 molecule. It follows that the average number of type 1 molecules per cluster (the "cooperative index" (16)) is:

$$CI = c_1 G_{11} + 1 \qquad (7\text{-}7)$$

In an ideal system, the activity coefficient is constant with water content. That is, Raoult's law, or at least Henry's law, is obeyed. The clustering function G_{11}/v_1 is then equal to minus one, or the cluster integral G_{11} is equal to minus one molecular volume. Under these conditions, a molecule of type 1 has no effect on other molecules except to exclude them from its own sorption site. If G_{11}/v_1 is greater than minus one, molecules will tend to cluster. If G_{11}/v_1 is less than minus one, molecules will exclude their own kind. Flory-Huggins mixing corresponds to G_{11}/v_1 equal to zero, where there is only enough clustering to overcome the excluded volume of the polymer (12).

Examination of equation 7-7 shows that a value of CI of less than one implies an apparent cluster size of less than one water molecule. The paradox resolves itself when it is remembered that a statistical model such as this treats all sites as being equally probable for random sorption. Starkweather (15) considered the cluster size of less than one water molecule to be indicative of preferred water-polymer contacts causing a greater separation between water molecules than would be expected in a random mixture. Therefore, the negative clustering function corresponds to a state of non-random sorption, or of preferred sorption onto specific sites. These specific sites have in the past been related to physical structures such as gaps or cavities (10, 17), or to polar sites such as hydroxyl or amide groups (18-20). For example, Zimm and Lundberg (12) found that for the sorption of small amounts of water onto collagen, the clustering function G_{11}/v_1 is less than minus ten, or G_{11} is less than minus ten molecular volumes. This was interpreted as indicating a very low concentration of initial sorption sites in the collagen. Within experimental error, the value obtained was the same as that determined from BET analysis of the isotherm.

In addition to the statistical or geometrical derivation, it has been pointed out that the cluster integral can be calculated from changes in the value of the χ parameter with water content (13, 18).

Starkweather (15) has derived a method to better quantify this theory. In his approach, w_1/CI is plotted vs. w_1, where w_1 is the weight of water sorbed (g per 100 g of polymer) and w_1/CI is the weight of water per cluster, directly related to the number of clusters present. The change in the slopes of these curves was interpreted in terms of the mechanism of cluster buildup and breakdown. For example, Starkweather suggested that a slope of plus one indicates random sorption while a slope of zero indicates that water is being sorbed with no change in the number of clusters. A negative slope would mean a decrease in the number of cluster, caused by the joining together of previously independent clusters, while a slope of greater than plus one would indicate non-random or preferred sorption.

B. Results

The sorption isotherms presented in the previous chapter were replotted as activity coefficients of water vs. activity of water. Slopes were taken from the hand smoothed curves, and equations 7-5, 7-6, and 7-7 were used to calculate the clustering functions and average cluster sizes. Table 7-1 shows the values of the clustering functions G_{11}/v_1 and of the average cluster sizes CI at regular intervals. Figures 7-1 to 7-7 illustrate the Zimm clustering plots and the Starkweather calculations. The Zimm clustering plots for cellulose monoacetate (D.S. = 0.89), cellulose acetate (D.S. = 2.45), and for ethyl cellulose are not shown. These curves are very similar in appearance to the cellulose plot (figure 7-3) except that the measurements for the latter two polymers terminated at a lower water content.

The slopes of the Starkweather curves are calculated from the second derivative of the hand smoothed Zimm clustering plots, and the third derivative of the original sorption isotherms. Therefore it is probably best to treat these in only a semi-quantitative fashion. The "saturation points" for the Starkweather curves described below are the concentration regions where preferred, non-random sorption ceases and clustering starts. Within the scatter of the isotherm points and the measured slopes, these correspond to the maxima in the Zimm clustering plots (or to the first point where the slope goes to zero), and to the place where the average cluster size goes from less than one to greater than or equal to one.

Table 7-1

Clustering Data for Cellulosic Polymers

	cellulose$^{(a)}$		CMA (sorption)		CMA (desorption)		CA		CTA		ethyl cellulose		HPC	
a_1	$\frac{G_{11}}{v_1}$	CI	$\frac{G_{11}}{v_1}$	CI	$\frac{G_{11}}{v_1}$	CI	$\frac{G_{11}}{v_1}$	CI	$\frac{G_{11}}{v_1}$	CI	$\frac{G_{11}}{v_1}$	CI	$\frac{G_{11}}{v_1}$	CI
0.025	-28.	0.6	-22.	0.7	---		-31.	0.9	-69.	0.9	-32.	0.9	3.2	1.0
0.05	-10.	0.5	-15.	0.6	-6.1	0.7	-15.	0.9	-7.8	1.	-27.	0.9	6.3	1.0
0.1	-15.	0.5	-12.	0.6	-5.5	0.6	-10.	0.9	-3.3	1.	-18.	0.9	6.4	1.1
0.2	-11.	0.5	-6.2	0.7	-4.3	0.5	-5.4	0.9	-1.0	1.	-10.4	0.9	8.1	1.1
0.3	-7.8	0.5	-1.0	1.0	-3.4	0.5	-2.7	0.9	0.68	1.	-1.0	1.0	8.1	1.2
0.4	-6.1	0.6	3.5	1.4	-3.3	0.4	4.5	1.2	0.81	1.	2.2	1.1	8.1	1.3
0.5	-3.8	0.7	1.0	1.1	-2.9	0.5	---		-1.0	1.	---		8.2	1.4
0.6	-1.4	0.9	1.3	1.2	-0.31	0.9	---		---		---		9.0	1.7
0.7	0.5	1.1	3.4	1.8	1.4	1.4	---		---		---		9.4	1.9
0.8	3.2	1.4	---		---		---		---		---		12.	2.6
0.9	4.1	1.7	---		---		---		---		---		16.	4.4
0.95	8.1	2.6	---		---		---		---		---		25.	9.6
0.975	14.	4.	---		---		---		---		---		---	

(a) Sorption data from reference 23

C. Discussion

1. Hydroxypropyl Cellulose (HPC)

Since HPC is miscible with water, sorption would be expected to proceed differently from adsorption on the other, insoluble cellulosics. This is seen in its Zimm clustering plot, figure 7-1. HPC is the only polymer that had a uniformly positive value of G_{11}/v_1, or a negative slope of the curve (a_1/ϕ_1) vs. a_1, down to very low water content. This corresponds to the existence of clustering even near infinite dilution, as shown in Table 7-1.

At the lowest water content, the slope of the Zimm curve is positive, rising from the infinite dilution value of a_1/ϕ_1. The difference between the infinite dilution value and the value extrapolated from finite concentration in figure 7-1 is equal to the suggested correction for the accessibility of the polymer to water (21). If this is not a coincidence, then it shows that any regions of inaccessibility disappear at an exceedingly low water content.

A Starkweather plot of w_1/CI vs. w_1 for HPC (figure 7-2) has a slope decreasing from one at infinite dilution to zero at higher water content, showing that sorption goes from random sorption at lowest water content to extensive clustering. The point at which the slope of the curve in figure 7-2 goes to zero is very close to an average concentration of three water molecules per HPC unit (2.95 ± 0.1), or one water molecule for every hydroxyl group. Since this concentration corresponds to an average cluster size of between two and three water molecules, most of the initial sorption must take place on a single site; possibly the one

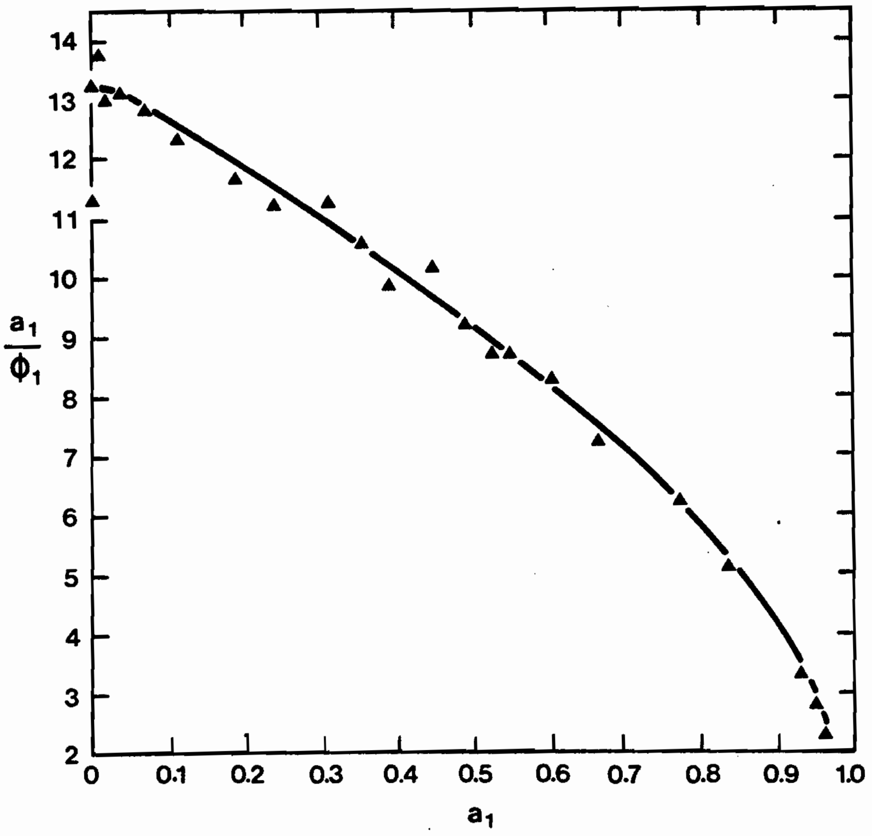

FIGURE 7-1 Zimm clustering plot (a_1/ϕ_1 vs. a_1) for hydroxypropyl cellulose. Values of the clustering function G_{11}/v_1 were calculated using the slopes of this curve and equation 7-5.

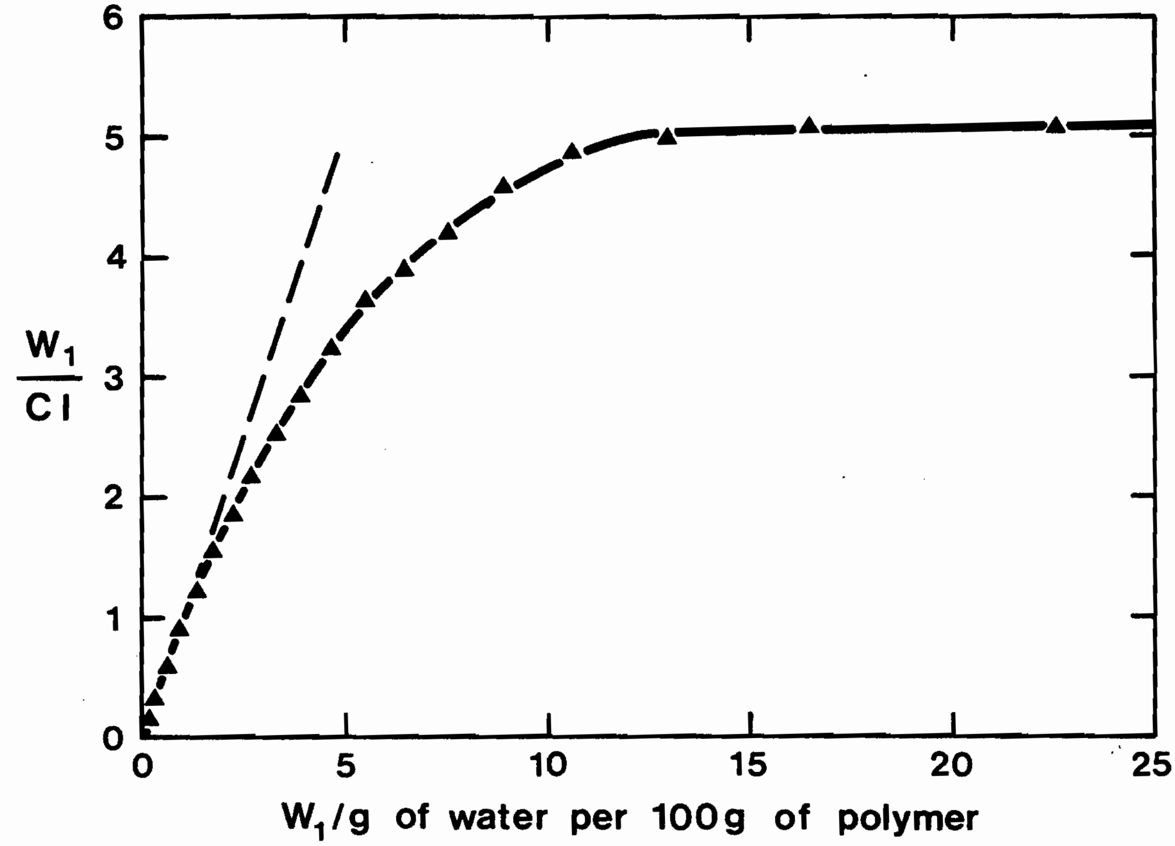

FIGURE 7-2 Starkweather plot (w_1/Cl vs. w_1) for hydroxypropyl cellulose. See text for explanation.

unsubstituted hydroxyl group believed to exist on the HPC backbone (22). This aspect is important to the discussion of the heats of mixing of water and HPC in Chapter 5 of this thesis. As shown in figures 5-4 and 5-5, the concentration of three water molecules per HPC unit, at a volume fraction of water of 0.145, is near the concentration where changes in the activites of water are first seen at the LCST. Furthermore, this is also the concentration where the ΔH curve (figure 5-5) shows a maximum.

2. Cellulose

The cluster calculations performed by Starkweather (15) on the data of Morrison and Dzieciuch for the sorption of water by cotton cellulose (23) were repeated. The Zimm clustering plot for cellulose (figure 7-3) shows a very strong antipathy to clustering at low water content (non-random, specific sorption), followed by clustering at higher water content. The Starkweather plot shown in figure 7-4 has three major regions. At low water content, the slope is greater than one, so that sorption is non-random. In the intermediate region, the slope is roughly zero, so that there is an increase in the size but not the number of clusters. At highest water content, the slope is negative, indicating a decrease in the number of clusters (joining together of previously independent clusters).

The boundaries between these regions in figure 7-4 occur at about 4.5 ± 0.5 and at about 13 ± 1 grams of water per one hundred grams of polymer, or about 0.43 and 1.2 water molecules per anhydroglucose unit. Since cotton cellulose is only about 40% accessible to water(24) -- changing

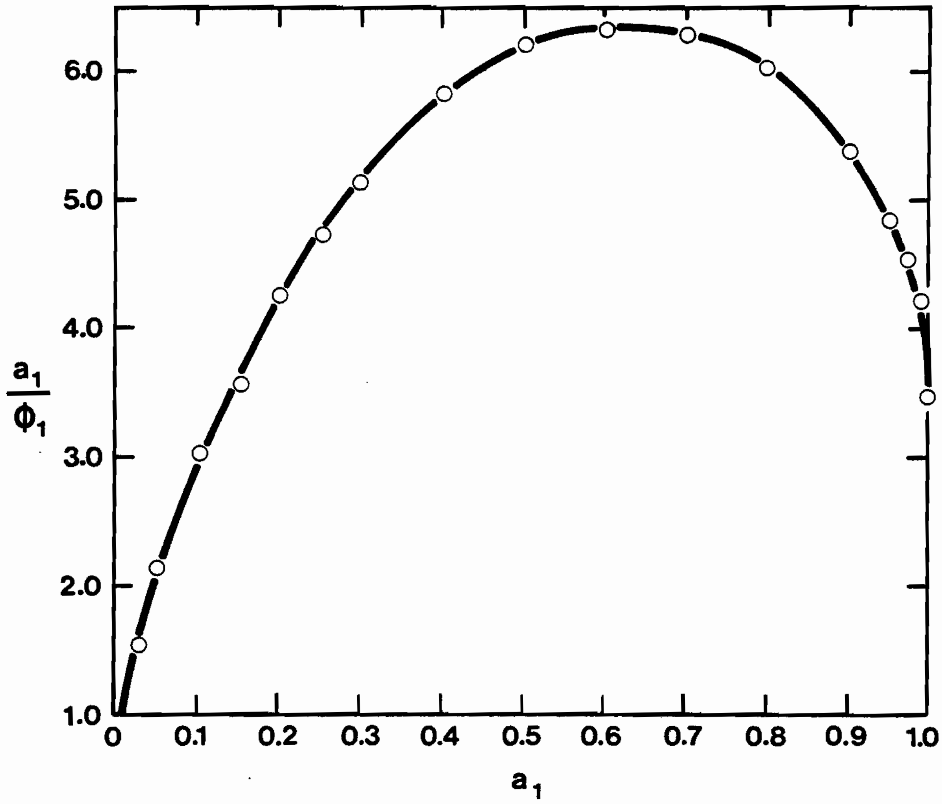

FIGURE 7-3 Zimm clustering plot for cellulose; data from reference 23.

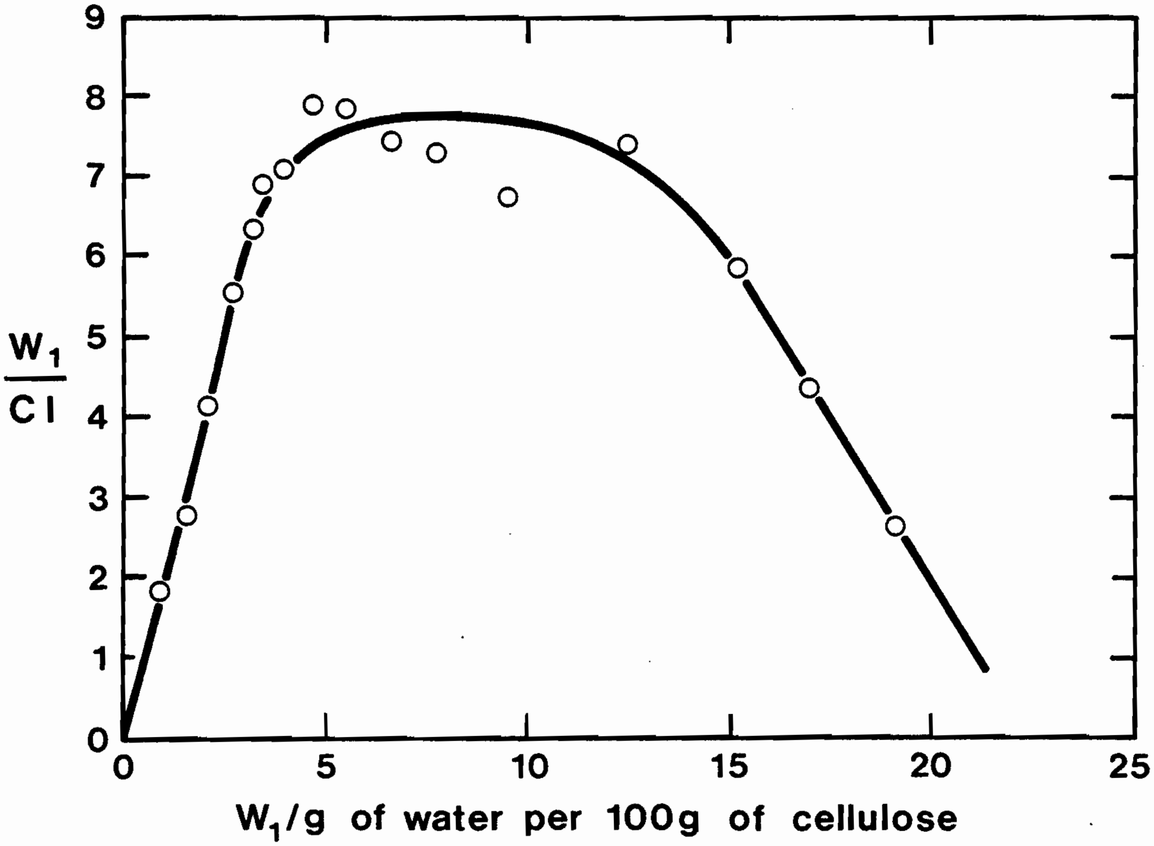

FIGURE 7-4 Starkweather plot for cellulose.

little with water content -- the values must be adjusted. The first boundary where the slope goes to zero is the area where clusters start to grow in size but not in number. This therefore occurs at one water molecule per unit. The second inflection, after which water sorbs by the joining together of previously separated clusters, occurs at three water molecules per unit, with an average cluster size of about two.

3. Cellulose Acetate (D.S. = 2.45) and Ethyl Cellulose

It has already been shown that these two polymers have similar sorption isotherms (25). The similarity carries over to the cluster calculations. In each case, G_{11}/v_1 was much less than minus one at low water content, indicative of an antipathy towards clustering, as in the case of cellulose. Clustering starts to occur at an intermediate water content ($a_1 \simeq 0.30$ to 0.35). The slopes of the corresponding Starkweather plots (figure 7-5) went from somewhat greater than one (non-random sorption) to zero. The zero slope, which occurs as the average cluster size reaches one molecule, was observed when a concentration of 0.37 ± 0.05 water molecules per anhydroglucose unit was reached. This concentration is lower than expected if a single water molecule associates with each hydroxyl group on the polymer. For cellulose acetate with an average of 0.55 hydroxyl groups per unit, this would mean an accessibility to water of (0.37/0.55) or about 70%, in reasonable agreement with admittedly variable literature sources (26,27).

Stannett and Williams (28) performed cluster calculations on sorption isotherms of cellulose acetate (D.S. = 2.25) and ethyl cellulose (D.S. = 2.55) at higher water content than reported here. They noted

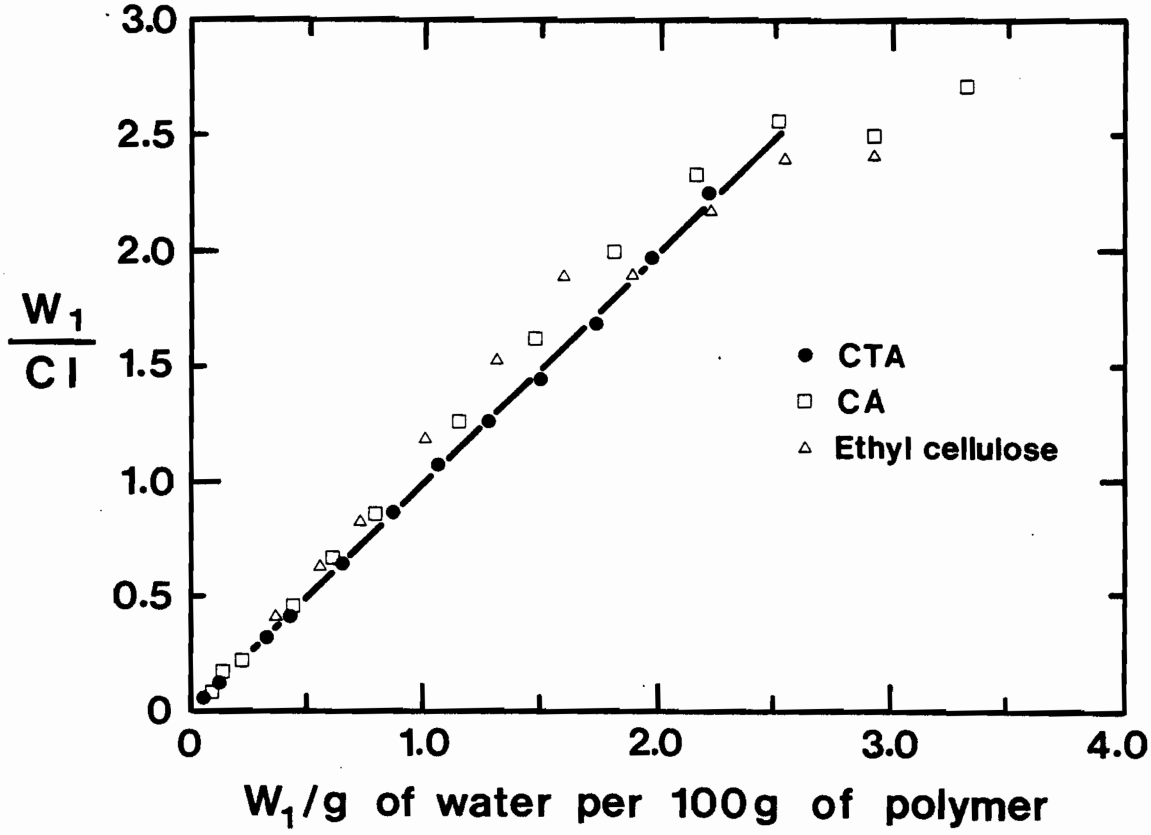

FIGURE 7-5 Starkweather plot for cellulose acetate (□); cellulose triacetate (●); and ethyl cellulose (△). The solid line was drawn with unit slope, for the sake of illustration.

that the existence of clustering in ethyl cellulose might be related to its inability to act as a membrane for reverse osmosis, or, conversely that cellulose acetate is effective in reverse osmosis since water does not cluster within it.

4. Cellulose Triacetate

At very low water content, G_{11}/v_1 is much less than one for CTA, again indicating highly non-random and specific sorption (figure 7-6 and Table 7-1). However, the clustering function very soon approached the value of minus one expected for ideal random sorption at a water content corresponding to 0.03 water molecules per anhydroglucose unit and an average cluster size of about one water molecule. This may result either from the existence of unsubstituted hydroxyl groups or from sorption onto other preferred sites such as gaps and voids or oxidation products. Part of the discrepancy may also be due to the non-ideal behavior of the GC chromatogram at very low water content (25).

The slope of the Starkweather plot did not follow the trend of the other cellulosics by going to zero at the saturation point. Instead, the slope was equal to unity from infinite dilution and upwards, indicating random sorption (figure 7-5). This difference in sorption behavior between CA and CTA has been the subject of speculation for many years (29). The mechanism based on clustering was confirmed by recent infrared measurements near the saturation point on CA and CTA samples of the same D.S. as those used here (30). In the latter work, the authors showed that water in CTA is present largely as monomers "dispersed" through the polymer, while water in CA is "dissolved" as clusters of up to three water molecules in size.

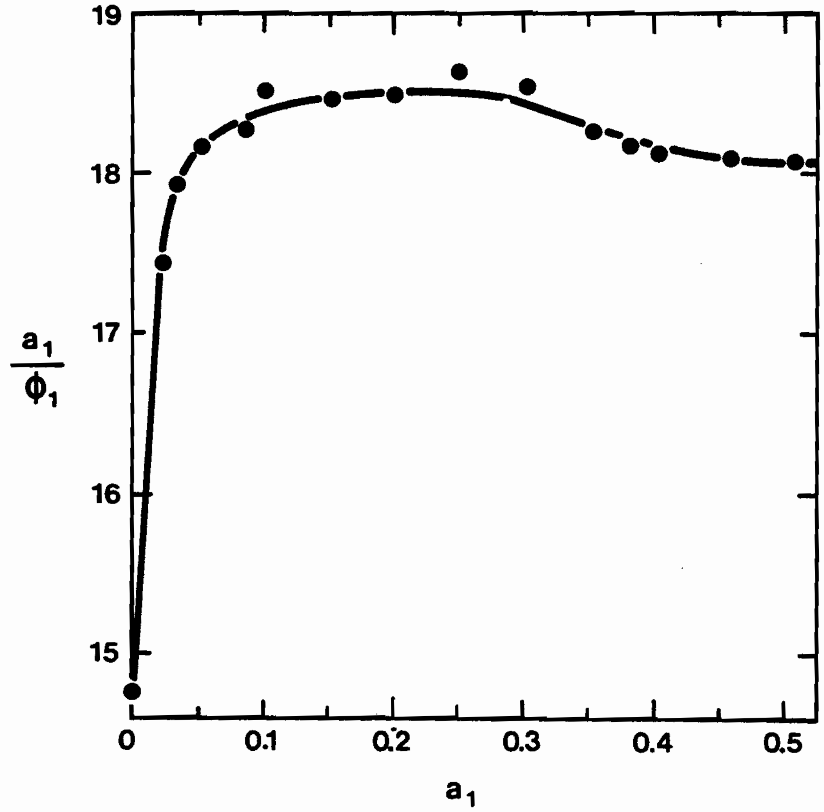

FIGURE 7-6 Zimm clustering plot for cellulose triacetate.

5. Cellulose Monoaceate

It should be noted that since both cellulose and CMA show a very distinct hysteresis in their sorption/desorption curves, it is not strictly correct to apply a theory such as this one which is based on equilibrium thermodynamics. Nevertheless, we apply it to the sorption and desorption curves in order to interpret them in molecular terms.

Figure 7-7 gives the Starkweather plots for both sorption onto and desorption from the CMA sample. In the sorption process, at the lowest water content, the antipathy towards clustering of the other cellulosics is seen. The first plateau of zero slope, which may be an artefact of the experimental scatter, exists between 0.4 and 1 water molecule per unit, and corresponds to sorption without increase in the number of clusters present. A brief period of random sorption (slope = 1) follows, until a second plateau is seen at a concentration of about 1.5 water molecules per unit. Since this material should have 2.1 free hydroxyl groups per unit, the conclusion is again that the polymer is not completely accessible to water. CMA is soluble in water, but with difficulty, so that this polymer provides an example of properties between the water soluble HPC and the insoluble cellulose. The high proportion of accessible hydroxyl groups in this polymer -- already cited as the cause of the hysteresis in the sorption isotherm -- would also account for the behavior of this polymer in the cluster model. At low water content, it would act as an insoluble cellulosic, but at higher water content, all hydroxyl groups must eventually become accessible, allowing it to dissolve in water. At high enough water content, the cluster model for CMA would then follow that of HPC.

In the desorption curve, the high concentration plateau occurs at

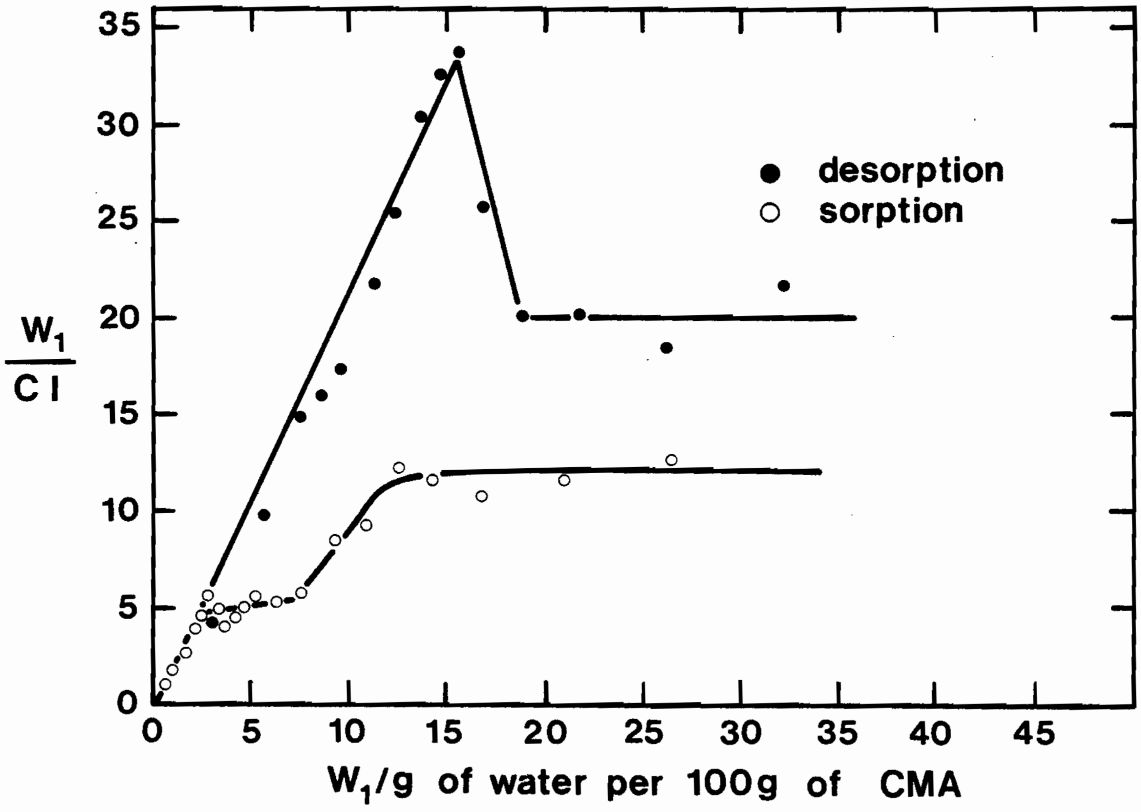

FIGURE 7-7 Starkweather plot for cellulose monoacetate: sorption (○) and desorption (●).

nearly twice the value of w_1/Cl, indicating that a greater number of clusters are contributing to this process. In this region, desorption occurs from pre-existing clusters, without a decrease in their number. Following the curve backwards, there is a very positive slope ($w_1 \simeq 19$ down to $\simeq 15$ g of water per one hundred g of polymer), indicating a sharp increase in the number of clusters as bridging molecules desorb. Finally the negative slope down to $w_1 = 0$ shows that the number of clusters is decreasing. Since the slope is constant down to zero, and since this represents the region of strong antipathy towards clustering, this region probably represents the desorption of individual molecules, especially since it coincides with the equivalent region in the sorption curve. This is in agreement with the suggestion (15) that the greatest tendency towards desorption occurs when two water molecules are together, since isolated molecules are more strongly held to the polymer.

D. References

1) A. Venkateswaran, Chem. Rev., 70, 619 (1970).

2) M. Kimura, H. Hatakeyama, M. Usuda, and J. Nakano, J. Appl. Polym. Sci., 16, 1749 (1972); also S. Svanson, J. Appl. Polym. Sci., 22, 571 (1978); E. Hsi, G.J. Vogt, and R.G. Bryant, J. Coll. Interface Sci., 70, 338 (1979).

3) Y. Taniguchi and S. Horigome, J. Appl. Polym. Sci., 19, 2743 (1975).

4) S. Brunauer, P.H. Emmett, and E. Teller, J. Am. Chem. Soc., 60, 309 (1938).

5) P.R. Tremaine and D.G. Gray, Anal. Chem., 48, 380 (1976).

6) A.J. Hailwood and S. Horrobin, Trans. Farad. Soc. 42B, 84 (1946).

7) C.H. Nicholls and J.B. Speakman, J. Text. Inst., 46, T264 (1955).

8) C.H. Nicholls and J.B. Speakman, ibid, T424 (1955).

9) D.S. Varma and D.K. Sadhir, J. Appl. Polym. Sci., 23, 393 (1979).

10) R.L. D'Arcy and I.C. Watt, Trans. Farad. Soc., 66, 1236 (1970).

11) B.H. Zimm, J. Chem. Phys., 21, 934 (1953).

12) B.H. Zimm and J.L. Lundberg, J. Phys. Chem., 60, 425 (1956).

13) J.L. Lundberg, J. Macromol. Sci. -- Phys., B3, 693 (1969).

14) H.W. Starkweather, Jr.,Polym. Lett., 1, 133 (1963).

15) H.W. Starkweather, Jr., Macromolecules 8, 476 (1975).

16) A.H. Nissan, in "Fibre-Water Interactions in Papermaking, Transactions of the Symposium held at Oxford, September, 1977", W. Clowes and Sons, Ltd., Oxford, 1978, p. 609.

17) R.M. Barrer and J.A. Barrie, J. Polym. Sci., 28, 377 (1958).

18) M. Yasuda and V. Stannett, J. Polym. Sci., 57, 907 (1962)

19) U. Coelho, J. Miltz, and S.G. Gilbert, Macromolecules 12, 284 (1979).

20) U. Coelho, J. Miltz, and S.G. Gilbert, J. Food Sci., 44, 1150 (1979).

21) This Thesis, Chapter 4.

22) R.J. Samuels, J. Polym. Sci. Part A2, 7, 1197 (1969).

23) J.L. Morrison and M.A. Dzieciuch, Can. J. Chem., 37, 1379 (1959).

24) O. Sepall and S.G. Mason, Can. J. Chem., 39, 1934 (1961).

25) This Thesis, Chapter 6.

26) M. Lewin, H. Guttman, and N. Saar, J. Appl. Polym. Sci., Appl. Polym. Symp., 28, 791 (1976).

27) L. Valentine, Text. Res. J., 45, 670 (1954).

28) V. Stannett and J.L. Williams, in "Fibre-Water Interactions in Papermaking, Transactions of the Symposium held at Oxford, September, 1977", W. Clowes and Sons, Ltd., Oxford, 1978, p.497.

29) P.T. Newsome and S.E. Sheppard, J. Phys. Chem., 36, 930 (1932).

30) C. Toprak, J.N. Agar, and M. Falk, J. Chem. Soc., Farad. Trans. 1, 75, 803 (1979).

CHAPTER 8

SUMMARY

The major emphasis of this thesis has been on the study of the interactions of cellulosic polymers with water by inverse gas chromatography. Throughout, an effort has been made to exploit the advantages of the GC method, while recognizing the problems that are inherent in its application to a system consisting of a polar probe plus a polar polymer.

Admittedly, these GC results do not achieve the very high precision of other GC data in the literature for some non-polar systems. On the other hand, for the first time direct measurements have been made in a concentration region that has been little studied in the past. Valuable illustrations of GC non-ideality and of possible corrections have also been shown. The results herein are more reliable than much of the data in the GC literature, where non-ideal effects are too often ignored. In addition, the work supplements older literature data for cellulosic systems by extending measurements to lower water contents.

The sorption measurements by classical static methods at finite concentration were a useful addition to the GC data. It was found that all of the various GC and static sorption methods gave the same answer, within the appropriate concentration range.

The first success of the work was in the examination of hydroxypropyl cellulose (HPC), a polymer that forms a liquid crystalline mesophase with cholesteric structure in a large number of solvents, including water. The behavior of HPC in water at very low water content was successfully described by Flory's theory for a system of very stiff or rod-like molecules. At higher concentration, the system deviated from the rod-like molecule theory and started to approach the behavior expected from the regular Flory-Huggins solution theory. This changeover from "rod-like" to "Flory-Huggins" mixing was seen to occur in the concentration region where optical measurements have shown the formation of the liquid crystalline mesophase from the isotropic solution.

Isotherms measured by inverse GC and static methods above and below the lower critical solution temperature (LCST) of HPC were used to calculate heats of mixing of water with HPC from 0 to 50% water. The measured activities and the calculated heats of mixing of water showed the effect of the LCST, in that the activities of water vapor went to unity at high concentrations above the LCST, and the heats of mixing went to zero. At an ideal phase separation, this would be expected, since effectively one is measuring the activity of pure water vapor over the precipitated polymer phase. The quantitative effect of the concentration of water in the liquid crystalline mesophase on this behavior is uncertain. However, it is suggested that there may be some type of "saturation point" at about three water molecules per HPC unit.

Results on the sorption of water by cellulosic polymers, including several cellulose acetates, showed the effect of non-ideal GC interactions. These were satisfactorily explained as having resulted from peak spreading due to slow diffusion within the polymer bulk. The necessary corrections were made, but the effect reduced the precision of the data. The order of the heats of mixing at infinite dilution with substituion on the cellulose backbone showed the importance of the interaction between water and the unsubstituted hydroxyl groups.

Zimm's cluster integral theory was used to interpret the finite concentration sorption isotherms. The modification derived by Starkweather was also applied. The theory leads to a plausible molecular picture of the adsorption of water by the cellulose derivatives, without requiring a detailed model for the mixing behavior.

In an appendix to this thesis, the sorption of a large number of organic probes onto HPC is investigated. Interaction parameters and heats of mixing at infinite dilution are measured. No correlation is observed between these values and the ability of HPC to form a liquid crystalline mesophase in a given solvent.

CLAIMS TO ORIGINAL RESEARCH

The studies described within this thesis should help to establish inverse gas chromatography as an adjunct to other methods of studying water-polymer interactions. The following claims to original research in the sorption of water by cellulosic polymers at low water content are made:

-- The experimental results represent the first time that water has been used as probe in a systematic fashion in the examination of polar polymers by inverse gas chromatography, and only the third or fourth time in which water has ever been used as probe. It is also the first time in which water has been used as a probe for cellulosic polymers.

-- Two gas chromatographic and two classical static methods of sorption isotherm measurement gave the same results within the appropriate concentration region.

-- The sorption isotherms of water on hydroxypropyl cellulose were measured between 15 and 55°C. At low water content, HPC fits very well Flory's theory for the mixing of a solvent with a collection of rod-like molecules. This is one of very few studies on the mixing of solvent with ordered polymer solutions, and the first involving GC measurements of solvent activity over such a solution.

-- The behavior of the sorption isotherms of HPC at a phase separation point was in accordance with expected behavior, in that calculated heats of mixing went to zero at temperatures above the phase separation point and at sufficiently high water content. This is the first reported attempt at GC measurements of a polymer phase separation.

-- Non-ideal (kinetic) GC effects resulting from polar interactions were examined in detail. The change in retention volume with gas flow rate and column loading was the reverse of that reported for kinetic effects on non-polar polymers that show linear isotherms. The effects were interpreted as resulting from a combination of isotherm curvature and slow solvent-polymer equilibration, and are most serious for the more polar polymers.

-- The results for the infinite dilution thermodynamic properties of water and cellulosic polymers were far more reliable than those in the literature measured by other techniques, although as a result of the kinetic effects, the precision is lower than found for many non-polar systems by inverse GC.

-- The heats of mixing at infinite dilution of water on cellulosic polymers were calculated for the first time. It was suggested that the most important contribution to the heat of mixing is from the interaction of water with unsubstituted hydroxyl groups on the polymers.

-- The sorption isotherms of water were measured on the cellulosic polymers at low water content by inverse GC techniques, and Zimm's cluster integral theory was used to analyze the sorption isotherms. Good agreement was found between the calculated saturation points and the accessibility of the cellulose acetates, as well as with results in the literature regarding their mechanism of sorption.

-- In an appendix to this thesis, the interaction of a range of organic solvents with HPC was investigated for the first time. No correlation was found between the polymer-solvent interactions at infinite dilution and the ability of the solvents to form a liquid crystalline mesophase with HPC.

Suggestions for Further Work

In light of the results shown in this thesis, several areas can be seen where further work might be profitable.

Now that the applicability of inverse GC on cellulose derivatives with water as probe has been shown, the interaction of water with other polymers at infinite dilution might be measured. Such measurements should cast light on the general problem of the nature of aqueous solutions. The measurement of heats of mixing for water and polymers by modern microcalorimetric techniques would supplement the data based on water activity measurements by GC.

For HPC, the results with organic probes would be put into better perspective if the phase diagrams and critical points with different solvents were known. The GC methods could also be applied to other rod-like or mesogenic polymers.

At finite concentration, Zimm clustering calculations on isotherms of polymers with well-defined inaccessible regions could settle the relationship between the cluster theory and the degree of accessibility. These could be compared to cluster sizes estimated from other techniques such as infrared spectroscopy or differential scanning calorimetry.

Finally, GC techniques can in general be applied to the measurement of sorption isotherms of water on both hydrophilic and hydrophobic polymers, once correction has been made for non-ideal GC effects. This might include a greater reliance on the "elution on a plateau" technique, especially for cellulose itself. However, there is as yet no rigorous theory for chromatography in situations where both kinetic effects and curved isotherms are encountered. The development of a tractable approach to this problem would be of great value.

APPENDIX A

THE SORPTION OF NON-AQUEOUS PROBES ONTO HYDROXYPROPYL CELLULOSE

ABSTRACT

Infinite dilution thermodynamic data are obtained for the interaction of a large number of organic probes with hydroxypropyl cellulose. No correlation is observed between the thermodynamic data and the tendency of this polymer to form a lyotropic liquid crystalline mesophase in a given solvent. A hitherto unreported glass transition temperature at about 10°C for hydroxypropyl cellulose is apparent from the gas chromatographic results.

A. Introduction

As part of the investigation of the solution properties of hydroxypropyl cellulose (HPC), the sorption of a large number of organic probes was measured by inverse GC. The initial impetus for this work was the discovery that HPC forms lyotropic liquid crystalline mesophases in several organic solvents (1) as well as in water (2). DiPaola-Baranyi and Guillet (3) recently proposed a method by which the solubility parameter of a polymer, δ_2, could be obtained from inverse GC measurements at a single temperature, using the infinite dilution retention of a series of probes. The applicability of the method to HPC was examined.

The solubility parameter of a substance, δ, has been defined as (4):

$$\delta \equiv [(\Delta H_v - RT)/V]^{\frac{1}{2}} \qquad \text{(A-1)}$$

where ΔH_v is the heat of vaporization and V the molar volume. This equation was combined with the Flory-Huggins solution theory to yield the interaction parameter as a function of the difference between the solubility parameters of solvent and substrate (4):

$$\chi_{12} = V_1(\delta_1 - \delta_2)^2/RT - \beta \qquad \text{(A-2)}$$

where β is the correction for the existence of the non-combinatorial entropy of mixing. DiPaola-Baranyi and Guillet rearranged the previous equation to obtain with $\beta = 0$ (3):

$$\left(\frac{\delta_1^2}{RT} - \frac{\chi_{12}}{V_1}\right) = \left(\frac{2\delta_2}{RT}\right)\delta_1 - \frac{\delta_2^2}{RT} \qquad \text{(A-3)}$$

and proposed that a plot of $(\delta_1^2/RT - \chi_{12}^{\infty}/V_1)$ vs. δ_1 would yield $2\delta_2/RT$ as slope and $-(\delta_2^2)/RT$ as intercept. Another version (5) takes advantage of the equation:

$$\Delta\bar{H}_m = V_1(\delta_1 - \delta_2)^2 \qquad \text{(A-4)}$$

After suitable rearrangement, the previous equation allows δ_2 to be determined from a plot of $\Delta\bar{H}_m$ vs. δ_1. A δ_2 value of 21.9 $(\text{J cm}^{-3})^{\frac{1}{2}}$ for HPC was recently derived from solubility measurements (6).

B. Results and Discussion

1. Infinite Dilution Results

Retention volumes were measured at 50.2°C for twenty five probes of different types. Peaks were extrapolated to zero height, but no correction was made for the effect of gas flow rate, which for a good solvent such as water was small (7). Values of χ_{12}^{∞} were calculated from equation 2-30. With water as probe, there was no need to correct for the second virial coefficient, B_{11}. However, the contribution from B_{11} for the organic probes was larger. Since the second virial coefficient changes with temperature, it was especially important to make this correction when retention was being measured as a function of temperature. Where available, values of B_{11} were taken from the literature (8). For several of the probes, values of B_{11} were calculated using the Bertholet equation (9):

$$B_{11} = \frac{9}{128} \frac{RT_c}{P_c} \left(1 - \frac{6T_c^2}{T^2}\right) \qquad \text{(A-5)}$$

where the value of B_{11} at a temperature T is a function of the critical temperature T_c and the critical pressure P_c. There were several probes for which critical data could not be found. As the probes concerned were only used at a single temperature and have a very low vapor pressure at 50°C, the error can be dismissed.

The vapor pressures of the probes at a temperature T were calculated from the Antoine equation:

$$\log_{10} P = A + \frac{B}{T + C} \qquad \text{(A-6)}$$

where A, B, and C are constants obtained from the literature (10-14). For several probes, vapor pressures at different temperatures were fitted to a polynomial function, and desired vapor pressures were interpolated from these functions. The heats of vaporization of the pure probes at a given temperature were calculated from the Clausius-Clapeyron equation (15):

$$-\frac{\Delta H_v}{2.303RT^2} = \frac{\partial(\log_{10}P)}{\partial(T)} \qquad \text{(A-7)}$$

The molar volumes of the probes were calculated from published densities and thermal expansion coefficients (10-14).

Table A-1 gives values of χ_{12}^{∞} for the twenty five probes. Also shown are values of the probe solubility parameter δ_1 calculated from equation A-1 and the quantities δ_1^2/RT and χ_{12}^{∞}/V_1 from equation A-3. Heats of mixing at infinite dilution, $\overline{\Delta H}_m^{\infty}$, were calculated from equation 2-34 using experimental activity coefficients at temperatures above 40°C for twelve probes. Results are shown in Table A-2. The errors given are the standard deviations of the least squares data.

The infinite dilution data presented in Tables A-1 and A-2 show the difficulties in the use of the derivation of DiPaola-Baranyi and Guillet (3) in the calculation of the polymer solubility parameter δ_2. The negative heats of mixing of HPC with most of the probes automatically invalidate the use of that derivation for this polymer. Even if the negative heats were not a problem, examination of the two terms on the left hand side of equation A-3 shown in Table A-1 reveals that the term δ_1^2/RT is much greater than the term χ_{12}^{∞}/V_1. Therefore any

Table A-1

Infinite Dilution Thermodynamic Data at 50.2°C for Organic Probes

Probe	χ_{12}^{∞}	δ_1 $(\mathrm{J\ cm^{-3}})^{\frac{1}{2}}$	δ_1^2/RT	χ_{12}^{∞}/V_1
water (a)	1.55	47.06	0.824	0.073
methanol (a)	0.47	28.96	0.312	0.011
ethanol (a)	0.38	25.56	0.243	0.006
1-propanol (a)	0.26	23.95	0.213	0.004
2-propanol	0.43	24.17	0.217	0.006
1-butanol	0.26	24.17	0.217	0.003
acetone	0.38	19.27	0.138	0.005
n-butyl acetate	0.14	17.22	0.110	0.001
1,4-dioxane (a)	0.06	19.34	0.139	0.001
tetrahydrofuran (a)	-0.12	18.62	0.129	-0.002
diethyl ether	-0.14	15.05	0.084	-0.001
cyclohexanol (b)	2.31	20.98	0.164	0.021
cyclohexanone	0.18	20.09	0.150	0.002
cyclohexane (b)	0.96	16.34	0.099	0.009
toluene (b)	0.17	17.71	0.117	0.002
n-heptane (b)	0.10	14.76	0.081	0.001
n-decane (b)	1.83	18.80	0.143	0.009
acetic acid (a)	-2.28	25.62	0.244	-0.038
acetic anhydride (a)	-1.65	20.82	0.161	-0.017
dimethyl sulfoxide (a)	-0.19	25.77	0.247	-0.003
N,N-dimethyl formamide (a)	-0.01	29.26	0.319	0.0
pyridine (a)	-0.42	21.04	0.165	-0.005
dichloromethane (b)	-0.38	19.78	0.146	-0.006
chloroform	-0.73	17.99	0.120	-0.009
carbon tetrachloride (b)	0.45	16.84	0.106	0.004

(a) forms liquid crystalline mesophase
(b) non-solvent

Table A-2

Partial Molar Heats of Mixing of Organic Probes with HPC

Probe	Temperature Range	$\Delta\bar{H}_m^\infty$ (kJ mol^{-1})
water	15 - 85°C	-5.7 ± 0.6
methanol	40 - 75°	-4.4 ± 1
ethanol	40 - 75°	-1.4 ± 0.7
1-propanol	40 - 75°	-1.8 ± 0.8
1-butanol	40 - 75°	-1.9 ± 0.8
acetone	40 - 60°	-3.1 ± 1.3
1,4-dioxane	40 - 85°	-0.7 ± 0.6
tetrahydrofuran	40 - 100°	0.2 ± 0.4
chloroform	40 - 70°	-4.8 ± 1
toluene	40 - 85°	0.2 ± 0.6
n-heptane	45 - 85°	2.6 ± 0.7
n-decane	40 - 70°	5 ± 2

calculations based on these experimental values of χ_{12}^{∞} would be open to serious scatter. In fact, insertion of the data in Table A-1 into equation A-3 yields a "value" of δ_2 close to the mean value of all the δ_1's (water omitted).

The data in Tables A-1 and A-2 were also examined in order to determine whether any trend exists with regard to the formation of liquid crystalline mesophases. No trend is evident. In fact, it now seems that HPC will form a liquid crystalline mesophase in any solvent in which the necessary high concentration can be achieved (19). Further correlations will require knowledge of the phase diagrams of the various solvents with HPC.

The heats of mixing in Table A-2 are of little additional help. The heats of mixing of the alcohols reflect more the changes in their own structure than any difference between mesogenic and non-mesogenic behavior. The mesogenic ethers dioxane and THF show smaller (more endothermic) heats of mixing than the non-mesogenic 1-butanol and acetone. Even chloroform, with the second most negative heat of mixing, is probably not a mesogenic solvent (19).

2. The Glass Transition

Figures A-1 and A-2 show the specific retention volumes at infinite dilution for n-heptane and tetrahydrofuran (THF), respectively a non-solvent and a fair solvent for HPC. A very clear glass transition temperature can be seen at about 10°C. In GC measurements, these Z-shaped curves are characteristic of a glass transition temperature, resulting from a change in retention mechanism from equilibrium surface

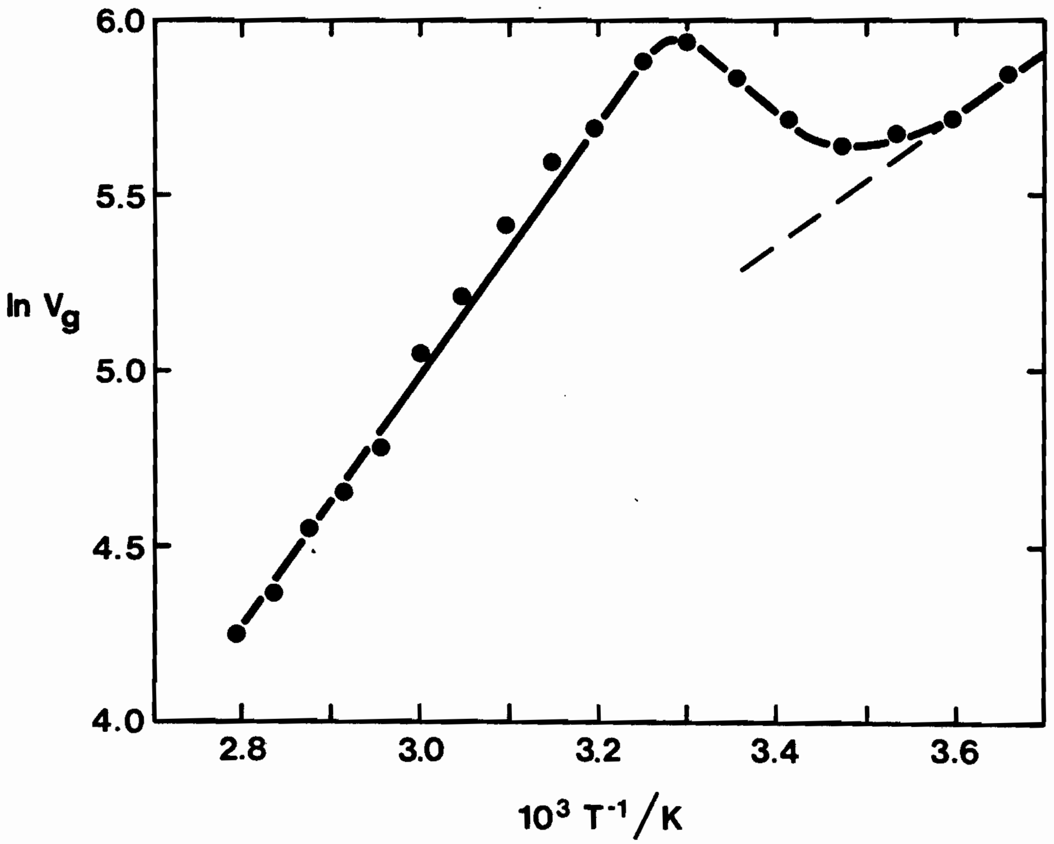

FIGURE A-1 Retention diagram of the log specific retention volume vs. inverse absolute temperature for n-heptane on HPC.

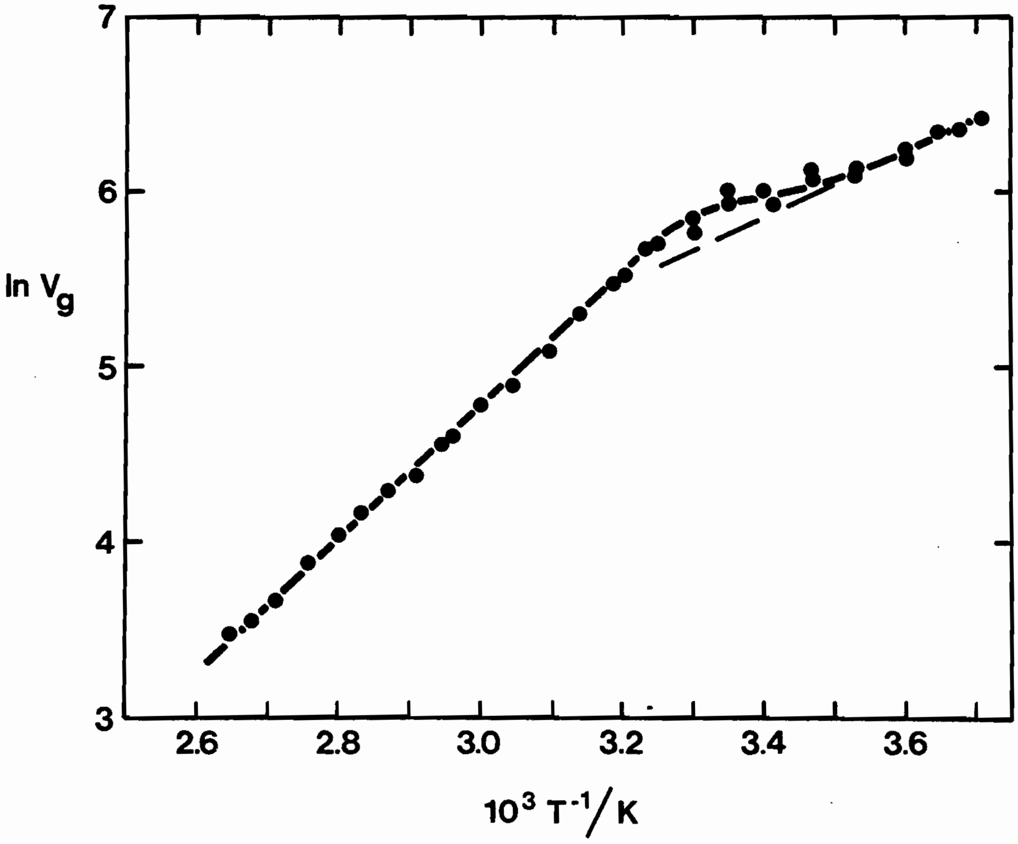

FIGURE A-2 Retention diagram of the log specific retention volume vs. inverse absolute temperature for THF on HPC.

adsorption below T_g to surface adsorption plus non-equilibrium bulk sorption in the region immediately above T_g. At a temperature sufficiently far enough above T_g, a state of equilibrium bulk sorption plus surface adsorption is reached. As is normal, the glass transition was taken to be the first point of deviation from linearity on the low temperature side of the curve. The existence of T_g was confirmed by differential scanning calorimetry.

The fundamental criterion for detection of a glass transition by inverse GC is that the probe be able to mix with the bulk of the polymer above T_g, but only adsorb onto the polymer surface below T_g (16). This behavior can clearly be seen for n-heptane in figure A-1 and for THF in figure A-2. No sign of a glass transition temperature was seen with good solvents such as water, ethanol, and methanol. This is generally accepted to be the result of the ability of a good solvent to penetrate even the glassy polymer, acting as a plasticizer to lower T_g. A non-solvent, toluene, did not show the glass transition temperature. This probably means that toluene is such a poor solvent that it cannot penetrate the polymer bulk, even above T_g. Discrepancies in the value of T_g from figures A-1 and A-2 may result from similar differences between n-heptane and THF.

3. Finite Concentration Results

Sorption isotherms at 25°C are shown in figure A-3 for three solvents (acetone, ethanol, and THF), and for one non-solvent (n-decane). The isotherm for n-decane was obtained by inverse GC, while the others were measured on the vacuum microbalance apparatus.

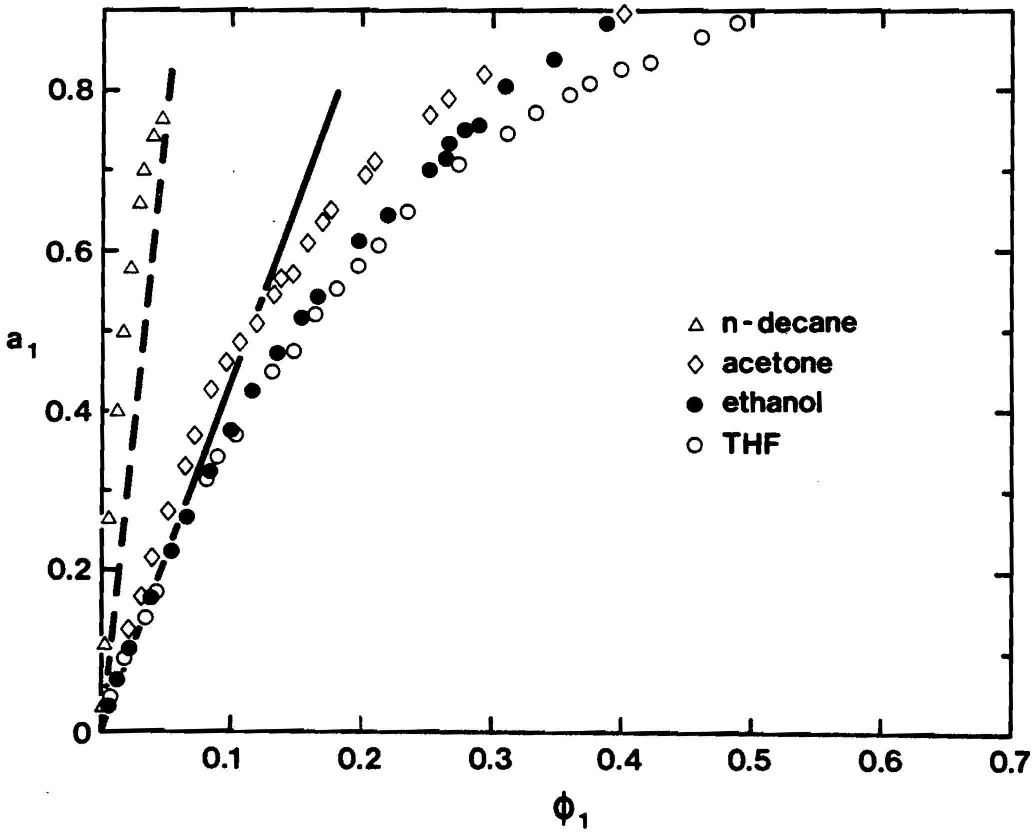

FIGURE A-3 Sorption isotherms on HPC at 25°C

(△) n-decane, measured by inverse GC; (◇) acetone, (●) ethanol, and (○) THF measured on the vacuum microbalance apparatus. The solid line and the dotted line were calculated assuming rod-like mixing for ethanol and n-decane, respectively. See text for details.

The solid line in figure A-3 was calculated for ethanol using Flory's equation for the solvent activity over an ordered polymer phase (17), as introduced in Chapter 2 of this thesis (equation 2-40). The value of the orientation parameter y was taken to be one, indicating perfect orientation of the polymer, while the rod-like model interaction parameter χ_R was obtained by subtracting unity from χ_{12}^{∞} for ethanol in Table A-1, after correction to 25°C. The dotted line in figure A-3 was calculated from the value of χ_R for n-decane.

It can be seen that the calculated solid line fits the ethanol sorption data at low ethanol concentrations. As in the case of water shown in Chapter 4 of this thesis, the system deviates from the ideal rod-like model behavior at a concentration of somewhat less than one solvent molecule per HPC unit. The fit between the rod-like molecule theory and the isotherms for the other solvents is poorer. It is possible that a better fit would result if preferential mixing with the side-chain had been considered, following Flory and Leonard (18). There is also a strong possibility that surface adsorption contributes significantly to the GC retention of n-decane and the other hydrocarbons.

C. References

1) R.S. Werbowyj and D.G. Gray, Macromolecules, 13, 69 (1980).

2) R.S. Werbowyj and D.G. Gray, Mol. Cryst. Liq. Cryst., 34, 97 (1976).

3) G. DiPaola-Baranyi and J.E. Guillet, Macromolecules, 11, 228 (1978).

4) J.H. Hildebrand and R.H. Scott, "The Solubility of Non-Electrolytes", third edition, Dover Publications Inc., New York, 1964.

5) M. Kawakami, M. Egashira, and S. Kagawa, Bull. Chem. Soc. Japan, 49, 3449 (1976).

6) G.A.F. Roberts and I.M. Thomas, Polymer, 19, 459 (1978).

7) This Thesis, Chapter 6.

8) "The Virial Coefficients of Gases: A Critical Compilation", J.H. Dymond and E.B. Smith, ed., Clarendon Press, Oxford, 1969.

9) D.D. Deshpande and S.L. Oswal, J. Chem. Soc., Farad. Trans. 1, 68, 1059 (1972).

10) "Handbook of Chemistry", tenth edition, N.A. Lange, ed., McGraw-Hill Co., New York, 1961.

11) "Chemical Engineering Handbook", J.H. Perry, ed., McGraw-Hill Co., New York, 1963.

12) "International Critical Tables", Vol. III, first edition, McGraw-Hill Co., New York, 1928.

13) R. Reid, J.M. Prausnitz, and T.K. Sherwood, "The Properties of Gases and Liquids", McGraw-Hill Co., New York, 1977.

14) "Handbook of Chemistry and Physics", 58th edition, CRC Press, Inc., West Palm Beach, 1977.

15) G.M. Barrow, "Physical Chemistry", second edition, McGraw-Hill Book Co., New York, 1966.

16) D.G. Gray, Progr. Polym. Sci., 5, 1 (1977).

17) P.J. Flory, Proc. Roy. Soc. London, Ser. A., 234, 73 (1956).

18) P.J. Flory and W.J. Leonard, Jr., J. Am. Chem. Soc., 87, 2101 (1965).

19) R.S. Werbowyj and D.G. Gray, unpublished results.

APPENDIX B

THERMODYNAMIC DATA FOR HPC AND WATER

Table B-1

Experimental Activities of Water Over HPC Solutions

Temp. 15.0°		Temp. 20.0°		Temp. 25.0°		Temp. 30.0°		Temp. 35.0°	
a_1	ϕ_1	a_1	ϕ_1	a_1	ϕ_1	a_1	ϕ_1	a_1	ϕ_1
$.01^{*}$	.001	$.006^{*}$	.001	$.03^{*}$	.002	$.03^{*}$	.002	$.03^{*}$	.002
$.03^{*}$	.003	$.01^{*}$	.002	$.07^{*}$	.006	$.06^{*}$	.005	$.06^{*}$	.005
$.053^{*}$	.005	$.102^{*}$	.009	$.113^{**}$	.009	$.106^{*}$	.009	$.106^{*}$	.009
$.085^{*}$	.008	$.154^{*}$	.014	$.206^{*}$	.017	$.164^{*}$	.013	$.164^{*}$	.013
$.127^{*}$	.012	$.197^{*}$	.018	$.239^{**}$	.021	$.208^{*}$	.017	$.208^{*}$	.017
$.169^{*}$	.016	$.253^{*}$	.023	$.313^{*}$	.028	$.218^{\dagger}$	.019	$.252^{*}$	.021
$.220^{*}$	.022	$.286^{*}$	.027	$.317^{\dagger}$	.028	$.252^{*}$	.021	$.283^{*}$	.024
$.260^{*}$	.025	$.323^{*}$	.031	$.356^{*}$	.034	$.283^{*}$	.024	$.322^{*}$	.029
$.300^{*}$	.030	$.340^{\dagger}$	.031	$.392^{**}$	.040	$.322^{*}$	.029	$.407^{\dagger\dagger}$	.031
$.338^{*}$	.037	$.472^{\dagger}$	.048	$.455^{\dagger\dagger}$	.042	$.373^{\dagger}$	.034	$.442^{\dagger\dagger}$	.037
$.378^{\dagger}$	.037	$.565^{\dagger}$	.067	$.486^{**}$	.053	$.529^{\dagger}$	.057	$.482^{\dagger\dagger}$	.039
$.447^{\dagger}$	.049	$.626^{\dagger}$	.081	$.527^{\dagger}$	.060	$.646^{\dagger}$	.081	$.601^{\dagger\dagger}$	.058
$.498^{\dagger}$	.057	$.677^{\dagger}$	.092	$.548^{**}$	.063	$.685^{\dagger}$	.095	$.771^{\dagger\dagger}$	.113
$.605^{\dagger}$	.078	$.679^{\dagger}$	.094	$.606^{**}$	.073	$.726^{\dagger}$	.110	$.885^{\dagger\dagger}$	.189

Table B-1 continued next page.../

* measured by GC (ECP technique)

** measured by GC (EP technique)

† measured on vacuum microbalance

†† measured over aqueous H_2SO_4

Table B-1 (cont'd.)

Temp. 15.0°		Temp. 20.0°		Temp. 25.0°		Temp. 30.0°		Temp. 35.0°	
a_1	ϕ_1	a_1	ϕ_1	a_1	ϕ_1	a_1	ϕ_1	a_1	ϕ_1
.699†	.107	.707†	.104	.668†	.092	.837††	.164	.916††	.225
.730†	.126	.725†	.115	.772††	.124	.864†	.186	.923††	.227
.801†	.179	.794†	.148	.835††	.164	.866†	.192	.929††	.233
.848†	.206	.816†	.167	.926††	.284	.883†	.209	.968††	.339
.876†	.249	.833†	.201	.948††	.345	.920††	.248	.970††	.441
.921†	.311	.862†	.208	.960††	.431	.950††	.329	.986††	.485
.924††	.327	.867†	.249	.987††	.613	.961††	.371		
.956††	.400	.894†	.288	.996††	.914	.973††	.413		
.972††	.407	.923††	.353			.987††	.597		
.974††	.483	.930††	.364						
.985††	.569	.956††	.435						
.992††	.612	.984††	.560						
		.989††	.577						
		.996††	.702						

† measured on vacuum microbalance

†† measured over aqueous H_2SO_4

Table B-1 continued next page.../

Table B-1 (cont'd.)

Temp. 40°		Temp. 45°		Temp. 50°		Temp. 55°	
a_1	ϕ_1	a_1	ϕ_1	a_1	ϕ_1	a_1	ϕ_1
.01*	.001			.01*	.001	.01*	.001
.04*	.003	.01*	.001	.04*	.002	.06*	.004
.098*	.007	.02*	.002	.06*	.004	.107*	.007
.167*	.013	.05*	.004	.111*	.008	.181*	.013
.210*	.017	.111*	.008	.170*	.012	.225*	.016
.284*	.023	.174*	.013	.224*	.016	.272*	.020
.352*	.030	.231*	.018	.343*	.027	.303*	.023
.470††	.043	.299*	.024	.490††	.031	.522††	.041
.600††	.058	.342*	.028	.510††	.032	.620††	.056
.801††	.128	.481††	.041	.583††	.048	.687††	.072
.880††	.168	.609††	.057	.631††	.061	.780††	.094
.905††	.197	.659††	.068	.712††	.079	.847††	.127
.940††	.238			.720††	.081		
.958††	.272	.823††	.131	.779††	.095	.857††	.132
.969††	.305	.897††	.183	.780††	.098	.902††	.156

Table B-1 continued next page.../

* measured by GC (ECP technique)

†† measured over aqueous H_2SO_4

Table B-1 (cont'd.)

Temp. 40°		Temp. 45°		Temp. 50°		Temp. 55°	
a_1	ϕ_1	a_1	ϕ_1	a_1	ϕ_1	a_1	ϕ_1
.979††	.338	.925††	.209	.843††	.129	.947††	.207
.990††	.407	.952††	.257	.885††	.152	.960††	.223
.996††	.472	.966††	.291	.906††	.161	.961††	.224
		.969††	.304	.911††	.190	.980††	.278
		.987††	.374	.935††	.203	.980††	.292
		.995††	.413	.960††	.236	.990††	.316
				.961††	.256	.993††	.377
				.973††	.283		
				.978††	.289		
				.982††	.323		
				.985††	.338		
				.990††	.344		
				.994††	.397		
				.996††	.420		

†† measured over aqueous H_2SO_4

Table B-2

Activities of Water Over HPC Solutions

Interpolated from Smoothed Isotherms

(1) Low Concentration Region: Average deviation in a_1 = 0.005, except as noted

* ±0.020 † ±0.015 ** ±0.010

a_1

ϕ_1 \ T	15°	20°	25°	30°	35°	40°	45°	50°	55°
0.005	0.057*	0.054*	0.063*	0.063†	0.061**	0.067	0.068	0.076	0.077
0.010	0.110*	0.115*	0.125*	0.124†	0.125**	0.132	0.138	0.145	0.151
0.015	0.159*	0.170†	0.183**	0.182	0.183	0.192	0.201	0.208	0.213
0.020	0.206*	0.219	0.237	0.239	0.237	0.248	0.256	0.268	0.272
0.025	0.259†	0.271	0.289	0.290	0.290	0.300	0.308	0.324	0.330
0.030	0.300**	0.318	0.331	0.334	0.330	0.350	0.360	0.372	0.374
0.040	0.378	0.406	0.408	0.436	0.472	0.445	0.473	0.497	0.516
0.050	0.454	0.476	0.482	0.486	0.555	0.536	0.563	0.589	0.591
0.060	0.512	0.535	0.538	0.542	0.618	0.608	0.630	0.636	0.644
0.070	0.562	0.578	0.591	0.600	0.648	0.652	0.672	0.682	0.685
0.080	0.609	0.625	0.632	0.640	0.680	0.688	0.700	0.716	0.727
0.090	0.644	0.665	0.665	0.670	0.710	0.717	0.726	0.756	0.770
0.100	0.682	0.696	0.698	0.702	0.734	0.738	0.756	0.782	0.795

Table B-2 continued next page.../

Table B-2 (cont'd.)

(2) Intermediate Concentration Region: Average deviation in a_1 = 0.003

a_1

ϕ_1 \ T	15°	20°	25°	30°	35°	40°	45°	50°	55°
0.11	0.708	0.722	0.728	0.730	0.765	0.760	0.782	0.802	0.816
0.12	0.724	0.742	0.750	0.756	0.784	0.784	0.804	0.823	0.836
0.13	0.742	0.760	0.774	0.776	0.805	0.808	0.821	0.848	0.854
0.14	0.756	0.778	0.792	0.795	0.820	0.828	0.840	0.862	0.875
0.15	0.772	0.797	0.810	0.816	0.836	0.848	0.856	0.879	0.893
0.16	0.789	0.810	0.824	0.834	0.850	0.865	0.868	0.892	0.908
0.17	0.800	0.820	0.833	0.847	0.864	0.881	0.882	0.903	0.919
0.18	0.813	0.828	0.844	0.858	0.874	0.893	0.896	0.913	0.926
0.19	0.826	0.835	0.854	0.869	0.886	0.904	0.909	0.920	0.935
0.20	0.838	0.842	0.862	0.880	0.894	0.914	0.917	0.929	0.944
0.21	0.846	0.846	0.872	0.888	0.904	0.921	0.926	0.939	0.950
0.22	0.853	0.853	0.883	0.898	0.915	0.929	0.934	0.947	0.958
0.23	0.860	0.858	0.892	0.906	0.925	0.935	0.941	0.954	0.964
0.24	0.868	0.865	0.900	0.914	0.930	0.942	0.944	0.960	0.967
0.25	0.876	0.870	0.906	0.922	0.937	0.948	0.950	0.962	0.973
0.26	0.884	0.876	0.912	0.927	0.942	0.955	0.956	0.965	0.975
0.27	0.889	0.883	0.919	0.932	0.948	0.958	0.960	0.970	0.978
0.28	0.896	0.890	0.924	0.936	0.951	0.964	0.963	0.974	0.981
0.29	0.905	0.895	0.929	0.941	0.955	0.968	0.969	0.978	0.983
0.30	0.910	0.900	0.932	0.943	0.958	0.972	0.969	0.980	0.986

Table B-2 continued next page.../

Table B-2 (cont'd.)

(3) High Concentration Region: Average Deviation in a_1 = 0.001

a_1

ϕ_1 \ T	15°	20°	25°	30°	35°	40°	45°	50°	55°
0.31	0.920	0.904	0.936	0.946	0.959	0.974	0.973	0.982	0.988
0.32	0.922	0.909	0.937	0.949	0.962	0.976	0.977	0.984	0.991
0.33	0.930	0.914	0.942	0.952	0.966	0.979	0.979	0.986	0.992
0.34	0.935	0.918	0.946	0.954	0.968	0.979	0.981	0.987	0.992
0.35	0.941	0.922	0.949	0.956	0.970	0.983	0.983	0.989	0.992
0.36	0.946	0.927	0.951	0.958	0.972	0.985	0.985	0.991	0.992
0.37	0.950	0.932	0.952	0.961	0.974	0.985	0.987	0.993	0.992
0.38	0.955	0.938	0.955	0.964	0.977	0.987	0.989	0.995	0.992
0.39	0.961	0.946	0.956	0.967	0.979	0.989	0.990	0.995	0.992
0.40	0.963	0.950	0.957	0.969	0.980	0.990	0.992	0.996	0.992
0.41	0.966	0.954	0.959	0.971	0.980	0.991	0.992	0.996	0.992
0.42	0.968	0.958	0.961	0.973	0.981	0.992	0.994	0.997	0.992
0.43	0.969	0.955	0.965	0.975	0.980	0.993	-	-	-
0.44	0.971	0.958	0.967	0.976	0.982	0.994	-	-	-
0.45	0.973	0.960	0.969	0.978	0.984	0.995	-	-	-
0.46	0.975	0.963	0.970	0.979	0.984	0.995	-	-	-
0.47	0.976	0.966	0.971	0.981	0.985	0.996	-	-	-
0.48	0.978	0.969	0.973	0.982	0.986	-	-	-	-
0.49	0.979	0.972	0.974	0.983	0.986	-	-	-	-
0.50	0.980	0.974	0.975	0.984	0.987	-	-	-	-

Table B-3

Heats of Mixing of Water with HPC

Calculated from Data in Table B-2

ϕ_1	15 - 55° $-\Delta\overline{H}$ kJ mol^{-1}	25 - 40° $-\Delta\overline{H}_1$ kJ mol^{-1}	45 - 55° $-\Delta\overline{H}_2$ kJ mol^{-1}
0	5.7 ± 0.6	-	-
0.005	7.6 ± 3.2	-	-
0.010	7.1 ± 1.4	-	-
0.015	5.4 ± 0.6	-	-
0.020	4.3 ± 0.3	-	-
0.025	4.1 ± 0.3	-	-
0.030	3.9 ± 0.3	-	-
0.040	4.8 ± .2	-	-
0.050	5.6 ± .2	-	-
0.060	4.8 ± .1	-	-
0.070	4.5 ± .1	-	-
0.080	3.6 ± .1	-	-
0.090	3.6 ± .1	-	-
0.100	3.1 ± .1	-	-
0.11	2.8 ± .1	-	-
0.12	2.8 ± .1	-	-
0.13	2.8 ± .1	-	-
0.14	2.8 ± .1	-	-
0.15	2.6 ± .1	2.7	-
0.16	2.7 ± .1	2.8	-

Table B-3 continued next page

Table B-3 (cont'd.)

ϕ_1	15 - 55° $-\Delta\overline{H}$ kJ mol^{-1}	25 - 40° $-\Delta\overline{H}_1$ kJ mol^{-1}	45 - 55° $-\Delta\overline{H}_2$ kJ mol^{-1}
0.17	2.6 ± .1	3.1	3.6
0.18	2.5 ± .1	3.1	2.9
0.19	2.5 ± .1	3.0	2.4
0.20	2.5 ± .1	3.0	2.5
0.21	-	2.9	2.3
0.22	-	2.7	2.2
0.23	-	2.5	2.1
0.24	-	2.3	2.3
0.25	-	2.3	2.1
0.26	-	2.4	1.7
0.27	-	2.2	1.6
0.28	-	2.2	1.6
0.29	-	2.2	1.3
0.30	-	2.3	1.5
0.31	-	2.1	1.3
0.32	-	2.1	1.2
0.33	-	2.0	1.1
0.34	-	1.8	0.97
0.35	-	1.8	0.79

Table B-3 continued next page.../

Table B-3 (cont'd.)

ϕ_1	15 - 55° $-\Delta\overline{H}$ kJ mol^{-1}	25 - 40° $-\Delta\overline{H}_1$ kJ mol^{-1}	45 - 55° $-\Delta\overline{H}_2$ kJ mol^{-1}
0.36	-	2.0	0.62
0.37	-	1.8	0.44
0.38	-	1.8	0.27
0.39	-	1.8	0.18
0.40	-	1.73	0
0.41	-	1.67	0
0.42	-	1.54	0
0.43	-	1.45	-
0.44	-	1.39	-
0.45	-	1.33	-
0.46	-	1.27	-
0.47	-	1.23	-
0.48	-	0.95	-
0.49	-	0.86	-
0.50	-	0.86	-

APPENDIX C

GLOSSARY OF SYMBOLS

Most of the symbols used in this thesis are shown here. If appropriate, the equation in which the symbol was first introduced is also shown. A subscript "1" refers to the volatile probe, while the subscript "2" refers to the stationary phase. A superscript "∞" indicates infinite dilution of the volatile probe in the stationary phase.

ROMAN SYMBOLS

a	gas phase volume per unit column length (equation 2-1)
a_1	activity of the probe solution in the stationary phase
a_s	surface coverage by the probe, mol g^{-1}
A	fractional accessibility of polymer to probe
A_L	surface area of stationary phase in GC column
B_{11}	gas phase second virial coefficient for component 1 (equation 2-30)
c	molar concentration of probe vapor in mobile phase
c_1	molar concentration of solvent in substrate (equations 7-6 and 7-7)
C	fractional crystallinity of polymer
C_A	GC calibration factor (equation 3-1)
F_2	molecular pair distribution function (equations 7-3 and 7-4)
$F(y)$	carrier gas flow rate for a mole fraction y of probe vapor (equation 2-46)
G_{11}	cluster integral (equation 7-3)
j	correction for gas phase compressibility (equations 2-4 and 2-5)
k	Boltzmann constant

K	mass distribution (partition) coefficient (equation 2-49)
K_a, K_b	partition coefficients for surface and bulk sorption, respectively (equation 2-39)
ℓ, L	column length
M_i	molecular weight of component i
N_i	number of molecules of component i
$\overline{p}$	average probe vapor pressure in the column
p_1	vapor pressure of probe in solution
p_1^o	vapor pressure of pure liquid probe
$P_{o,flo}$	saturated vapor pressure of water at flow meter (ambient) temperature (equation 2-3)
$P_{o,sat}$	saturated vapor pressure of water at gas saturator temperature (equation 3-2)
P_i, P_o	inlet (back) pressure and outlet (atmospheric) pressures, respectively
q	amount of probe vapor in the stationary phase (mol g^{-1})
R	gas constant
t_M	retention time of non-interacting marker
t_R	retention time of probe
T_g	glass transition temperature
T_m	melting temperature
T, T_c	column or experimental temperature
$\dot{V}$	carrier gas flow rate (mL min^{-1})
$\dot{V}_{CORR}$	carrier gas flow rate corrected for the presence of water vapor (equations 2-3 and 3-2)

V_g	specific retention volume (equations 2-6 and 2-8)
V_m	volume of mixing
V_M	retention volume of non-interacting marker (equation 2-1)
V_N	net retention volume (equation 2-5)
$V_{R'}$	retention volume of sample, corrected for column dead volume (equations 2-2 and 2-9)
w	weight of stationary phase
w_i	weight fraction of component i
x	ratio of molar volumes, V_2/V_1
x_i	mole fraction of component i
y	degree of orientation of a collection of rod-like molecules ($1 \leq y < x$) (equation 2-40)
$\overline{y}$	average mole fraction of probe in the mobile phase
y_o	mole fraction of probe in the mobile phase at the GC outlet
y	mole fraction of probe in the mobile phase
z	lattice coordination number (equation 2-14)

THERMODYNAMIC PARAMETERS

$\Delta\overline{G}_m$, $\Delta\overline{H}_m$, $\Delta\overline{S}_m$	partial molar free energy, enthalpy, and entropy of mixing of probe in polymer
$\Delta\overline{G}_m^{\infty}$, $\Delta\overline{H}_m^{\infty}$, $\Delta\overline{S}_m^{\infty}$	partial molar free energy, enthalpy, and entropy of mixing at infinite dilution of probe in stationary phase (equations 2-32, 2-33, 2-35)

ΔG_m, ΔH_m, ΔS_m	free energy, enthalpy, and entropy of mixing (equations 2-15 and 2-16)
$\Delta G_{m,comb}$	combinatorial (statistical) contribution to ΔG_m (equation 2-18)
$\Delta G_{m,noncomb}$	all other contributions to ΔG_m (equation 2-18)
$\Delta \overline{H}_s$	heat of solution of probe in stationary phase (equations 2-37 and 2-38)
ΔH_v	latent heat of vaporization of pure liquid probe (equations 2-37 and 2-38)

GREEK SYMBOLS

α, α'	areas defining sorption regions on GC chromatogram (equations 2-47 and 2-48; figure 2-3)
β	area defining non-sorption region of GC chromatogram (equation 2-48, figure 2-3)
β	specific partition coefficient for equilibration of probe between the vapor and stationary phases, mL g^{-1} (equations 2-7, 2-8, and 2-9)
γ_i	mole fraction based activity coefficient of component i
Γ	surface concentration or Gibbs excess (mol cm^{-2})
δ_i	solubility parameter of component i (equation A-1)
π	osmotic pressure of solution (equation 4-2)
ϕ_i	volume fraction of component i (equations 2-19 and 2-20)
χ_{12}, χ_{FH}	Flory-Huggins interaction parameter for component 1 in stationary phase 2
χ_{crit}	value of χ at a critical (phase separation) point (equations 2-24 and 2-25)

χ_H, χ_S	enthalpic and entropic contributions to χ (equation 2-17)
χ_R	interaction parameter for a system of rod-like molecules (equation 2-40)
Ω_1	weight fraction based activity coefficient of component 1 in stationary phase 2 (equation 2-27)

APPENDIX D

ORIGINAL DATA FOR HEATS OF SOLUTION OF WATER ON CELLULOSIC POLYMERS*

* Activity coefficients as y coordinate in the form of natural logarithms

```
*IN PROGRESS
COMPILE =   0.51 SEC
INF. DIL. HEAT OF MIXING OF WATER ON CELL. ACETATE (DS=0.89)


 SLOPE =   -1974.713000 INTERCEPT =       6.3940
 STANDARD DEVIATION OF THE SLOPE =  0.151E 03
 STANDARD DEVIATION OF THE INTERCEPT =  0.436E 00
 LINEAR CORRELATION COEFFICIENT =   -0.9913E 00


     1/T           Y-EXPERIMENTAL     Y-CALCULATED
    0.002874         0.7320             0.7186
    0.002792         0.8680             0.8806
    0.002821         0.8300             0.8233
    0.002850         0.7920             0.7660
    0.002873         0.7150             0.7206
    0.002906         0.6310             0.6554
    0.002939         0.5830             0.5903
    0.002973         0.5030             0.5231
    0.003007         0.4800             0.4560
EXEC =   0.05 SEC
*END
```

```
*IN PROGRESS
COMPILE =   0.51 SEC
INF. DIL. HEAT OF MIXING OF WATER ON CELL. ACETATE (DS = 2.45)


 SLOPE =   -1137.782000 INTERCEPT =       4.5825
 STANDARD DEVIATION OF THE SLOPE =  0.172E 03
 STANDARD DEVIATION OF THE INTERCEPT =  0.498E 00
 LINEAR CORRELATION COEFFICIENT =   -0.9958E 00


     1/T           Y-EXPERIMENTAL     Y-CALCULATED
    0.002998         1.1810             1.1714
    0.002951         1.2200             1.2249
    0.002910         1.2630             1.2715
    0.002869         1.3190             1.3182
    0.002827         1.3590             1.3659
    0.002789         1.4190             1.4092
EXEC =   0.04 SEC
*END
```

```
/ENDRUN
*IN PROGRESS
COMPILE =   0.50 SEC
INF. DIL. HEAT OF MIXING OF WATER ON CELLULOSE TRIACETATE


 SLOPE =    -614.811500 INTERCEPT =       4.6715
 STANDARD DEVIATION OF THE SLOPE =  0.124E 03
 STANDARD DEVIATION OF THE INTERCEPT =  0.360E 00
 LINEAR CORRELATION COEFFICIENT =   -0.6817E 00


      1/T           Y-EXPERIMENTAL      Y-CALCULATED
    0.002997          2.7100              2.8289
    0.002954          2.8630              2.8553
    0.002912          2.8800              2.8812
    0.002869          2.8530              2.9076
    0.002826          2.9120              2.9340
    0.002788          2.9570              2.9574
    0.002824          2.9400              2.9353
    0.002861          2.9510              2.9125
    0.002901          2.9190              2.8879
    0.002941          2.8990              2.8633
    0.002983          2.8550              2.8375
    0.003008          2.8840              2.8221
EXEC =   0.07 SEC
*END
```

```
/ENDRUN
*IN PROGRESS
COMPILE =   0.51 SEC
INF. DIL. HEAT OF MIXING OF WATER ON METHYL CELLULOSE


 SLOPE =   -2225.081000 INTERCEPT =       9.5564
 STANDARD DEVIATION OF THE SLOPE =  0.170E 03
 STANDARD DEVIATION OF THE INTERCEPT =  0.491E 00
 LINEAR CORRELATION COEFFICIENT =   -0.9957E 00


      1/T           Y-EXPERIMENTAL      Y-CALCULATED
    0.002789          3.3690              3.3507
    0.002828          3.2480              3.2639
    0.002865          3.1880              3.1816
    0.002909          3.0600              3.0837
    0.002950          2.9960              2.9924
    0.003002          2.8880              2.8767
EXEC =   0.04 SEC
*END
```

```
INF. DIL. HEAT OF MIXING OF WATER ON ETHYL CELLULOSE

 SLOPE =   -1348.464000 INTERCEPT =        6.6165
 STANDARD DEVIATION OF THE SLOPE =  0.146E 03
 STANDARD DEVIATION OF THE INTERCEPT =  0.426E 00
 LINEAR CORRELATION COEFFICIENT =   -0.9589E 00


      1/T            Y-EXPERIMENTAL      Y-CALCULATED
    0.002829           2.8010              2.8017
    0.002865           2.6930              2.7532
    0.002912           2.6810              2.6898
    0.002954           2.6400              2.6332
    0.002996           2.5560              2.5765
    0.002914           2.7220              2.6871
    0.002952           2.6400              2.6359
    0.002994           2.5730              2.5792
    0.002997           2.5710              2.5752
    0.002954           2.6480              2.6332
    0.002914           2.7120              2.6871
    0.002874           2.7360              2.7411
    0.002829           2.8220              2.8017
EXEC =   0.06 SEC
*END
```